Distributed source coding schemes for wireless sensor networks

Tang, Zuoyin

Award date:
2007

Awarding institution:
University of Bath

Distributed Source Coding Schemes for Wireless Sensor Networks

submitted by

Zuoyin Tang

for the degree of Doctor of Philosophy

of the

University of Bath

Department of Electronic and Electrical Engineering

September 2007

Dedicated in loving memory of

Xinshi Tang

1937-2007

Abstract

Recent advances in micro-electro-mechanical systems (MEMS) fabrication have made it possible to construct miniature devices containing an embedded system with strong computing capabilities. New generations of low cost sensor nodes can be created small with powerful computing and sensing capabilities. The small sensor nodes together with distributed wireless networking techniques enable the creation of innovative self-organized and peer-to-peer large scale wireless sensor networks (WSNs). A coordinated network of sensor nodes can perform distributed sensing of environmental phenomena over large-scale physical spaces and enable reliable monitoring and control in various applications. WSNs provide bridges between the virtual world of information technology and the real physical world. They represent a fundamental paradigm shift from traditional inter-human personal communications to autonomous inter-device communications.

This thesis investigates the problems of target detection and tracking in WSNs. WSNs have some unique advantages over traditional sensor networks. However, the severe scarcity of power, communication and computation resources imposes some major challenges on the design and applications of distributed protocols for WSNs. In particular, this thesis focuses on two aspects of remote target detection and tracking in WSNs: distributed source coding (DSC) and sensor node localization. The primary purpose is to improve the application performance while minimizing energy consumption and bandwidth overhead.

Theoretically, DSC schemes can be used to compress multiple sensor readings without inter-node communications. Both the bandwidth and the power consumption of sensor nodes can, therefore, be reduced. However, previously proposed DSC schemes can only jointly compress one sensor reading with the uncompressed readings at a time. To address this problem a practical random-binning based DSC algorithm for application to remote source estimation in WSNs is proposed. The algorithm is shown to be simple and efficient by analytical model and simulation. The random-binning based DSC algorithm is then applied to the design of a distributed compression scheme. The

problems in the construction and utilization of side information, and the control of coding rate, are solved. The decoding error performance of the DSC scheme is analyzed and simulated. The signal to distortion ratio (SDR), bandwidth, and energy efficiency performance of the DSC scheme are analytically modeled as functions of the DSC scheme parameters and network conditions. Using these models, an adaptive control mechanism is proposed to adapt to the changing network environment and improve end-to-end remote signal estimation performance. A detailed packet format and communication protocol are implemented to assist in adaptively controlling the number of sensor nodes participating in DSC coding process. The DSC coding and transmission parameters are also adapted to the changing network conditions. The performance of the proposed adaptive DSC control mechanism is investigated in detail.

The importance of location information in wireless sensor networks has motivated much research on the design of localization protocols. However, it is very important to understand how a localization protocol can work well and be optimized for specific applications in WSNs. Since simulation is inefficient to evaluate the performance of large scale WSN localization algorithms, a Cramer-Rao bound (CRB) based analytical approach is proposed to evaluate the feasibility and estimation performance of several existing localization algorithms for target detection and tracking applications. The analytical approach is simple and scalable, which makes it especially suitable for large scale WSN applications. Simulation results of the localization algorithms for some WSNs show the CRB based analytical approach to be very efficient. The application of CRB based analytical approach and localization algorithms for target detection and tracking applications is also investigated.

Acknowledgments

I'm indebted to many individuals for their care and support given to me during my doctoral studies. First of all I would like to express my deep gratitude to my supervisor, Dr. **Ian Glover**. Without his assiduous instruction and continuous encouragement, no progress in my research work is possible. His wise guidance and great concern have provided tremendous help to my professional growth. I enjoyed very much the discussion with him and the time working with him.

I would also like to express my cordial thanks to Professor **Don Monro**. He provided me constant encouragement and invaluable suggestions on my research, especially during the starting phase of my PhD studies. I would also like to thank Dr. **Adrian Evans**. He provided me constant encouragement especially during my most difficult time. His insightful comments on my thesis will benefit not only my PhD research, but also my career in a long time to come.

Appreciation is also extended to all the staffs in the Department of Electronic and Electrical Engineering, for their efforts in providing a friendly research environment.

The scholarship granted by ORS is gratefully acknowledged.

I would also like to thank my friends and my fellow postgraduate students **Fei Tong**, **Dexin Zhang**, **Wei Huo**, **Xiaopeng Wang**, for their friendship, discussion, and advice. I am also thankful to **Bingjie Fu**, **Aimin Wang**, **Wei Ding**, and **Yanwu Guo** for their friendship and enjoyable technical discussion.

My special thanks should go to my parents since they have always loved me, believed in me and encouraged me in my study. I am also grateful to my husband and my younger sister for their forever love and support.

Table of Contents

List of Figures

List of Tables

Acronyms and Abbreviations

3G	third-generation
ADC	analog-to-digital converter
ADSID	Air Delivered Seismic Intrusion Detector
ARQ	automatic repeat request
AWGN	additive white Gaussian noise
BMA	bit-map-assisted
B-MAC	Berkeley Media Access Control
C4ISRT	command, control, communications, computing, intelligence, surveillance, reconnaissance, and targeting
CEO	chief executive officer
CL-basic	centralized, basic
CL-refine	centralized, with local refinement
CMOS	complementary metal-oxide-semiconductor
CODA	COngestion Detection and Avoidance
COTS	commercial-off-the-shelf
CPU	Central Processing Unit
CRB	Cramer-Rao Bound
CSMA	Carrier Sense Multiple Access
DAC	digital-to-analog converter

DSC distributed source coding

DV-hop a method to determine multi-hop distance, in hops, based on distance-vector

DV-Min distance determined by DV-hop method, location computed by Min-max method

DV-Lat distance determined by DV-hop method, location computed by trilateration method

ESB Embedded Sensor Board

ESRT Event-to-Sink Reliable Transport

FEC forward error correction

FFT fast Fourier transform

FIM Fisher information matrix

GPRS General Packet Radio Service

GPS global positioning system

GSM Global System for Mobile communications

HMAC Hybrid MAC

IFA intermediate frequency amplifier

ISM industrial, scientific, and medical

LDPC low-density parity-check

LEACH Low Energy Adaptive Clustering Hierarchy

LLC Logical Link Control

LNA low noise amplifier

LO local oscillator

MAC media access control

MANet mobile ad-hoc network

MEMS micro-electro-mechanical systems

Min-max a method to compute location, based on minimum and maximum of coordinates for intersection of bounding boxes

MQAM M-order Quadrature Amplitude Modulation

MSE mean square error

ns-2 network simulator

PA power amplifier

PAN personal area network

PAR peak to average ratio

PDA personal digital assistant

PSFQ Pump Slowly, Fetch Quickly

RAM random access memory

ReInForM Reliable Information Forwarding using Multiple paths

RF radio-frequency

RFID radio-frequency identification

RMST Reliable Multi-Segment Transport

ROM read-only memory

RSS received signal strength

SD-Min distance determined by Sum-dist method, location computed by Min-max method

SD-Lat distance determined by Sum-dist method, location computed by trilateration method

SDR signal to distortion ratio

S-MAC sensor-MAC

SMP Sensor Management Protocol

SNMP Simple Network Management Protocol

SNR signal to observation noise ratio

SoC system-on-a-chip

SPIN Sensor Protocol for Information via Negotiation

SQDDP Sensor Query and Data Dissemination Protocol

Sum-dist a method to determine multi-hop distance, based on sum of distance each hop along path

TDMA time division multiple access

TDOA time-difference-of-arrival

T-MAC Timeout-MAC

TOA time-of-arrival

TRAMA TRaffic-Adaptive Medium Access protocol

UHF ultra high frequency

UWB ultra-wideband

VHF very high frequency

VLSI very-large-scale integration

WINS wireless integrated network sensors

WLAN wireless local area network

WMAN wireless metropolitan area network

WPAN wireless personal area network

WRAN wireless regional area network

WSN wireless sensor network

Z-MAC Zebra MAC

μAMPS micro-Adaptive Multi-domain Power-aware Sensors

Chapter 1

Introduction

With the popularity of laptops, cell phones, personal digital assistants (PDAs), global positioning system (GPS) devices, radio-frequency identification (RFID), and intelligent electronics in the post-PC era, computing devices have become cheaper, more mobile, more distributed, and more pervasive in daily life. The rapid advances in micro-electro-mechanical systems (MEMS) fabrication makes it now possible to construct computing devices with small-size embedded system and strong computing capabilities. As the Moores's Law marches on, computing devices will get smaller and grow more powerful at a given size. This will enable the development of new generations of sensors that are small and cheap with powerful computing and sensing capabilities [1–3].

In addition, during the past decade, wireless communications has experienced a worldwide momentous revolution and brought the world into a completely new era. It is becoming an essential feature of everyday life. Not only are computer networks becoming mobile, but also each device such as laptop, camera, phone will eventually have one or several wireless interfaces. These wireless interfaces can provide communication capabilities for ubiquitous wireless data services driven by explosive growth of the Internet and mobile networks. The commu-

nication capabilities also enable direct communication between devices without control or management of central stations.

Powerful computing capabilities together with distributed wireless networking techniques enable the creation of innovative self-organized and peer-to-peer large scale wireless networks. Wireless sensor networks (WSNs) have appeared as one kind of such networks in the last few years [1–3]. In a WSN a large number of powerful sensors are networked by wireless communication technologies and send measurement data to sink(s) for further processing. The networked sensors coordinate to perform distributed sensing of environmental phenomena over large scale of physical space, thus enable reliable monitoring and control in various applications. WSNs provide bridges between the virtual world of information technology and the real physical world. They represent a fundamental paradigm shift from traditional inter-human personal communications to autonomous inter-device communications. They promise unprecedented new abilities to observe and understand large-scale, real-world phenomena at a fine spatial-temporal resolution. WSN was identified by Business Week as one of the most important and impactive technologies for the 21st century in September 1999. The MIT's Technology Review stated that WSN is one of the top ten emerging technologies in January 2003.

WSNs are powerful in supporting a lot of different applications and have the potential to engender new breakthrough scientific advances. They also, however, present many research and engineering challenges because of this flexibility and the severe scarcity of energy, computation and communication resources [2–18, 20–24, 116]. In the remainder of this chapter, the application framework to be investigated by this thesis will be introduced in Section 1.1. The research challenges and the research motivations associated with the applications are identified in Section 1.2 and Section 1.3, respectively. The specific

contributions presented in this thesis are listed in Section 1.4, and the thesis is outlined in Section 1.5.

1.1 Application Framework

With simple processing, storage, sensing and communication capabilities integrated into small-scale low cost sensors, WSNs promise an unprecedented fine-grained interface between the virtual and physical worlds. It is one of the most rapidly developing new information technologies, with applications in a wide range of fields including industrial process control, security and surveillance, environmental sensing, and structural health monitoring. Karl and Willig pointed out that many of the applications for WSNs share some basic characteristics and most of them have a clear difference between the sources of data and the sinks [3]. There are three typical interactive patterns to distinguish the interaction between the sources and the sinks, which include:

- Event detection: Once sensor nodes detect the occurrence of a specific event, they should report to the sink(s). If several different events occur at the same time, event classification will be required. In this application pattern, sensor nodes can stay in sleeping state in most of time and wake up occasionally.

- Target Tracking: In the case of the source of an event being mobile (such as tanks in the battlefield), the sensor nodes that detect the occurrence of the source will report and update the source's position to the sink(s). In this application pattern, sensor nodes behave the same as they do in the application pattern of event detection if no source of events is detected. Once the sources of events are detected, however, they can behave differently. The number of active sensor nodes deployed around to detect the source and the

sampling frequency can be increased to track the trajectory of the mobile source with a satisfactory resolution.

- Periodic measurement: WSNs can also be designed to periodically report measured values. The measurement can be made periodically or triggered by some specific events. There is a trade-off between reporting frequency and measurement resolution.

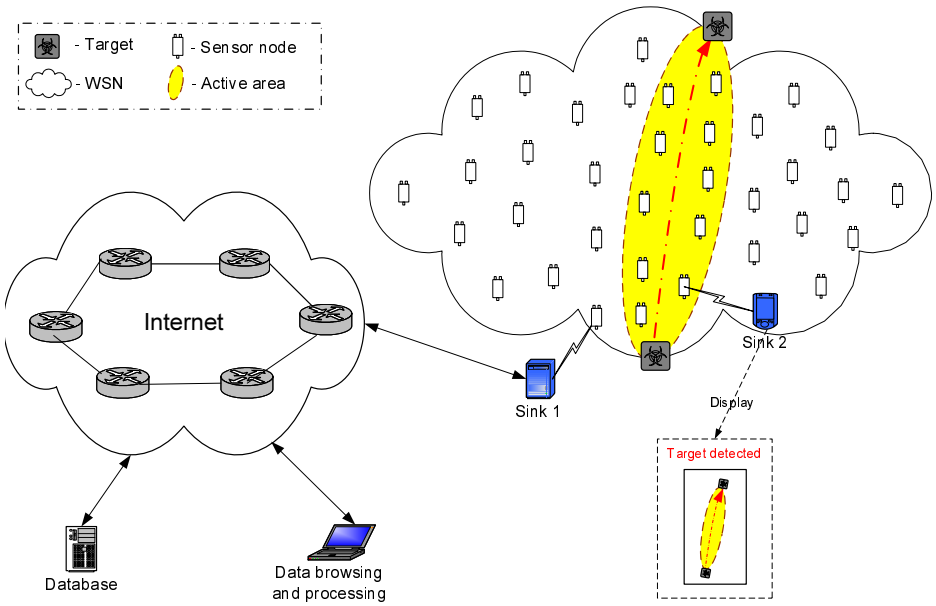

Figure 1-1: Scenario of target detection and tracking in wireless sensor networks.

In this thesis, target detection and tracking is taken as the background application for research. Event detection and tracking in WSNs has a wide range of applications in both military and civilian fields. For example, WSNs can be used to detect the occurrence of enemy soldiers and vehicles in battlefield, and detect intruders in civilian surveillance applications. It is noted that the research achievements of the work in this thesis can be extended to other application patterns. Figure 1-1 illustrates the framework of remote source detection and tracking. In this framework, sensor nodes are connected by wireless links and equipped with one or more sensors. Accordingly to the scale of WSNs, sensor

nodes can be randomly deployed in an ad-hoc approach if there are a large number of nodes in the network, or be deployed in well-planned fixed locations. The sensor nodes have to function unattended for a long time without maintenance or energy supply.

Sensor nodes are used to detect the occurrence of specific events. Once events are detected, the sensor nodes will cooperatively transmit measured data to the sink(s). As shown in Figure 1-1, multiple sinks may connect the WSN. In addition to the function of collecting the measurement data from the sensor nodes, they have other different types of functions, such as data processing and control. For example, Sink 1 in Figure 1-1 acts only as a bridge between the WSN and the control systems connected to the Internet. After receiving the measurement data from the WSN, Sink 1 forwards data to and/or receives control commands from the central data processing and control station. Sink 2 in Figure 1-1 is, however, more powerful. It has data processing function and can react immediately to the events detected by the sensor nodes.

1.2 Research Challenges

1.2.1 Comparison to Traditional Sensor Networks

As a new technology for applications of target detection and tracking, WSNs have several specific features and advantages. Currently wired sensor networks are widely used for target detection and tracking. They are, however, expensive to install and maintain and limited in range. The promise of a wireless solution is not feasible because of difficult technical challenges associated with reliability, power consumption, costs and complexity of network installation and expansion. Traditional point-to-point wireless networks are not adequate to solve these challenges, as they are prone to failure when facing the demanding and dy-

namic Radio-Frequency (RF) landscape which is crowded with transmissions from cordless telephones, Wi-Fi networks, and common business equipments such as bar-code scanners and person-to-person radios.

In contrast to traditional sensor networks, WSNs can provide performance beyond traditional point-to-point solutions, particularly in areas of fault tolerance, power consumption and installation cost:

- Improved sensing accuracy: With the advanced MEMS technologies, individual wireless sensor nodes can be manufactured in small size and with ultra low power consumption, which enables them to last for a long time, from several months to tens of years. This long service life is especially suitable for target detection and tracking applications in inaccessible areas without renewable power sources. The low production cost allows deploying sensor nodes densely in area of interest and providing a very large coverage through the union of small sensor coverage. Higher sensing accuracy is, therefore, achievable.

- Higher fault tolerance: Since sensor nodes are deployed in close proximity to the object of interest, WSNs can efficiently overcome ambient environmental effects that might otherwise interfere with sensor observations. Higher fault tolerance is also achievable through the high level of redundancy due to dense deployment.

- Easier deployment and management: WSNs can be easily deployed and capable of self-organizing. Unlike the wired sensor networks, the position of sensor nodes in WSNs need not be predetermined or engineered, which allows random deployment in inaccessible regions or dangerous operations. In addition, WSNs do not need infrastructure support or complex network configuration. The management work will, therefore, also be minimized.

WSNs can also be easily extended.

- Stronger adaptation capabilities: Wireless sensor nodes have memory storage, computation and signal processing capabilities on board. This not only enables sensor nodes to collaborate locally to enhance the observing confidence, but also enables WSNs to dynamically adapt to changing environments. Using adaptation mechanisms, WSNs can automatically respond to the changes in network topologies, events, or task requirements.

1.2.2 Design Challenges

Although WSNs have many advantages over tradition sensor networks, they present a number of serious challenges that cannot be easily solved by existing technologies. In what follows, the requirements on service and network mechanism for application of WSNs to target detection and tracking will be analyzed. Many challenges come from protocol designs to satisfy services and network mechanisms requirements [3].

Services Requirements

Several services are very important for target detection and tracking applications and should be provided by WSNs. Serious challenges are posed on the design of protocols and mechanisms to satisfy these services requirements:

- Lifetime: WSN nodes are generally severely energy-constrained due to battery limitations. Hardware improvements in battery design and energy harvesting techniques offer, however, only partial solutions. Due to the expense and potential infeasibility of recharging/replacing batteries for a large network, lifetime is a big challenge for protocol designs in WSNs. Long lifetime is desired and energy efficiency should be taken as the primary goal of most protocol designs.

There can be several definitions of network lifetime. A simple definition is using the time until a certain number of sensor nodes, for example, until the first sensor node, or a specific percentage of sensor nodes, run out of energy. The time until the network is partitioned, or a specific point in the monitored area is not covered by the network, or the desired detection accuracy can not be obtained, can also be defined as the network lifetime.

- Detection accuracy and responsivity: For applications of target detection and tracking, the occurrence of target is unpredictable in advance. If the detection of target or the transmission of detection results to central control station is delayed, the best opportunity of taking actions may be missed. In addition, if detection results are wrong, disaster loss may be caused due to wrong actions being taken. Accurate and quick detection of target is, therefore, important for central control station to be aware of the events, make correct decisions, and take necessary actions. This is critical for the success of WSNs. However, as described in previous section, sensor nodes may only be woken up occasionally to monitor surrounding environment in order to reduce energy consumption. If there are not enough sensor nodes that are active when the target appears, the detection responsivity and accuracy may be severely affected. It is challenging to properly schedule the sleeping of sensor nodes to achieve the desired responsivity and accuracy while minimizing the energy consumption and cost of sensor nodes.

- Coverage and robustness: Due to unpredictable locations where targets may occur, it is desirable that the whole area to be monitored should be covered by active sensor nodes. Due to the large number of wireless sensor nodes, however, it is difficult to deploy sensor nodes in a well-planned way. The number of nodes in a unit area may vary considerably over space. In addition, inexpensive devices may often be unreliable and prone to failures.

The number of nodes may further vary with time and space due to node failure or sleep. It is, therefore, important and challenging to control and monitor the number of deployed sensor nodes and active sensor nodes over time and space, in order to maintain the necessary service coverage, and to ensure that the target detection and tracking services are not too sensitive to individual device failures.

- Location: Since sensor nodes do not generally have an ID, measured data need to be associated with the location information where the source of events is detected, otherwise it may become meaningless. The location information can be either carried by data packets sent from sensor nodes to sink(s) explicitly, or be obtained implicitly by sink(s). For example, the sink can send out a query message to a specific region of monitored area and request only the sensor nodes in that region to send back measured data. In this way, the sink can implicitly obtain the location information associated with the data packets received from sensor nodes. Although much research effort has been dedicated to the localization problem and a number of algorithms have been proposed, the problem remains challenging. Further research effort on assessing the accuracy, scalability, and energy efficiency of the proposed algorithms is required.

- Privacy and security: Privacy and security have to be protected by almost every kind of networks. This holds true for WSNs, especially for military target detection and tracking applications. The constrained energy, computing and storage capabilities, however, limit the use of advanced algorithms in WSNs. How to protect sensitive measured data under these constraints is very interesting and remains an open research issue. The security problem will, however, not be investigated in this thesis.

Network Mechanisms Requirements

The challenges not only come from the design of innovative mechanisms to realize the services requirements for WSN-based target detection and tracking, but also from the management of WSN itself and fitting for the specific features of WSNs. Several network mechanism requirements are analyzed below [3].

- Scalability: As described in the service requirements for high detection accuracy and full coverage of target detection, high density of sensor nodes are required to be deployed. WSNs can therefore be extremely large scale (tens of thousands and perhaps even millions of nodes). With the continuing drop of sensor node cost, this is also economically possible. To provide the scalability, protocols designed for network management and service provision have to be inherently distributed, involving localized communication, and utilizing hierarchical architectures. It is, however, still challenging to deploy and manage a large number of nodes in practice, especially in the aspects of failure handling, sensor nodes programmability, and capacity limits in large scale networks.

- Auto-configurable: As assumed in the application framework, due to difficulty and potential infeasibility of network maintenance, WSNs for target detection and tracking have to operate unattended. Mechanisms have to be designed for sensor nodes to be able to configure their own network topology, localize, calibrate themselves and determine other important operating parameters. Autonomous configuration of network and protocol parameters is still a key network design challenge.

- Self-adaptive: In target detection and tracking, there is often significant uncertainty about the occurrence of targets over time and space prior to deployment. In addition, the network conditions, such as node density, en-

ergy status and network traffic, may change dynamically over time. It is challenging for WSNs to autonomously learn environmental dynamics in an online manner, and adapt to changing environment by using the learned information. Various trade-offs between mutually contradictory goals (such as energy, detection accuracy, lifetime, and node density) should be exploited to improve network performance.

- Collaborative and in-network processing: For economic considerations of reducing cost and size per node, it is possible that the capabilities of individual nodes remain constrained to some extent. In target detection and tracking applications, a single sensor node may not be able to achieve the required detection accuracy on the occurrence of a target. Several sensor nodes have to collaborate and only the joint data of many sensor nodes can provide sufficient information. There will be, however, much spatial and temporal redundancy among the measured data from sensor nodes. The challenges are, therefore, those of designing collaborative mechanisms to minimize the number of sensor nodes simultaneously participating measurement process, and those of efficiently reducing the amount of data sent to sink(s) to improve energy, computation and communication efficiency.

1.3 Research Motivations

For target detection and tracking applications, WSNs have some unique advantages whilst also present many challenges to achieve the required services levels and network mechanisms properties. During the last decades, there has been extensive research on protocol and mechanism design for data services and network management services. Hardware design, routing and MAC protocols, and physical layer techniques have received most of research effort. Recently reliability

and congestion control for WSNs have received more research interests.

This thesis will focus on several challenging problems identified in Section 1.2 for applications of target detection and tracking. The first one is the challenging problem of collaborative and in-network signal processing. Application of a distributed signal processing technique, namely distributed source coding (DSC), is investigated for improving detection accuracy, bandwidth and energy efficiency. The second one is on the localization problem. The network self-configuration, self-adaptation and optimization problems are also investigated.

For scalability and robustness considerations, it is necessary to organize WSNs in distributed fashion. When the network is organized in distributed fashion, sensor nodes in the network will not only send their own or pass on other nodes' packets. They can also actively participate in the network management and optimization, through localized communication and collaborative in-network signal processing. Several collaborative in-network processing techniques exist, including aggregation and DSC [5]. DSC is a technique to exploit the correlation among the measured signals by adjacent sensor nodes on the same source of event. Using this technique, the number of transmitted bits can be reduced whilst still satisfy the detection accuracy requirement. It has advantage over aggregation technique, which condenses and sacrifices the information on measured data in order not to transmit all the bits of data from all active sensor nodes to the sink. The challenge of applying DSC to WSNs is, however, that the measured data provided by multiple sensor nodes must be distributively coded with very limited or even zero communication for joint coding. How to implicitly provide the joint information among adjacent nodes is still an open research issue. It is the primary objective of this thesis to design practical DSC schemes for WSNs.

On the other hand, for networks where there is often significant uncertainty about operating conditions prior to deployment and where resource availability

changes dynamically, it is important to have a flexible execution strategy. This strategy allows algorithms to adapt to current network conditions. Since the recovered signal by DSC method will be affected by not only the coding method itself but also the end-to-end information delivery, some information redundancy may be required to combat noisy channel and packet erasures. It is important to design efficient mechanisms to control coding parameters and transmission strategies to adapt to changing network conditions. The second objective of this thesis is, therefore, to design adaptive control mechanisms to investigate various trade-offs between the performances of detection accuracy, bandwidth and energy efficiency, and network control complexity.

Furthermore, in target detection and tracking applications, the received signal is meaningless without localization information. Due to the large scale of WSNs, however, sensor nodes do not have global IDs. It is impractical to equip each sensor node with a GPS. How to accurately and efficiently locate sensor nodes in a scalable way is one of the most challenging problems in target locating. Investigation of localization algorithms is, therefore, another research focus of this thesis. The obtained location information, either local or global, can be associated with measured data for identification of targets, and can also assist in the control of DSC procedures.

In the next section, more details on the research activity and achievements of this thesis will be presented.

1.4 Key Contributions

This thesis primarily focuses on two aspects of target detection and tracking in WSNs: remote signal estimation and sensor node locating. While extensive research work has been done in both of these areas, a lot of challenges still remain, for example, in the solution design to satisfy the requirement of detection

accuracy, energy and bandwidth efficiency, self-adaption, and scalability. In this thesis, these requirements and specific features of WSNs are taken into account in protocol designs, to improve application performance while minimizing energy consumption and bandwidth overhead.

A number of research contributions are made in this thesis that improve the state of the art in target detection and tracking in WSNs. These are:

- Based on the analysis of current DSC techniques for WSNs, a practical random-binning based DSC algorithm is proposed for application to remote source estimation in WSNs. The algorithm is simple and efficient. Its performance is evaluated by analytical model and simulation.

- The random-binning based DSC algorithm is used in the design of a distributed compression scheme. The scheme overcomes the limitation in previous DSC schemes that only one sensor reading at a time can be compressed jointly with uncoded sensor readings. In the proposed scheme, multiple sensor readings are jointly encoded with the side information implicitly provided by the sink at the same time. The challenges in the construction and utilization of side information, and the control of coding rate are also overcome. By fully utilizing the spatial correlation between multiple sensor observations, this scheme achieves high coding efficiency and reduces bandwidth consumption. Since only simple encoding operations are required at sensor nodes, the proposed scheme is feasible and desirable for resource-constrained wireless sensor nodes. The decoding performance of the DSC scheme is also analyzed and simulated.

- To make efficient trade-off between signal to distortion ratio (SDR), energy consumption and bandwidth efficiency under the changing WSN environment, analytical models are proposed to understand the impacts of DSC

algorithm parameters, transmission strategies and network conditions. The SDR, bandwidth and energy efficiency performances of the DSC scheme are modeled as functions of the number of active sensor nodes, observation noise, quantization distortion, DSC decoding errors, network bandwidth constraint and network packet losses. A multi-mode power model for wireless sensor communications is used for the evaluation of the overall network energy consumption performance.

- With the developed models, a new adaptive control mechanism is proposed to adapt to changing network environment and improve end-to-end remote signal estimation performance. Detailed packet format and communication protocol are implemented to assist in adaptively controlling the number of sensor nodes participating in the coding process, the source coding and transmission parameters to the changing network conditions. Simulation results show that the proposed adaptive DSC control mechanism can either save up to more than 30% of energy without decreasing SDR or maximize SDR with up to nearly 10% energy saving. To the best of the author's knowledge, this is also the first research effort on the evaluation of energy consumption performance for DSC schemes.

- In addition, the performance of localization protocols in a multi-hop WSN is studied. Due to the importance of location information for target detection and tracking applications, much effort has been devoted to the design of sensor localization algorithms. Since simulation is inefficient to evaluate the performance of the proposed algorithms for large scale WSNs, there are some theoretic analysis and comparison research effort. To the best of the author's knowledge, however, theoretic analysis of range-based localization algorithms for multi-hop WSNs has not been reported in the literature. In order to evaluate the feasibility and performance of existing localization

protocols for target detection and tracking applications, this thesis further proposes a general evaluation tool based on Cramer-Rao bound (CRB), for localization algorithms in multi-hop WSNs.

- With the CRB-based evaluation tool, two centralized localization algorithms (with and without local refinement, respectively) are analyzed and compared with four distributed localization algorithms, in order to get insights into the location estimation performance. The sensitivity of localization performance to distance measurement error, network size, and anchor node density are also investigated. Although CRB-based analysis has been previously used to provide performance bounds on localization error of various locating protocols, this study fills up the gap in the previous work on multi-hop range-based locating protocols. The complex tradeoff of centralized and distributed locating protocols between location estimation accuracy and complexity is studied. Compared to discrete-event simulation method, the proposed analytical evaluation tool is more efficient and scalable. The obtained results can provide valuable suggestions on design, selection, configuration, and optimization of localization algorithms for large scale WSNs.

1.5 Outline of Thesis

This thesis begins in Chapter 2 by presenting the relevant aspects of WSNs as the background for the subsequent contents regarding the research on DSC and localization protocols. The architecture of WSNs and overall protocol stacks will be introduced. Several existing collaborative in-network processing techniques will also be presented and briefly compared.

The design and analysis of random-binning based DSC algorithm is presented in Chapter 3. After summarizing the related work on DSC, a random-binning

based DSC algorithm is developed and used in the transmission scheme for target detection and tracking applications. Analytical and simulation results are also presented.

Then in Chapter 4, an adaptive end-to-end DSC control mechanism is proposed. The energy model used for design and evaluation of the mechanism is introduced. The details on performance modeling, protocol design, adaptation mechanism, and performance evaluation are presented.

In Chapter 5, localization algorithms for WSNs are briefly introduced. The general CRB-based analysis method is also introduced. An CRB-based analytical approach is developed to evaluate two centralized localization algorithms in both single-hop and multi-hop WSNs. The location estimation performance of the two centralized algorithms is compared with that of four distributed localization algorithms. The application of the CRB-based analytical approach to target detection and tracking applications is also discussed.

Chapter 6 concludes the research work and the achievements obtained in this thesis, and identifies several future research directions.

Chapter 2

Architecture of Wireless Sensor Networks

This chapter will provide a background of WSNs for the later research work. Section 2.1 introduces the application and technical driving forces for WSNs. Section 2.2 introduces a typical sensor node architecture and some developed prototypes of sensor nodes. Section 2.3 presents a protocol stack used for target detection and tracking applications. Section 2.4 summarizes the chapter.

2.1 Overview

2.1.1 Technical and Application Driving Forces

Technology is generally shaped and formed by the applications to be supported. This is also true for WSN technologies, as it is thought as a technology-driven development in some extent [3]. In this subsection, the technical driving forces for WSNs will be analyzed.

Military Applications

Like many other innovative network technologies, e.g. the Internet and mobile ad hoc networks, WSNs were also designed and developed for military applications [2]. The importance of WSNs lies in their excellent capabilities of measuring and collecting battlefield information. In battlefields, being discovered equals being destroyed. If the enemy's information such as vehicle, weapon and troop statuses can be closely monitored, the information can be used to assist in determining the best actions. Dominant advantages can, therefore, be obtained. Due to their advantages of passive and close monitoring, no human exposure, self-organization/self-healing, high spatial/temporal resolution and fault-tolerance, WSNs have become a critical part of military command, control, communications, computing, intelligence, surveillance, reconnaissance, and targeting (C4ISRT) systems [2].

Early military application of wireless networked sensors dates back to the 1970s. The Air Delivered Seismic Intrusion Detector (ADSID) system was used by the US Air Force in the Vietnam war [25]. Each ADSID node was about 48 inches in length, 9 inches in diameter, and 38 pounds in weight. The ADSID nodes were equipped with sensitive seismometers, and planted along the Ho Chi Minh Trail to detect vibrations from moving personnel and vehicles. Each node directly transmits sensed data to an airplane, over a channel with unique frequency. Although the ADSID nodes were large and their lifetime was only a few weeks, the system successfully demonstrated the concept of WSNs.

In the 1990s when wireless technologies and low-power VLSI design became feasible, large-scale embedded WSNs for dense sensing applications started to be investigated. Such WSNs can play more important roles. Examples of applications include monitoring of friendly and enemy forces; equipment and ammunition monitoring; targeting; and nuclear, biological, and chemical attack detection [25].

The future wars can be even described as wars of WSNs. By deploying WSNs with various sensors in critical areas, enemy troop and vehicle movements can be tracked in detail. Sensor nodes can be programmed to send notifications whenever movement through a particular region is detected. Unlike other surveillance techniques, WSNs can be programmed to be completely passive until a particular phenomenon is detected. Detailed and timely intelligence about enemy movements can be relayed, in a proactive manner, to a remote base station for optimal decision-making.

Smart Environment and Ambient Intelligence

Research on WSNs is also driven by the huge markets of smart environment and ambient intelligence [26, 27]. A smart environment is a small world where all kinds of smart devices are continuously working to make inhabitants' lives more comfortable [26]. Here the word smart means the ability to autonomously acquire and apply knowledge, while environment refers to our surroundings. Knowledge about an environment can, therefore, be acquired and applied to adapt to its inhabitants in order to improve user experiences in that environment. It represents the next step of automation of building, utilities, industrial, home, shipboard, and transportation systems.

The desire to create smart environments has existed for decades, motivated by the dream that the space around us could adapt to our needs and intentions, and ideally, the environments that we live in were able to commune with us [27]. Then our lives could be much simpler and we would be more productive. The dream will, however, become a reality only with advances in such areas as pervasive computing, machine learning, and wireless sensor networking. The smart environment relies first and foremost on multiple sensors of different modalities in distributed locations. The smart environment needs information

about its surroundings as well as about its internal working. There are numerous challenges in detecting relevant quantities, monitoring and collecting data, assessing and evaluating information, formulating meaningful user displays, and performing decision-making and alarm functions [26]. There is an urgent need for distributed WSNs, that are responsible for sensing as well as for the first stage of processing hierarchy, to provide the information needed by smart environments.

Similar to smart environments, Ambient Intelligence has also been investigated to provide design criteria for an intelligent infrastructure [27]. The word intelligent means not only because it can interpret actions and intentions, but also because it can change our environment to help us with transparent solutions. It is a term that was introduced by the European Community to identify a paradigm by equipping environments with advanced technology and computing to create an ergonomic space for occupant users [27]. The paradigm of Ambient Intelligence is wider in scope, even though some of the ideas were inspired by the smart room concept [27]. Smart Rooms were introduced to offer a new solution to the human-machine interface problem.

The Ambient Intelligence can be realized only through a number of technologies, all involving modern computing hardware and software. In particular, an Ambient Intelligence system also requires the use of distributed sensors and actuators to create a pervasive technological layer, which is able to interact transparently with a user. The interaction can be not only passive by observing and trying to interpret what the user actions and intentions are, but also active by learning the preferences of user and adapting system parameters to improve the quality of life and work of the occupant.

Ubiquitous Computing and Networking

From another aspect, research on WSNs can be thought to be motivated by the desire to exploiting the capabilities of ubiquitous computing and networking integrated in small size devices.

Since the beginning of last century, telecommunications have experienced considerable changes, from traditional telephony-oriented services to data-based services; from homogeneous to heterogeneous networks; from non-intelligent devices to smart handhelds, PDAs, and mobile computers. To enable the growth in these expanding markets, computing anywhere, anytime, and personalized mobile computing (ubiquitous computing) have been envisioned as two targets for the evolution of telecommunications and computing field. The primary goal of ubiquitous computing is to embed small and highly specialized devices within the everyday environment so that they operate seamlessly and become transparent to the person using them.

To enable ubiquitous computing and communication in an evolving, heterogeneous network, a critical need is of wireless appliances and network devices with integrated computing and communication capabilities. Next generation wireless network must provide flexible network access and bit rates, and both local and wide area coverage. The heterogeneous infrastructure of next generation wireless network will comprise different wireless access systems, ranging from current cellular systems with nomadic wireless-access systems to personal-area networks (PANs): cellular networks of Global System for Mobile Communication (GSM) (called 2G) [28,29], to its extension General Packet Radio Services (GPRS) (called 2.5G) [28, 29], and third-generation (3G) wireless systems with full coverage [30]; IEEE 802.16 standard based wireless metropolitan area networks (WMAN) for higher data rate and larger coverage area [31]; IEEE 802.22 standard based wireless regional area network (WRAN), which would operate in VHF/UHF spectrum

below 900MHz for unlicensed devices [32]; IEEE 802.11 standard based wireless local area networks (WLAN) in organizations and home use due to its flexibility and facilities [33, 34]; and IEEE 802.15 standard based wireless personal network (WPAN) [35].

Integration of wireless appliances and infrastructure devices with ubiquitous computing and communication capabilities will enable a new era of mobile and wireless information technology. A wide range of esoteric applications come to mind, in order to exploit the benefits from the capabilities. An example is the data-centric WSN. Different from the general telecommunication network-centric wireless networks, the major tasks of WSNs are monitoring the physical world and sending measurement data to the sink for further processing and control. The abilities of WSNs communicating with the physical world make them take a position in the future 4G networks [30]. A coarse description of the relationship of WSNs with other types of wireless networks is illustrated in Figure. 2-1.

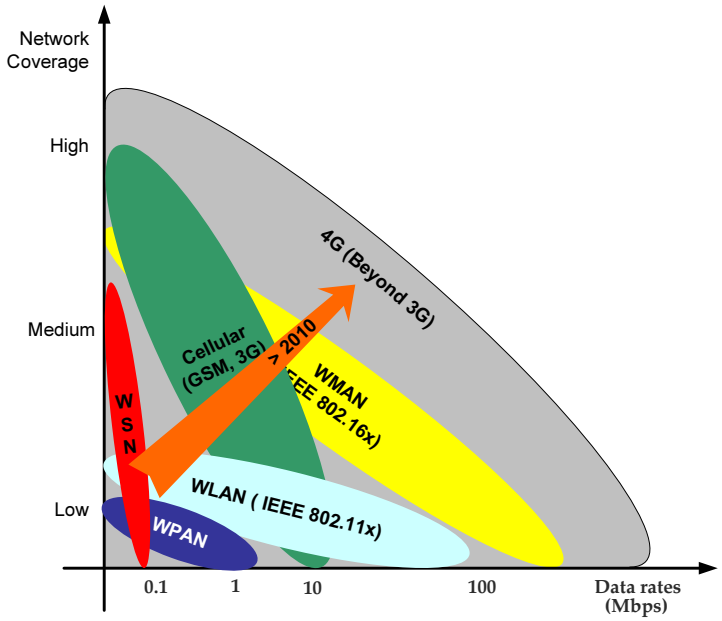

Figure 2-1: Coexistence of WSNs and other wireless networks. Various existing wireless technologies will fuse to 4G services with increase in data rate and mobility.

It is noted that WSNs are also quite different from the current wireless mobile networks, e.g. cellular network, WLAN, WMAN, and WPAN. Compared with these wireless networks, WSNs have many more nodes in a network, and the transmission range is much shorter, typically around ten meter. In addition to being tiny in size and low in cost, wireless sensor nodes have low mobility. Due to low event rate and limited memory storage and processing capabilities, WSNs have small packet size (on the order of hundreds of bits) and may have very low application data rate (e.g less than 1 Kbps). Unlike other wireless networks that the traffic flow is usually bidirectional or down-link, the traffic in WSNs is mostly up-link from sensor nodes to information sink. In addition, since battery lifetime is crucial, the power consumption of sensor nodes is kept much lower. Due to large scale and high density, WSNs also have more inherent redundancy and can get higher level of reliability. The characteristics of WSNs and other wireless networks are compared in Table 2.1.

Table 2.1: Comparison of WSNs and other wireless networks

Characteristic	Cellular	WLAN	WMAN	WPAN	WSN
Number of nodes	large	small	medium	small	very large
Communication range	long	medium	long	short	short
Mobility	high	medium	high	low	low
Data rate	medium	high	high	medium	very low
Power consumption	high	medium	high	low	very low
Redundancy/Reliability	low	low	low	low	high

2.1.2 Enabling Techniques

Although the early application of WSNs dates back to the 1970s, the major research and development of WSNs started in the 1990s only with the advances in hardware techniques, wireless communication and networking, and digital signal

processing [25].

Hardware Techniques

The critical factors needed for WSNs to achieve success and advantages include size and cost of individual sensor nodes, capabilities of computing and communication, and power consumption. There are several techniques which have driven WSNs to achieve these advances.

The first technique advance is on System-on-Chip (SoC) technology, which is capable of integrating complete systems on a single chip. Commercial SoC based embedded processors from Atmel, Intel, and Texas Instruments have been used for sensor nodes [25]. By integrating complete systems on sensor nodes, all the necessary functions to construct a large-scale WSN can be implemented in single sensor node, while the size, cost, and power consumption can all be controlled and significantly reduced.

The second technique advance is on commercial radio frequency (RF) circuits [25]. Current commercial RF circuits products can enable short distance wireless communication, while consuming extremely low power. The commercial radios can usually achieve a data rate of tens to hundreds of Mbps or even higher, while consuming less than 20 mW of power for both packet transmission and packet receiving [25]. Single sensor node can, therefore, work for several months and even several years without recharging. This is critical for large scale WSNs, where human based power recharging is almost impossible.

The third technical advance is from MEMS technology, which is now available to integrate a rich set of sensors onto the same CMOS chip. Commercially available sensors now include thermal, acoustic, and seismic sensors, accelerometers, and chemical and biological transducers [25]. These sensors can be used in a broad range of applications, including acoustic ranging, motion tracking,

vibration detection, and environmental sensing. The sensing capabilities of an individual sensor node can, therefore, be largely enhanced, while the size, cost and power consumption can be reduced at the same time.

The above technologies, together with advanced packaging techniques, have made it possible to integrate sensing, computing, communication, and power components into a small-sized sensor node.

Wireless Communications and Networking

Besides hardware technologies, the development of WSNs is also enabled by the advances on wireless communications and networking [25]. In the early research and development effort on WSNs, IEEE 802.11 protocols was the standard specified for the physical and MAC layers due to the wide availability and low cost of 802.11 products. Although 802.11 protocols offer high data rate, the complex protocol operations and high power consumption make them not suitable for WSNs. Some research effort has been motivated to design energy efficient MAC protocols to satisfy the requirements of WSNs. The 802.15.4-based ZigBee protocol is one of the outcome of the research effort, which has been released and is specifically designed for short range and low data rate WPAN [35, 36]. Its applicability to wireless sensors has been supported by several commercial sensor node products such as MICAz [37].

In addition to the advances in wireless communications, the advances in wireless networking techniques are also important for WSNs. Due to the requirement of low power consumption and long lifetime for WSNs, short-range communication is one of the design principles for WSNs. In a large scale WSN, direct communication between wireless sensor nodes and the sink may not be achievable in general. Multi-hop routing protocol is, therefore, a necessity to connect the individual sensor nodes and make them work as a whole in this case. Although

the early routing protocols proposed for mobile ad hoc networks (MANET) can be used for the purpose of networking nodes in WSNs, these protocols are designed for application-centric networks, with reduced power consumption constraints and without consideration on the specific communication patterns in WSNs, therefore, are hardly applicable to WSNs. Dense research effort has been made on designing energy efficient and robust routing protocols tailed for WSNs. Widely known routing protocols include Direct Diffusion [38] and LEACH [39].

Digital Signal Processing

Due to economic consideration on the size and cost of sensor nodes, single sensor node is generally severely constrained in sensing, power, computation, communication, and storage [2, 25]. For target detection and tracking applications, the measurement data sent from a sensor node to the sink may be lost during the delivery, or may be insufficient to achieve the expected detection reliability. It is necessary for a certain number of sensor nodes to work jointly and use advanced digital signal processing techniques to detect the occurrences of targets even in harsh signal to noise situations.

On the other hand, in the raw data collected by sensor nodes from the environment, only useful information is of importance. It is desirable to process the raw data locally at the sensing nodes and send back only processed data to the sink, in order to save energy consumption in sending large volume of raw data. Due to the weak sensing and processing capabilities of each individual node, signal processing is often required to be performed by a set of sensor nodes. Such signal processing techniques will be very beneficial for target detection and tracking applications in WSNs. The advances in digital signal processing, especially collaborative signal processing, enable developing more energy and bandwidth efficient protocols for WSNs [25]. For example, sensor readings are usually imprecise due

to strong variations of the monitored entity or interference from the environment. Information fusion can be used to process data from multiple sensor nodes in order to filter noisy measurements and provide more accurate interpretations of the information generated by a large number of sensor nodes. Other techniques, including DSC, data aggregation, Kalman filtering, Bayesian inference, time synchronization, and localization are also applicable to WSNs [25]. The advances in digital signal processing algorithms can efficiently reduce bandwidth and power consumption, and significantly extend network lifetime.

2.1.3 Applications

The above described specific features ensure a wide range of applications for WSNs, including industrial, environmental, health care, military, home and commercial areas [40–52]. Next, some civilian applications of WSNs will be introduced.

Industrial applications: In industrial manufacturing plants, equipment performance is critical. Currently manual monitoring is used to predict failures and schedule maintenance or replacement to avoid costly manufacturing downtime. Instead of manual monitoring, WSNs can be used to increase equipment performance through continuous monitoring, and lower installation and maintenance costs. Besides equipment maintenance and calibration, wireless sensor nodes can be used for machine health monitoring [40]. WSNs can continuously collect information such as pressure and motion, provide full visibility of vital machines, and allow end users to quickly diagnose conditions, identify problems that might otherwise disrupt production, and take corresponding actions.

In process control, essential information collected by sensor nodes can be used to control industrial processes, real-time monitor production and direct

activities without human intervention [41]. A quick response to changing conditions is enabled by identifying significant variations in operational performance, determining original causes, and making corrections to meet production goals. For example, in a chemical processing plant, the information on temperature, chemical concentration and pressure may be collected by a WSN and used to adjust the amount of a particular ingredient or change the heat settings.

Environmental applications: WSNs embedded in a natural environment enable the collection of long-term data for both microscopic and macroscopic physical phenomenon on a large scale and high resolution that are previously unattainable. Obtaining localized and detailed measurements in a wide area becomes possible, based on which some environmental applications have been envisioned for WSNs, such as precision agriculture [42], forest fire detection, habitat monitoring, animal tracking, and disaster relief.

Take forest fire detection as an example of environmental application. The FireBug project at the University of California Berkeley (UC Berkeley) has used a sensor network to monitor a controlled burn in a forest park in California [43]. Currently, the detection of forest fire is usually based on satellite monitoring, but the high cost, low resolution of satellites and long scan period restrict the effectiveness of traditional method. Moreover, satellites cannot forecast fires before they spread uncontrollably. Figure 2-2 shows a scenario of forest fire detection with the help of a WSN. Wireless sensor nodes deployed in a forest self-organize into networks to collect real time data in wild environments, such as temperature, humidity, smoke, barometric pressure, and windy speed [44]. The collected raw data can be potentially used to predict the behavior of a fire. When a fire starts in a forest, WSNs

not only can accurately locate the fire disaster and report to the command center, but also can track the fire and predict the future path of the fire. This would help save fire fighters' lives and also improve the effectiveness of fire rescue.

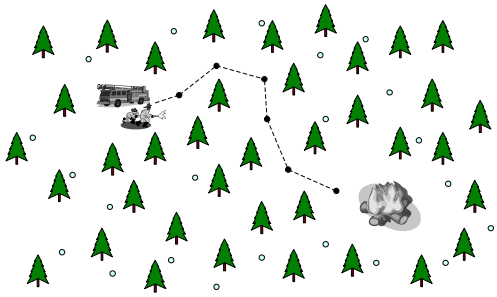

Figure 2-2: Application of WSNs for forest fire detection.

For scientific research, WSNs have also been applied in habitat monitoring to allow researchers to obtain detailed measurements of wildlife ecological environment in a non-intrusive and non-disruptive way. Scientific studies of ecological habitats, including animals, plants, and microorganisms, are traditionally conducted by hand by field investigators. The presence and potentially intrusive activities of human being may affect the behavior of organisms in the monitored habitat, especially for the species sensitive to human being, thus lead bias into the observed results. This is usually referred to as "observer effect". WSNs, on the other hand, provide a cleaner, remote-controllable approach to habit monitoring. WSNs can be deployed prior to habitat monitoring, and after that they require no maintenance. The impact on the wildlife being monitored will, therefore, be minimal. Furthermore, large scale and highly dense WSNs can benefit scientific research by providing rich experimental data. One of the earliest WSN deployments for habitat monitoring is on Great Duck Island by researchers at UC Berkeley, to monitor the nesting burrows of Leach's Storm Petrels [45].

Other ecological application examples include the PODS project at University of Hawaii, James Reserve project at UCLA, and ZebraNet project at Princeton University [46–48].

Health care: Wireless sensor nodes can be deployed to improve people's health and quality of life while reducing overwhelming health care bill. For example, monitoring the activities of elders is an important aspect of eldercare, but the traditional monitoring can be intrusive for the elder and exhausting for the caregiver. The researchers in Intel Research Seattle at University of Washington have developed a Caregiver's Assistant based on wireless sensors to detect the activities of an elder without requiring direct observation by a caregiver, which allows the caregiver to focus on the quality of care rather than tedious tasks [49]. In another medical application, sensors are sent into the body of a patient to take pictures and produce a global view of an infected organ. This makes it possible for doctors to inspect the infected organ without surgery. The information can also be used in a robot-aided surgery to control a robot arm.

Furthermore, recent advances in WSNs have made a significant impact on current e-health and telemedical systems, and impelled the emergence of pervasive mobile health care. Patients with wearable or implanted wireless sensors can be monitored at home or outdoors, for not only physiological signals such as heart rate and blood pressure, but also physical activities such as movement and fall. Sensors can network and communicate wirelessly, and collaborate to give the patients' accurate position and report raw sensor data to the control center. Then the control center can use the raw sensor data to detect the patients' health status in a real time manner, which can therefore assist in monitoring and diagnosing patients, sending alerting messages and deploying emergency services if necessary.

Home and commercial applications: WSNs can also be widely applied in home and commercial areas. Some typical applications include structural testing and energy conserving in intelligent buildings, seismic monitoring in bridges, traffic monitoring on roads, and inventory control in warehouses [50–52].

For example, WSNs can be used to monitor power usage, lighting levels and room temperature in intelligent buildings. Researchers at UC Berkeley have designed a WSN for commercial lighting control, based on some artificial intelligence techniques [52]. With the information provided by WSNs, the central controller can have a better understanding of the energy consumption distribution throughout the building and accordingly control the power usage to save energy. This would be very helpful in areas suffering from a power supply shortage. By placing wireless sensor nodes along highways, police will have real-time and more detailed monitoring of traffic flow and better control of stoplights. In the case of traffic jams, motorists can even be informed of alternate routes by the wireless sensor nodes along roadside.

2.2 Architectures of Wireless Sensors Nodes

During the last few years, many different versions of wireless sensor nodes, commonly known as motes, have been designed and built by various universities and research labs. This section will introduce the typical sensor node architecture and some developed sensor node prototypes.

2.2.1 Schematic of Wireless Sensor Node

A typical wireless sensor node is usually made up of five major components: sensors, microprocessor unit, memory, radio transceiver, and energy supply, as

shown in Figure 2-3 [2]. In what follows, each key component will be introduced in detail.

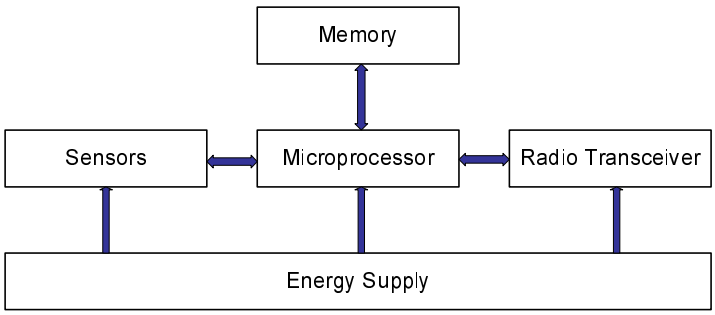

Figure 2-3: Schematic of a typical wireless sensor node.

- **Sensors:** Due to the constraints of bandwidth and energy/power supply in WSNs, wireless sensor nodes mainly support sensing at a low data rate. Since many WSN applications require multi-modal sensing of the environmental phenomena, each sensor node may have more than one sensor on board. Depending on the specific applications that the WSN is deployed for, sensors installed on board may include temperature sensors, heat sensors, humidity sensors, light sensors, chemical sensors, pressure sensors, barometers, accelerometers, magnetometers, acoustic sensors, or even low resolution cameras. Sensors are generally associated with analog-to-digital converters (ADC), which convert the analog signals produced by the sensors to digital signals that are suitable for operation in the processing component.

- **Embedded microprocessor:** The computational tasks on a wireless sensor node are accomplished by a embedded processor, which processes both locally sensed information and data for communication with other sensor nodes over wireless networks. Due to the size, energy and production cost constraint of wireless sensor node, low-power embedded

microprocessors are used. These microprocessors have limited computational speed and processing capability, which put constraints on the operating systems, software, and middleware that they can run. Accordingly designed are the component-based embedded operating system TinyOS [53] and the query processing system TinyDB [54].

- **Onboard memory/storage:** Wireless sensor node has a small storage component onboard, in the form of random access memory (RAM) and read-only memory (ROM). This includes both data memory, to store raw and processed sensor measurements and other local information, and program memory, from which embedded microprocessor reads and executes instructions to carry out the assigned sensing tasks. The size and cost constraint of wireless sensor nodes also results in the limited quantities of memory and storage onboard. However, given Moore's law, future wireless sensor nodes may each possess more memory.

- **Low-power radio transceiver:** Wireless sensor node has a low-rate, short-range radio transceiver for wireless communication with each other. Because of constraint in processing capability and power, the data rate of transceivers on sensor nodes is currently limited to about 200 Kbps, and the communication range is limited to tens of meters. However, the capabilities of these radio devices are likely to improve over time, including the improvements in cost, tunability, spectral efficiency, and immunity to noise, fading, and interference. Since radio communication is usually the dominant factor in power consumption in a wireless sensor node, the radio transceiver must incorporate energy efficient modes such as sleeping and waking up.

- **Energy supply:** One of the most important components on a wireless sen-

sor node is the energy supply. For flexible deployment wireless sensor nodes are battery-powered. Usually the power usage on a sensor node is dominated by radio transmission and reception, while sometimes the microprocessor uses large amount of power to do complex computation such as encryption. Moore's law indicates that the transistor density of integrated circuits doubles every 24 months, but battery technology has far lagged. Energy capacity decreases as battery gets smaller. Although power scavenging techniques such as solar cells may provide energy renewal in some cases, the finite battery capacity is still the scarcest resource in wireless sensor nodes and results in corresponding constraints in computational speed and processing capability in most WSN applications.

2.2.2 Example Wireless Sensors

Within academic community, the mote platform developed at UC Berkeley has become the standard for research on mote prototype and deploying new WSN applications. At UC Berkeley, researchers in the long term project "Smart Dust" focus on developing millimetric-sized sensor nodes [1, 2]. Using commercial-off-the-shelf (COTS) components, the prototypes of mote, called macro motes or COTS Dust, were developed and built in a short time. COTS Dust have all the basic functions of Smart Dust, but the devices are a cubic inch instead of a cubic millimeter in size. They were used as a platform to run various algorithms to test the behaviors that Smart Dust would present.

Figure 2-4 shows the evolution of the Berkeley mote platforms, from the earliest COTS Dust to the up-to-date Spec mote. This involves the advances in miniaturization, integration, and energy management. RF mote is an early mote version of COTS Dust using an RF transceiver to communicate wirelessly. Its

successors, Mini mote and weC mote, are smaller versions of RF mote. weC mote is also more computationally powerful and supports remote reprogramming over a wireless link. In order to manage the different functions on board, motes family use TinyOS, a compact and simple event-based operating system [53, 54]. It is after the introduction of weC mote that began the development of TinyOS at UC Berkeley.

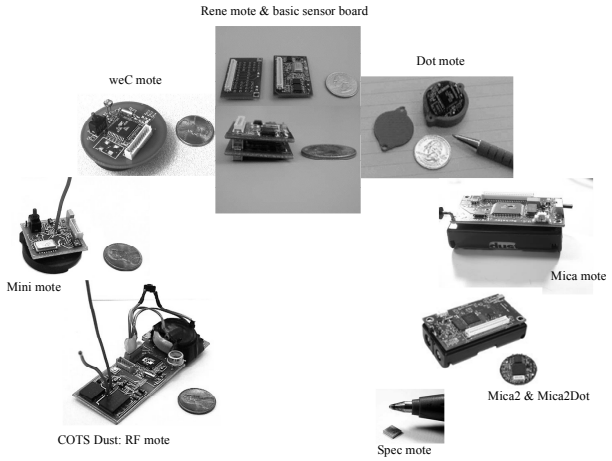

Figure 2-4: Evolution of Berkeley mote platforms: from COTS RF mote to Spec, chronologically ordered in clockwise direction.

Rene mote is the first generation commercial mote platform manufactured by Crossbow Technology. Based on a modular design, it is built by stacking a main processor-radio board and one or more basic sensor boards through a 51-pin sensor board interface. It allows sensor expansion and enables various applications. Dot mote is architecturally the same as Rene but shrinks into a one-inch-diameter circular platform. Mica mote is the second generation commercial mote module. Its architecture has been significantly improved to increase radio performance and memory efficiency. Mica mote then evolved to Mica2 and Mica2Dot, the third generation commercial motes. Compared to Mica mote, Mica2 mote has larger memory storage and more powerful radio communication capabilities. It allows a routing function and supports remote reprogramming over the sensor network.

Mica2Dot mote is a coin sized version with reduced input/output capabilities. The up-to-date most advanced hardware platform is a newer generation mote, called Spec, which is an integrated single-chip CMOS device measuring just 2.5 mm $\times$ 2.5 mm. It represents the complete integrated CMOS vision that wireless sensor nodes will be manufactured for pennies and deployed in millions.

Besides UC Berkeley, there are many other universities undertaking research projects in this area. The developed mote platforms include the micro-Adaptive Multi-domain Power-aware Sensors (μAMPS) and Wireless Integrated Network Sensors (WINS) by UCLA, the BTnode by ETH Zurich, and the Embedded Sensor Board (ESB) by FU Berlin.

In industrial community, a lot of companies including Intel, the leader in semiconductor manufacture, are participating in the design and development of novel motes and WSN applications. The aim of the "Intel Mote" project is to create a new platform design that delivers a high level of integration, ultra low-power operation, and hardware reconfiguration in a single microchip. The project team is focusing on developing a mote with more CPU power for digital signal processing and complex tasks, more reliable radio links, and better security features. Figure 2-5(a) presents the prototype of Intel Mote. Another example of commercial mote platform is the wireless sensor Pod produced by Accsense company. Accsense system consists of multiple sensor Pods, which can measure a wide range of physical phenomena, and a gateway, which can handle up to sixteen Pods and connects to the Internet or a local server. Figure 2-5(b) shows a pair of Accsense Pod and gateway.

2.3 Protocols Stack

In WSNs, each sensor node has the capabilities to sense the environment and route data back to the sink via a distributed multi-hop networking. To ensure

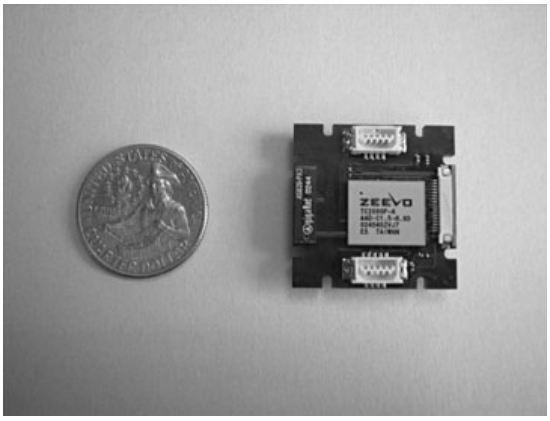

(a) Prototype of Intel Mote, measuring 3mm×3mm

(b) Accsense wireless sensor Pod and Gateway

Figure 2-5: Examples of mote platforms developed by industry.

that all sensor nodes and the sink work as a whole and satisfy the service and network requirements, proper protocols and mechanisms must be designed and deployed. A protocol stack used by the sink and all sensor nodes is given in 2-6 [2, 3]. The protocol stack consists of two planes: data plane and management plane, which combines power and location awareness, and integrates target sensing with networking protocols and energy efficient wireless communication. It also promotes collaborations among sensor nodes [3].

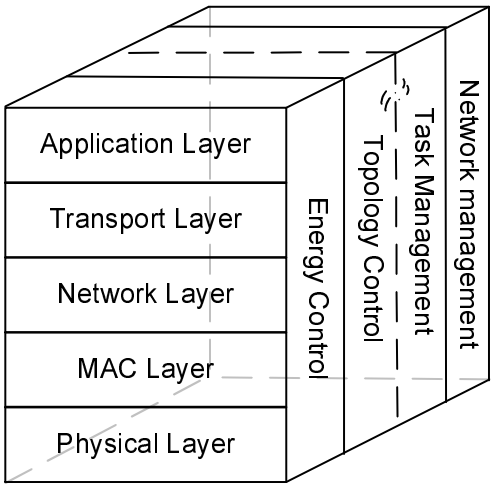

Figure 2-6: Protocol stack proposed for target detection and tracking.

2.3.1 Data Plane

The data plane consists of physical layer, data link layer, network layer, transport layer, and application layer [2, 3]. The functions of these layers will be briefly discussed below.

- The physical layer is mostly concerned with modulation and demodulation of digital data, transmission and receiving techniques. The responsibilities of the physical layer include frequency selection, carrier frequency generation, signal detection, and modulation. It is commonly known that the properties of wireless transmission channel and the physical layer techniques have significant impacts on protocol stack. Thus far, the 915 MHz industrial, scientific, and medical (ISM) band has been suggested for WSNs. The physical layer is, however, a largely unexplored area in WSNs. Open research issues range from power-efficient transceiver design to modulation schemes. Simple and low-power modulation schemes need to be developed for WSNs. Tiny, low-power, low-cost transceiver, sensing, and processing units also need to be designed.

- The data link layer is responsible for multiplexing of data streams, data frame detection, medium access and error control [8]. It ensures reliable point-to-point and point-to-multipoint connections in a communication network. The data link layer includes two sublayers: Logical Link Control (LLC) sublayer and Medium Access Control (MAC) sublayer. The responsibilities of LLC protocol includes error control and flow control. Error control is to ensure transmission reliability by using automatic repeat request (ARQ) and forward error correction (FEC) techniques. The flow control regulates transmission rate to protect a slow receiver from being overwhelmed with data.

  The fundamental task of MAC protocol is to regulate the access of a large number of sensor nodes to a shared wireless medium. It has to achieve the goal of fairly and efficiently sharing of communication resource among sensor nodes. Thus far, both fixed and random access version of MAC protocols have been proposed. The balance of requirements for WSNs is, however, different from that of tradition wireless networks. The requirement of energy efficiency is most important for WSNs, while many classical protocols such as ALOHA and CSMA do not provide schemes to address this requirement. Other typical performance metrics, like throughput, delay and fairness, play a minor role in WSNs, while further important requirements for the MAC protocol of WSNs are scalability and robustness.

- The network layer is responsible for routing data from the transport layer. In large-scale WSNs, special multi-hop wireless routing protocols are needed [9]. As discussed in Section 2.1.2, traditional ad hoc routing protocols do not usually fit the requirements of WSNs. Instead of addressing individual nodes as in traditional routing protocols, data is the focus of interests in WSNs. According to the intended frequency of request-answer interaction,

the protocol solutions proposed to data-centric networking can be classified into two groups [2]. One group contains protocols that target single request single answer interactions, where measurement data is sent back to the sink only for a single request. Sensor Protocol for Information via Negotiation (SPIN) is an example protocol in this group, which is also the first data-centric dissemination protocol for WSNs [55]. Another group contains protocols that target single request multiple answers interactions, where measurement data is periodically sent back to the sink. Example protocols include Directed Diffusion [38] and LEACH [39]. The periodical reading of measurement data makes it beneficial of setting up a routing structure, especially when data aggregation can be used.

- The transport layer helps to maintain data flow and ensure reliable data transport if the applications request it. The tasks commonly attributed to the transport protocols include reliable data transport and congestion control. Reliable data transport requires the ability to detect and repair lost packets. The particular challenges for transport protocols in WSNs are multi-hop networking, stringent constraints regarding power, storage or computation of sensor nodes, and variable network topologies [2]. For target detection and tracking applications, the reliability to be achieved by reliable transport protocols is application dependent. Example reliable data transport protocols include ReInForm using multiple paths for single block delivery [56], PSFQ for block delivery from the sink to sensor nodes [57], and RMST for block delivery from sensor nodes to the sink [58].

  Congestion control requires the ability to detect and react to the situation that more packets are delivered into the network than the network can carry. In target detection and tracking applications, when there are no target detected, the background traffic for network maintenance and man-

agement can be light. After the targets are detected, heavy traffic may be generated and congest the network due to periodic packets generated to report the occurrences and tracks of the targets. Two example approaches proposed for congestion detection and control are the COngestion Detection and Avoidance (CODA) protocol [59] and the Event-to-Sink Reliable Transport (ESRT) protocol [60].

- In the application layer, the services of target detection and tracking can be requested by the sink or the control unit and be provided by sensor nodes. Although there are many application areas defined and proposed for WSNs, the application layer protocols for WSNs remain a largely unexplored region. For target detection and tracking applications, geographic forwarding and geographic addresses can be used and incorporated into the application layer protocols. In addition to data aggregation, DSC, network coding, and other advanced signal processing techniques can be used to help detect targets and reduce energy consumption [5, 13, 14]. DSC is the research focus of this thesis and will be described in more detail in the remainder of the thesis.

2.3.2 Management Plane

The management plane of the protocol stack for target detection and tracking applications is responsible for monitoring the network, coordinating the sensing task, and lowering the overall power consumption. These responsibilities can be accomplished through the cross-layer management of energy consumption, topology control, collaboration, task management and other functions.

- The energy control function manages how a sensor node uses its power [2,16]. Different layers of the data plane can be involved. For example, in the MAC sublayer, sensor node can be controlled and scheduled to turn on

and turn off its receiver for listening to the channel for messages from its neighbors. In the network layer, if a sensor node observes its power level low, it can broadcast a message to its neighbors that it cannot participate in routing messages due to the low power level. In the transport layer, the number of active sensor nodes participating in sensing the environments should be minimized in order to reduce energy consumption while achieving the expected coverage and sensing reliability.

- For the application of target detection and tracking, certain geographical areas are required to be monitored [17]. Topology control is important with two most concerned functions: network deployment and control of active sensor nodes [14, 18, 20, 116]. In network deployment, the challenge is how to deploy sensor nodes in order to cover the given geographical areas with a certain density of sensor nodes. The expected network lifetime should be taken into account in the problem of network deployment. The control of the number of active sensor nodes is required to balance the requirements between energy consumption and target detection reliability. Given the deployment and survival of sensor nodes, the challenge is how to schedule the active periods of sensor nodes. It can be observed that the topology control function has a close relationship with the energy control function. For data-centric networks, they may be designed together in order to achieve the optimized performance.

- The task management plane is concerned with the problem of disseminating interest and data, in addition to the problem of scheduling sensing task by sensor nodes [2]. One approach to the first problem is sending interest by users, on a certain attributes (e.g. locations) or on a triggering event, to the WSN. Another approach can be advertising the available data at sensor nodes to users, followed by the interested users sending out queries

about the data. Task management protocols are useful for the operations of different data plane protocols. Sensor Query and Data Dissemination Protocol (SQDDP) is a task management protocol proposed with interfaces to issue queries, respond to queries, and collect incoming replies [2].

- For a large-scale WSN, it is important to monitor network status, such as power status, the number and locations of survival sensor nodes. Simple Network Management Protocol (SNMP) is used for the purpose of network management in traditional networks. However, as sensor nodes in WSNs do not have global IDs and are usually infrastructureless, sensor node can only be accessed by using attribute-based naming or location-based addressing. Sensor Management Protocol (SMP) is designed for sensor network management, which provides the operations needed to perform administrative tasks: for example, introducing the rules related to data aggregation, sensor naming and clustering; exchanging the data related to location finding algorithms; time synchronization; querying network configuration and node status; reconfiguring sensor network; authentication and security in data communication [2].

2.4 Summary

This chapter has introduced the relevant background of WSNs for the research work in subsequent chapters. The architecture and overall protocol stack of WSNs are presented. For general target detection and tracking applications, most of the data plane and management plane functions are necessary and will be required to satisfy the services and network requirements. There are still many research challenges. As an application layer technique that can help improve target detection and energy efficiency, DSC is an important technique for WSNs while is

also a challenging problem which has not been solved by research to date. The subsequent chapters of this thesis will focus on practical DSC schemes for WSNs, with consideration on bandwidth, energy, location, and network management. The overviews of DSC and sensor localization for WSNs are, therefore, not given in this chapter but will be given in Chapter 3 and Chapter 5, respectively.

Chapter 3

Distributed Source Coding Scheme

3.1 Introduction

As introduced in previous chapters, due to the limited power, processing capability and network bandwidth in large-scale WSNs, bandwidth and energy efficient schemes are required in the design of algorithms and protocols. Distributed source coding (DSC) is one such scheme. Recently, the application of DSC to remote target location and tracking in WSNs has received much attention.

DSC was proposed and studied in the 1970s, to compress correlated sources without intercommunication between the sources. It has, therefore, the potential to save bandwidth and energy for the applications of target location and tracking in WSNs in which multiple sensor nodes may detect a target and send correlated sensor readings to an information sink for joint decoding. By exchanging the computational complexity of the encoder for the decoder, DSC transfers the burden of computing and processing from sensor nodes to the sink. The low-complexity encoder is critical for prolonging the lifetime of a wireless sensor node since sim-

ple encoding operations consume low battery energy. DSC compresses multiple correlated sensor readings in a distributed way, while reducing the consumption of network bandwidth and transmission power as well as the probability of packet collision network. Although many data aggregation techniques have been proposed to compress identical or nearly identical sensor readings transmitted through a sensor node in the transmission paths, they do not work when the readings are correlated instead of being identical. Moreover, different readings may be transmitted to the sink over different paths. DSC becomes, therefore, an important alternative approach to data compression in WSNs.

Prior work on the application of DSC in WSNs has focused on information-theoretic aspects such as achievable rate-distortion regions, although some existing work has addressed the construction of distributed source codes. Challenges remain, however, in the design of practical DSC schemes which can efficiently construct and utilize side information in order to compress sensor observations. This chapter proposes a simple and efficient random-binning based DSC scheme for application to remote source estimation in WSNs. The scheme jointly encodes data from multiple sensor nodes with side information. It achieves high coding efficiency and reduces power and bandwidth consumption.

The rest of this chapter first gives an overview on the fundamentals of DSC and discuss the current state of the art on the applications of DSC in WSNs. Based on the overview, Section 3.3 formulates the problem and introduces the general DSC scheme. Section 3.4 proposes a random-binning based DSC scheme, including the encoding method, control of the coding rate, and the decoding method. Its decoding performance is also analyzed. In Section 3.5 the simulation method and simulation results for the proposed random-binning coding and the DSC source estimation scheme are presented and discussed. Section 3.6 summarizes the chapter.

3.2 Related Work

3.2.1 Fundamentals of DSC

A paper on the noiseless coding of correlated information sources written by Slepian and Wolf in 1973, formulated what has become known as the Slepian-Wolf theorem and encapsulated the fundamental concept of DSC [61]. The paper considered the problem of coding two correlated sources when constraining the encoder of each source to operate without knowledge of the other source. The decoder, however, has available both encoded binary messages. To ensure accurate reconstruction of both sources by the decoder, the admissible coding rate region is given. The principal theorem and main results are briefly introduced below. For a more detailed description and proof on the theorem, the reader is referred to [61].

Suppose X and Y are a pair of correlated discrete random variables with the joint probability distribution of $p_{XY}(x, y)$. Two correlated information sequences $X_1, X_2, \ldots, X_n$, denoted by $\boldsymbol{X}$, and $Y_1, Y_2, \ldots, Y_n$, denoted by $\boldsymbol{Y}$, are composed of n independent sample pairs of the correlated variables. $\boldsymbol{X}$ and $\boldsymbol{Y}$ can also be regarded as two corresponding blocks of n-characters produced by two correlated information sources. The admissible rate R is defined as for every $\varepsilon > 0$ there exists an encoder-decoder pair with coding rate R such that the probability of error in decoding of the source is less than ε.

For the independent decoding of both encoded sequences, [61] showed that, irrespective of whether the two correlated sources are encoded independently or not, the admissible rate region $\mathcal{R}$ is the same, bounded by the entropies of the two sources $H(X)$ and $H(Y)$, which are determined by the marginal distributions of X and Y, i.e. $p_X(x)$ and $p_Y(y)$, respectively. The admissible rate region for these cases is shown as the dotted region in Figure 3-1.

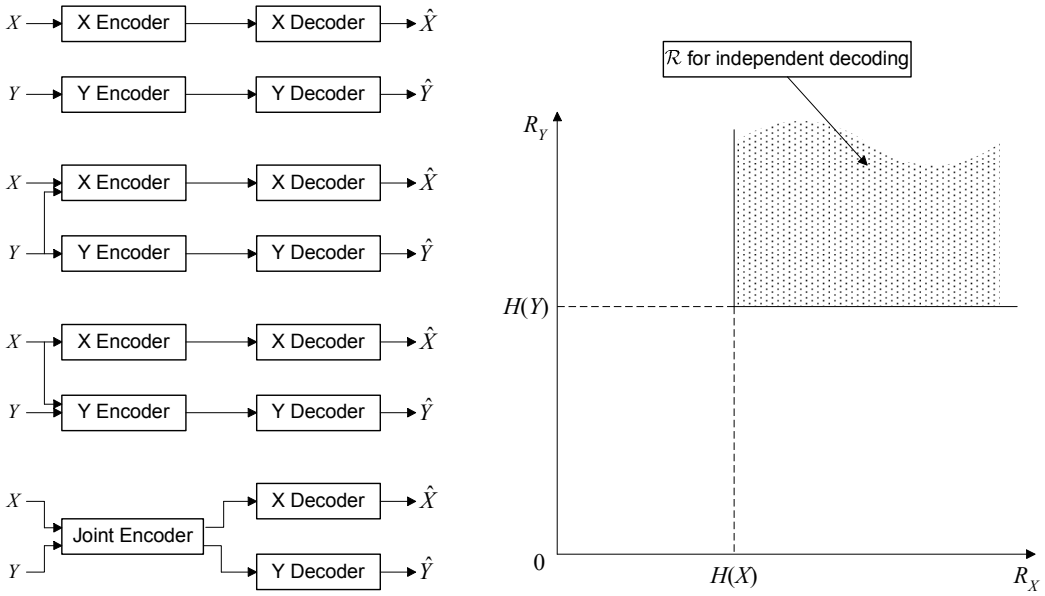

Figure 3-1: Admissible rate region $\mathcal{R}$ for independent decoding cases: always bounded by the entropies of two sources.

When the two correlated sources are encoded independently while both encoded sequences are decoded jointly, [61] proved that the admissible rate region $\mathcal{R}$ is bounded by two conditional entropies, $H(X|Y)$ and $H(Y|X)$, and a line giving $R_X + R_Y = H(X,Y)$, where $H(X,Y)$ is the joint entropy of two sources X and Y. The admissible rate region for this case, shown in Figure 3-2, has one more striated region compared to the admissible rate region for independent decoding cases.

There is an important part of $\mathcal{R}$ in Figure 3-2, i.e., the line segment $\overline{\text{AB}}$ connecting point A and point B. Point A represents $R_X = H(X|Y)$ and $R_Y = H(Y)$, whilst point B represents $R_X = H(X)$ and $R_Y = H(Y|X)$. Slepian and Wolf proved in their work [61] that this line segment is always a part of the boundary of the admissible rate region for joint decoding cases, irrespective of whether the two correlated sources are encoded independently or not. This shows that, for the joint decoding cases, when assigning coding rate R_X and R_Y using the points on the line segment $\overline{\text{AB}}$, even if the two sources are encoded

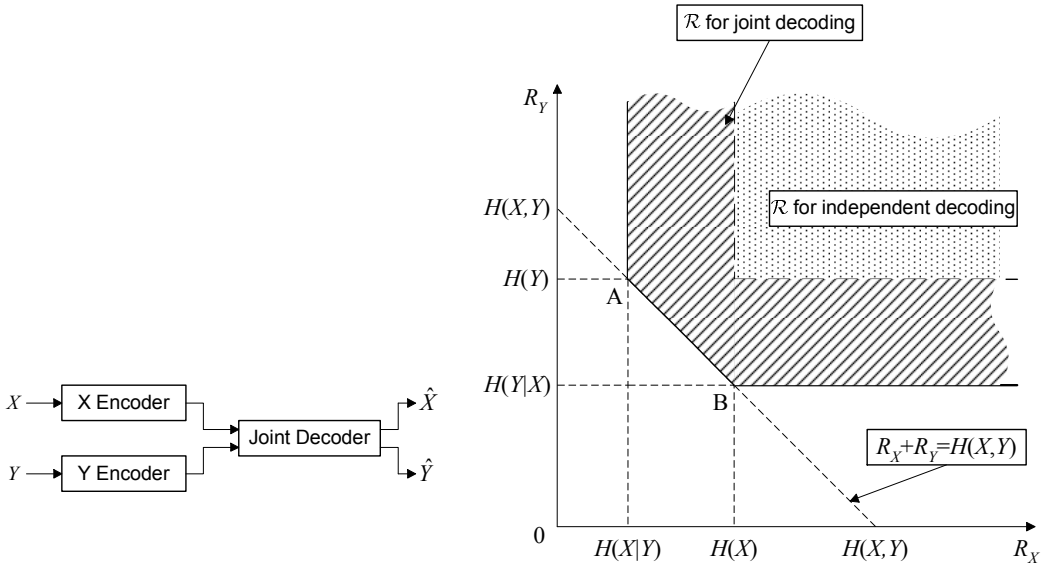

Figure 3-2: Admissible rate region $\mathcal{R}$ for independent encoding and joint decoding case: bounded by two conditional entropies and a line, larger (striated region) than $\mathcal{R}$ for independent decoding cases.

separately, the same coding performance can be achieved as if they are encoded jointly. Among the points on $\overline{\text{AB}}$, point A is often used for the application of DSC, as shown in Figure 3-3. If the encoder of source X does not know source Y, X can still be compressed using only $H(X|Y)$ bits. This is the same as the case when the encoder of X knows Y. Here the uncompressed source Y is usually deemed as the side information for DSC. The cost is, as indicated in [61], a somewhat more complicated decoder for X.

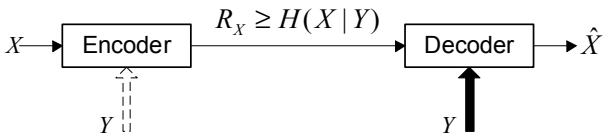

Figure 3-3: Application of Slepian-Wolf theorem to DSC: the dashed and hollowed arrow for Y at the encoder means the same effect with or without knowledge of Y at the encoder.

The proof of the Slepian-Wolf theorem is based on typical sequences (see [62]) and random-binning. As a key concept of DSC, random-binning partitions the

space of all possible outcomes of a random source into disjoint subsets or bins [63]. To encode a realization of the source, the index of the subset, instead of the index of the outcome, is sent to the decoder. The side information Y at the decoder helps determine the outcome in the subset and thus reconstruct the source X. Figure 3-4 illustrates the encoding and decoding processes of random-binning based DSC.

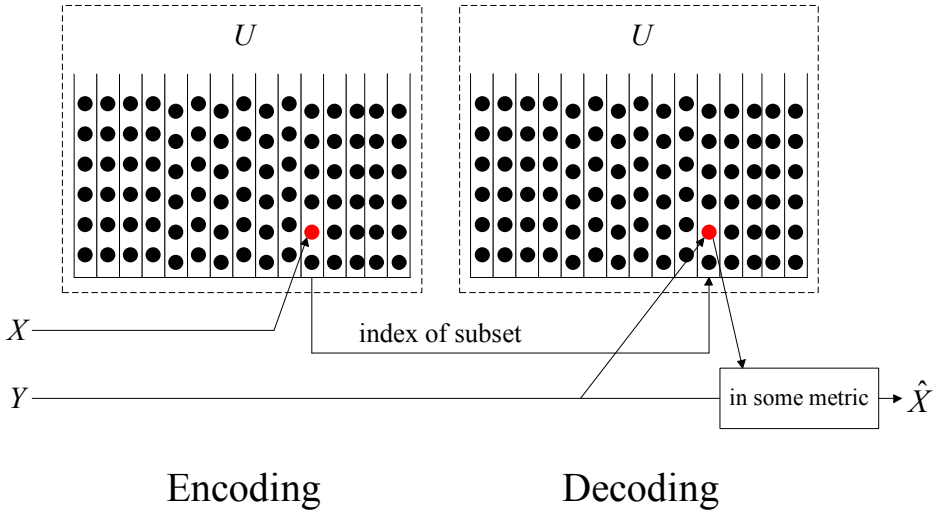

Figure 3-4: Encoding and decoding of random-binning based DSC: U is the outcome space of the source. The decoder finds the outcome of the source in the subset with the help of the side information Y.

Following is a simple example of random-binning [65]:

Suppose X and Y are equiprobable 3-bit binary words correlated in the sense that the Hamming distance between X and Y is no more than one. To encode X by random-binning, the outcome space of X is partitioned into 4 disjoint subsets: {000,111},{001,110},{010,101},{100,011},composed of pairs of words whose Hamming distance is three. If Y is available to the decoder, the index (2 bit) of the subset where X belongs to is sent to the decoder. Since Y is known to be within Hamming distance 1 of X, the decoder can resolve the uncertainty by checking which word in the subset is closer in Hamming distance to Y and declar-

ing it as the value of X. This compression is possible even if Y is not available to the encoder.

In 1976 Wyner and Ziv extended the Slepian-Wolf theorem to the case of lossy coding of continuous-valued sources, by showing that a similar result holds where the side information Y is the sum of the Gaussian source X and another Gaussian random variable which is independent of X [64]. With lossless knowledge of Y at the decoder, the rate-distortion performance for lossy coding X is identical irrespective of whether the encoder knows Y or not [65]. This is known as the Wyner-Ziv theorem.

Although the Slepian-Wolf theorem relates to compression of two correlated sources, it also marked the beginning of research in the field of multiterminal source coding, which considers compressing multiply correlated, but physically separated, sources and jointly reconstructing them at the decoder. There has been much research effort devoted to determining the general achievable rate-distortion region with respect to a fidelity criterion [66–68]. The most recent theoretical work has focused on the special case of conditionally independent sources [69] and Gaussian sources [70–73].

3.2.2 Applications of DSC in Wireless Sensor Networks

As a signal processing approach to achieving high coding efficiency, the application of DSC in resource-limited WSNs has received much research attention. Oohama provided a complete characterization of the rate-distortion region for the quadratic Gaussian chief executive officer (CEO) problem when the source is an independent identically distributed (i.i.d.) Gaussian random variable and observations are corrupted by independent Gaussian noise [72]. It was assumed that the communication links between the encoders and the decoder are reliable. When applying the result of the quadratic Gaussian chief executive officer (CEO)

problem to DSC in WSNs, Ishwar et al. extended Oohama's work to networks with sensor nodes and communication links subject to failure [74]. Their work assumed, however, that a certain number of encoded sensor readings, each with the same rate, are guaranteed to be successfully transmitted to the sink. This is a hard requirement to satisfy in dynamic WSNs, where network bandwidth is shared by a large number of sensor nodes and may change from time to time during communications. It is also unnecessary for all observing sensor nodes to transmit their measurements back to the sink in order to optimize system performance.

Although prior work on the application of DSC in WSNs has focused on information-theoretic aspects, some existing work has addressed the problems of constructing distributed source codes. Pradhan et al. constructed a DSC framework based on algebraic trellis codes [65, 75–77]. Garcia-Frias et al. [78–80] and Aaron et al. [81] proposed DSC construction using turbo codes for symmetric and asymmetric DSC, respectively. However, both trellis codes and turbo codes are computationally complex and hardware-costly in the context of resource-limited wireless sensor nodes. Stankovic et al. investigated practical distributed source code designs using advanced channel codes and constructed a code for binary sources with the parity-check matrix of a systematic Hamming channel code, by assuming the correlation among sources is such that their sum is a Bernoulli-p process [82]. However, their assumed correlation model is less general for practical sensor readings, which may make this approach to code construction not suitable for DSC in most WSNs. Some other effort on the construction of practical distributed source codes for WSNs have focused on low-density parity-check (LDPC) codes [83–85]. When applied to DSC, LDPC codes can perform close to the Slepian-Wolf limit and are less complex to design and more flexible than other codes. The proposed decoding algorithm in [85] prevents error propagation

among the sources. Chou et al. constructed a tree-based distributed compression code to adaptively compress spatially and temporally correlated sensor readings [86]. In their proposed DSC scheme, however, only one sensor reading can be compressed jointly at a time with the uncompressed sensor readings and the decoded sensor readings, and the joint compression is based on the feedback from the sink, which makes it not efficient in terms of coding efficiency. Furthermore, the indirect inter-node communication between sensor nodes and the sink results in a high system processing delay and control overhead.

Obviously, the requirement of very little or even zero inter-node communication puts challenge for the sink to implicitly provide the side information for joint coding in a DSC scheme. It is, therefore, necessary to design a practical DSC scheme which can efficiently construct the side information and effectively utilize the side information to compress multiple sensor observations. The research effort to this aim is presented in detail in the remainder of this chapter.

3.3 Problem Formulation

This section investigates a WSN designed to monitor remote targets. For simplicity, it is assumed that there is at most one active target at any time. Once the target becomes active, it is observed by the surrounding wireless sensor nodes deployed in the sensor field. The surrounding sensor nodes generate observation signals and transmit the signals via single-hop or multi-hop paths to an information sink for further processing. The received sensor observation signals are then used by the sink to estimate the target signal and take corresponding action. Since the focus of this chapter is on the DSC algorithm, it is assumed that, for simplicity, there is no packet delivery loss in the network. Furthermore, the bandwidth constraint is not considered. (The problem of packet loss and bandwidth constraint will be discussed in Chapter 4.) Figure 3-5 shows the system

framework for remote signal estimation for WSNs.

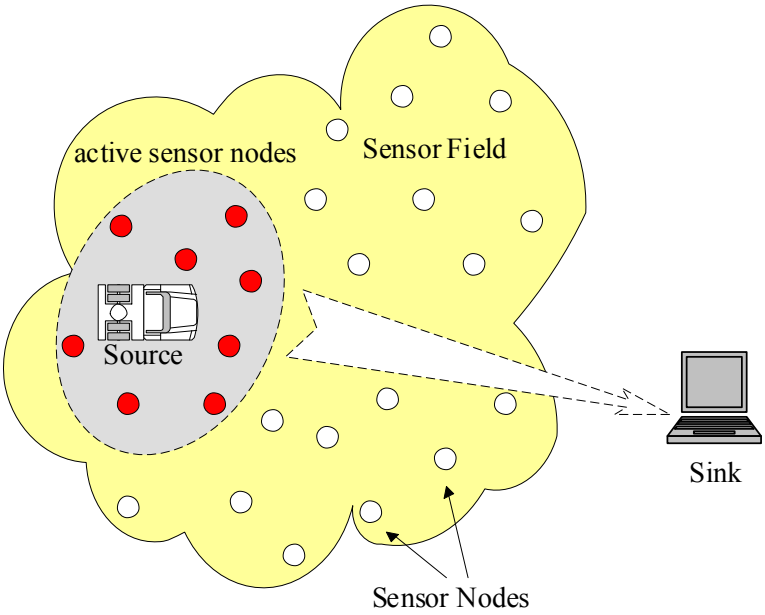

Figure 3-5: System framework for remote signal estimation for WSNs.

For each active target, it is assumed that n individual sensors in the surrounding sensing field make synchronous, correlated and noisy measurements of the signal generated by the target (represented by a source process X). The n noisy observations $Y_1, \ldots, Y_n$ are quantized yielding $U_1, \ldots, U_n$. These quantized signals can be transmitted directly to the sink for further processing. This simple remote source estimation scheme is denoted as the basic transmission scheme and will be discussed in more detail in Chapter 4. To improve network performance by fully utilizing the correlations between sensor readings and also to compress sensor data in one step, a random-binning based DSC scheme is used. Note that although network bandwidth can be saved by reducing the number of quantization levels, the cost is increased signal distortion. DSC, however, saves network bandwidth without increasing signal distortion.

The operation of the proposed scheme is divided into *rounds*. In each round, $s(\geq 1)$ quantized readings U_j $(j = n - s + 1, \ldots, n)$ are selected to be sent

uncoded to achieve a certain level of signal estimation reliability. With the s uncoded readings as the condition of joint encoding, the other $n-s$ quantized readings U_i $(i = 1, \ldots, n-s)$ are randomly divided into groups of k $(1 \leq k \leq n-s)$ readings and jointly encoded with random-binning rate R_k, yielding $n-s$ indices I_i $(i = 1, \ldots, n-s)$. The $n-s$ indices are then transmitted with the s uncoded quantized readings through the WSN to the sink. After the sink receives the s uncoded readings U_j $(j = n-s+1, \ldots, n)$ and the $n-s$ indices I_i $(i = 1, \ldots, n-s)$, it decodes I_i yielding $\hat{U}_i$, and subsequently reconstructs the source signal by first averaging U_j and $\hat{U}_i$ and then dequantizing the averaged quantization value to give $\hat{X}$. The general DSC scheme is illustrated in Figure 3-6. The problem to be solved now becomes that of designing a simple random-binning based coding method to compress multiple and highly-correlated sensor readings and the control of source estimation quality.

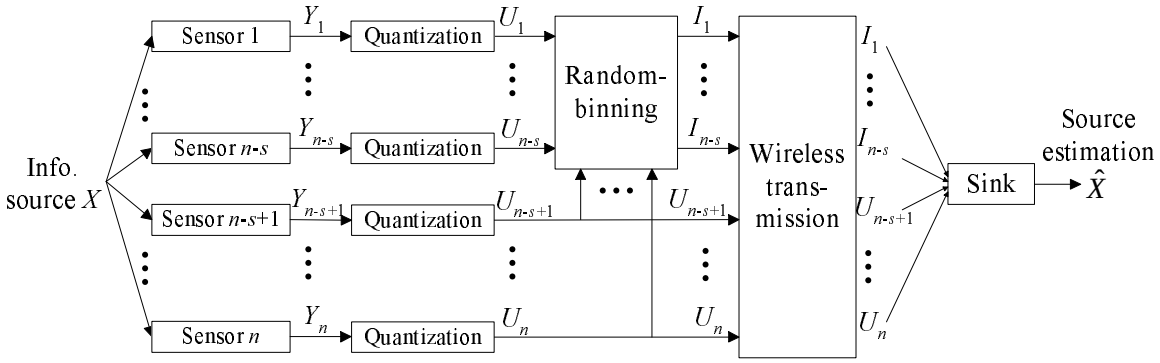

Figure 3-6: General distributed source coding scheme. s quantized readings are uncoded as the condition of joint coding, $n-s$ quantized readings are jointly encoded by random-binning.

For simplicity, it is further assumed that the source process $\{X(t)\}_{t=1}^{\infty} \sim \mathcal{N}(\overline{x}, \sigma_X^2)$ is an i.i.d. Gaussian source and

$$Y_i(t) = X(t) + N_i(t),\ i = 1, \ldots, n, \tag{3.1}$$

are the noisy measurements generated by the n sensors at time t. Suppose that across time, the observation noise processes $\{N_i(t)\}_{t=1}^{\infty} \sim \mathcal{N}(0, \sigma_N^2)$ are i.i.d. Gaussian and independent of the source process. The noisy sensor observations $\{Y_i(t)\}_{t=1}^{\infty} \sim \mathcal{N}(\overline{x}, \sigma_X^2 + \sigma_N^2)$ are therefore conditionally independent and symmetrically correlated given the $X(t)$ samples. Let

$$U_i(t) = \frac{1}{\Delta}[Y_i(t) - y_0] + q_i(t) \tag{3.2}$$

be the uniformly-quantized noisy reading of sensor i at time t, where y_0 is the reference point for the uniform quantizer, Δ is the quantization step, and $\{q_i(t)\}_{t=1}^{\infty}$ are the quantization noise processes with mean $\overline{q}$ and variance σ_q^2. With an appropriate choice of y_0 and Δ for high resolution quantization, $q_i(t)$ can be assumed to be approximately uniformly distributed in $(-0.5, 0.5]$. Since $\overline{q} \approx 0$ and $\sigma_q^2 \approx \frac{1}{12} \ll \frac{1}{\Delta^2}(\sigma_X^2 + \sigma_N^2)$, the quantized readings are assumed to be Gaussianly-distributed, i.e.

$$\{U_i(t)\}_{t=1}^{\infty} \sim \mathcal{N}\left[\frac{1}{\Delta}(\overline{x} - y_0) + \overline{q}, \frac{1}{\Delta^2}(\sigma_X^2 + \sigma_N^2) + \sigma_q^2\right],$$

and are also conditionally independent and symmetrically correlated given the $X(t)$ samples. Note that the work presented in this chapter, however, can be extended to the case with general signal and noise distributions. Since all operations are assumed for a certain round t, for concision of description, t will be omitted from the arguments of variables such as $X(t)$, $Y_i(t)$ and $U_i(t)$, $i = 1, \ldots, n$, in the subsequent subsections.

3.4 Random-binning Coding

Since the n quantized sensor readings U_i $(i = 1, \ldots, n)$ are symmetrically correlated, this section will discuss the encoding of k quantized readings U_i, $i = 1, \ldots, k$, and the decoding of k received indices I_i, $i = 1, \ldots, k$, with s uncoded readings U_j, $j = n-s+1, \ldots, n$. To encode more than k quantized readings and decode more than k indices, the coding operations can be repeated.

3.4.1 Encoding Method

Random-binning coding reduces the complexity of the encoding process by transferring the burden of computing to the decoding process at the sink. The joint encoding method is similar to that of the simple distributed source code proposed in [86], and begins with the codebook construction.

Assume that all the noisy sensor readings are quantized with n_0 bits. The root level of the codebook contains 2^{n_0} representative values, with equal (unit) distance between any two adjacent values. Firstly, the root codebook is partitioned into two level 1 sub-codebooks (i.e. bins), each comprising 2^{n_0-1} values with equal distance 2 between any two adjacent values within the same sub-codebook. The two level 1 sub-codebooks are indexed "0" and "1" respectively, and are then repeatedly partitioned into further sub-codebooks $n_0 - 1$ times, until at level n_0, each of the 2^{n_0} sub-codebooks contains one value. Each time when two sub-codebooks are generated from a higher level sub-codebook they are indexed with an additional "0" and "1" respectively. The values in an R^{th} level sub-codebook are, therefore, spaced by a distance of 2^R $(1 \leq R \leq n_0 - 1)$. At each level of the codebook, every sub-codebook has a unique bin index, which is determined by either choosing the smallest value in the sub-codebook or reading the codebook tree backwards from the sub-codebook to the root codebook. Figure 3-7 illustrates the process of the codebook construction for random-binning based

DSC.

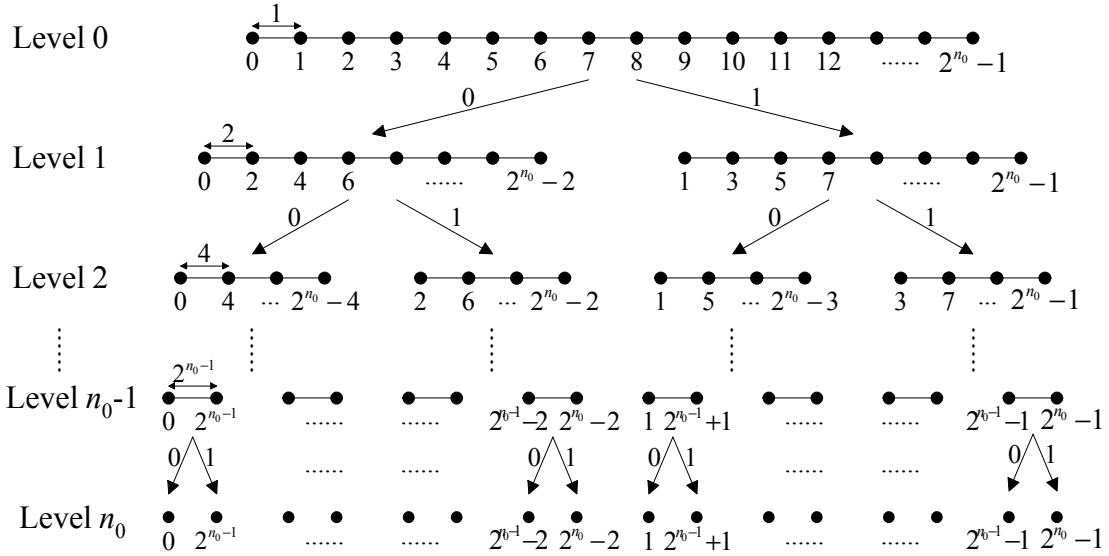

Figure 3-7: Encoding process of random-binning based DSC: codebook construction for sensor readings quantized with n_0 bits.

The advantage of random-binning is that joint encoding of multiple sensor readings can be accomplished distributedly with the joint coding rate known. Denote $\mathcal{C}_{R,I}$ as the I^{th} sub-codebook at level R. For a known coding rate R, encoding of a quantized reading U_i $(i = 1, \ldots, k)$ is easily done by mapping U_i to the index I_i of an R^{th} level sub-codebook $\mathcal{C}_{R,I_i}$, which includes the value of U_i. The mapping is given by:

$$I_i = index(U_i) \ mod \ 2^R, \tag{3.3}$$

where $index()$ is a mapping of a quantization value to its index in the root level of the codebook. The property of this code is that when using R bits to encode an original value, the decoded value will always be equal to the original value if, and only if, the value of the side information at the decoder is no further than 2^{R-1} away from the original value [86].

3.4.2 Coding Rate

Random-binning implements joint source coding in a distributed way. The sensor does not need information from other sensors to perform this distributed encoding. The determination of the operational coding rate R_k, however, is not easy and has a large impact on the performance of random-binning decoding and the DSC estimation scheme. Several basic requirements on the value of R_k are listed as following:

1. $R_k \in [1, n_0]$ and should be an integer.
2. R_k should be larger than the theoretical coding rate determined by the entropy of the sensor readings.
3. R_k should be large enough to make the decoding error probability small.

In what follows, the theoretical optimal coding rate will be derived and used to give the operational coding rate.

Let $\hat{U}_i$ be the decoded value corresponding to a quantized reading U_i ($i = 1, \ldots, k$). Define R_{kc} and $D(\hat{U}_i)$ as the theoretical rate-distortion tuple for the achievable random-binning coding quality for a group of k readings, U_i, $i = 1, \ldots, k$, to be jointly encoded with s uncoded readings, U_j, $j = n-s+1, \ldots, n$. The decoding quality is measured by mean square error (MSE), i.e.:

$$D(\hat{U}_i) = \mathbb{E}\left[\left(U_i - \hat{U}_i\right)^2\right]. \tag{3.4}$$

For optimal decoding, when $D(\hat{U}_i) = 0$, the theoretical optimal rate, denoted as R_{kc}, is determined by the average entropy of k quantized readings with the condition of s quantized readings already available, i.e.:

$$R_{kc} = \frac{1}{k} H\left[(U_1, \ldots, U_k) | (U_{n-s+1}, \ldots, U_n)\right]$$

$$= \frac{1}{k}\left[H(U_1, \ldots, U_k, U_{n-s+1}, \ldots, U_n) - H(U_{n-s+1}, \ldots, U_n)\right]. \quad (3.5)$$

As the quantized readings are assumed to be conditionally independent, symmetrically correlated and Gaussian, the joint entropy of multiple quantized readings is the entropy of a multivariate normal process, determined by the covariance matrix of the multiple variates [62]. Specifically, as assumed in Section 3.3, for $i = 1, \ldots, n$, the quantized reading $U_i \sim \mathcal{N}\left[\frac{1}{\Delta}(\overline{x} - y_0) + \overline{q}, \frac{1}{\Delta^2}(\sigma_X^2 + \sigma_N^2) + \sigma_q^2\right]$, the variances of U_i $(i = 1, \ldots, n)$ are, therefore, the same value:

$$\sigma_U^2 = \frac{1}{\Delta^2}(\sigma_X^2 + \sigma_N^2) + \sigma_q^2, \quad (3.6)$$

and the entropies of U_i $(i = 1, \ldots, n)$ are given by:

$$\begin{aligned} H(U_i) &= \frac{1}{2}\log\left(2\pi e\sigma_U^2\right) \\ &= \frac{1}{2}\log\left\{2\pi e\left[\frac{1}{\Delta^2}(\sigma_X^2 + \sigma_N^2) + \sigma_q^2\right]\right\}. \end{aligned} \quad (3.7)$$

Let $\mathbb{C}_s$ denote the covariance matrix of $(U_{n-s+1}, \ldots, U_n)$. Since U_i $(i = n - s + 1, \ldots, n)$ are conditionally i.i.d. Gaussian and symmetrically correlated, their covariance matrix is circulant, given by:

$$\mathbb{C}_s = \begin{bmatrix} \frac{1}{\Delta^2}(\sigma_X^2 + \sigma_N^2) + \sigma_q^2 & \frac{1}{\Delta^2}\sigma_X^2 & \cdots & \frac{1}{\Delta^2}\sigma_X^2 \\ \frac{1}{\Delta^2}\sigma_X^2 & \frac{1}{\Delta^2}(\sigma_X^2 + \sigma_N^2) + \sigma_q^2 & \cdots & \frac{1}{\Delta^2}\sigma_X^2 \\ \vdots & \vdots & \ddots & \vdots \\ \frac{1}{\Delta^2}\sigma_X^2 & \frac{1}{\Delta^2}\sigma_X^2 & \cdots & \frac{1}{\Delta^2}(\sigma_X^2 + \sigma_N^2) + \sigma_q^2 \end{bmatrix}. \quad (3.8)$$

The eigenvalue λ of matrix $\mathbb{C}_s$ is determined by the characteristic polynomial of $\mathbb{C}_s$ to be zero:

$$\det(\lambda \mathbb{I}_s - \mathbb{C}_s) = 0, \tag{3.9}$$

where det() is the determinant of a matrix, and $\mathbb{I}_s$ is the identity matrix of size s. It is easily to get the s eigenvalues of $\mathbb{C}_s$, i.e. $\left[\frac{1}{\Delta^2}(s \cdot \sigma_X^2 + \sigma_N^2) + \sigma_q^2\right]$ with multiplicity 1 and $\left(\frac{1}{\Delta^2}\sigma_N^2 + \sigma_q^2\right)$ with multiplicity $(s-1)$. The determinant of $\mathbb{C}_s$ is:

$$\det(\mathbb{C}_s) = \left[\frac{1}{\Delta^2}(s \cdot \sigma_X^2 + \sigma_N^2) + \sigma_q^2\right] \left(\frac{1}{\Delta^2}\sigma_N^2 + \sigma_q^2\right)^{s-1}. \tag{3.10}$$

The joint entropy of s quantized readings $(U_{n-s+1}, \ldots, U_n)$ is then given by:

$$\begin{aligned} H(U_{n-s+1}, \ldots, U_n) &= \frac{1}{2}\log\left[(2\pi e)^s \det(\mathbb{C}_s)\right] \\ &= \frac{1}{2}\log\left\{(2\pi e)^s \left[\frac{1}{\Delta^2}(s \cdot \sigma_X^2 + \sigma_N^2) + \sigma_q^2\right] \right. \\ &\quad \left. \cdot \left(\frac{1}{\Delta^2}\sigma_N^2 + \sigma_q^2\right)^{s-1}\right\}. \end{aligned} \tag{3.11}$$

Similarly, the joint entropy of $k+s$ quantized readings $(U_1, \ldots, U_k, U_{n-s+1}, \ldots, U_n)$ is:

$$\begin{aligned} &H(U_1, \ldots, U_k, U_{n-s+1}, \ldots, U_n) \\ &= \frac{1}{2}\log\left\{(2\pi e)^{k+s}\left\{\frac{1}{\Delta^2}[(k+s)\sigma_X^2 + \sigma_N^2] + \sigma_q^2\right\}\left(\frac{1}{\Delta^2}\sigma_N^2 + \sigma_q^2\right)^{k+s-1}\right\} \end{aligned} \tag{3.12}$$

Using (3.5), (3.11), and (3.12), the theoretical optimal random-binning coding rate is found as a function of the number of uncoded readings as the condition of joint encoding, s, and the number of joint encoding nodes, k, given by:

$$R_{kc}(s,k) = \frac{1}{2}\log\left[2\pi e\left(\frac{1}{\Delta^2}\sigma_N^2 + \sigma_q^2\right)\left(1 + \frac{k \cdot \sigma_X^2}{s \cdot \sigma_X^2 + \sigma_N^2 + \Delta^2\sigma_q^2}\right)^{\frac{1}{k}}\right]. \tag{3.13}$$

The operational coding rate R_k is required to be no less than the theoretical optimal coding rate $R_{kc}(s,k)$.

Due to the property of the random-binning code, a received index I_i ($i = 1, \ldots, k$) with coding rate R_k will be correctly decoded only when the constructed side information is less than 2^{R_k-1} away from U_i. Since U_i are symmetrically correlated and Gaussianly distributed, the most desirable side information we may construct is the mean of U_i ($i = 1, \ldots, n$), denoted by U_0. Define

$$d(U_i, U_0) = U_i - U_0 \tag{3.14}$$

as the offset of U_i from U_0. The index I_i can, therefore, be correctly decoded with the side information U_0, only when the absolute value of $d(U_i, U_0)$ satisfies:

$$|d(U_i, U_0)| < 2^{R_k-1}. \tag{3.15}$$

For a particular source sample value x, U_i and U_0 are given by $U_i = \frac{1}{\Delta}(x + N_i - y_0) + q_i$ and $U_0 = \frac{1}{\Delta}(x - y_0) + \overline{q}$, where N_i and q_i are the observation noise and the quantization noise for sensor i, respectively. $d(U_i, U_0)$ is, therefore, given by

$$d(U_i, U_0) = \frac{1}{\Delta}N_i + (q_i - \overline{q}). \tag{3.16}$$

Since $\overline{q} \approx 0$ and $\sigma_q^2 \approx \frac{1}{12} \ll \frac{1}{\Delta^2}\sigma_N^2$, $d(U_i, U_0)$ is approximately Gaussianly distributed, i.e. $d(U_i, U_0) \sim \mathcal{N}\left(0, \frac{1}{\Delta^2}\sigma_N^2 + \sigma_q^2\right)$. With some prediction error probability, P_{err}, $d(U_i, U_0)$ is bounded by

$$d(U_i, U_0) \leq \delta, \tag{3.17}$$

where δ is determined by:

$$1 - P_{err} = \int_{-\delta}^{\delta} \frac{1}{\sqrt{2\pi}\sigma} e^{-\frac{x^2}{2\sigma^2}} dx, \text{ where } \sigma = \sqrt{\frac{1}{\Delta^2}\sigma_N^2 + \sigma_q^2}. \tag{3.18}$$

Using (3.13), (3.15), and (3.17), the optimal coding rate R_k^* is chosen as the minimum integer satisfying:

$$\begin{cases} R_k^* > log_2\delta + 1; \\ R_{kc} \leq R_k^* \leq n_0 - 1. \end{cases} \tag{3.19}$$

3.4.3 Decoding Method

The decoding method of the random binning indices I_i ($i = 1, \ldots, k$) is different to that used in [86]. In [86], s and k are both set to 1, and the uncoded reading U_n is taken as the side information. I_1 is simply decoded to $\hat{U}_1$ by choosing the value in the sub-codebook $\mathcal{C}_{R_k,I_1}$ closest to U_n. In the random-binning based DSC scheme proposed in this chapter, however, the side information is not directly available and needs to be constructed from not only the uncoded readings U_j ($j = n - s + 1, \ldots, n$) but also the indices I_i ($i = 1, \ldots, k$) to efficiently utilize the data correlation. The method of constructing the side information and jointly decoding I_i is proposed as following.

Intuitively, to decode I_i, the information compressed with rate R_{kc} (determined by (3.13)) should be recovered. Two auxiliary random variables V_1 and V_2 are defined, respectively given by:

$$\begin{aligned} V_1 &= \frac{1}{s} \sum_{j=n-s+1}^{n} U_j; \\ V_2 &= \frac{1}{k+s} \left(\sum_{i=1}^{k} U_i + s \cdot V_1 \right), \end{aligned} \tag{3.20}$$

as the algebraic mean of the s and $k+s$ uncoded quantized readings, respectively. The distributions of V_1 and V_2 are, respectively, given by:

$$V_1 \sim \mathcal{N}\left\{\frac{1}{\Delta}(\overline{x}-y_0)+\overline{q}, \left[\frac{1}{\Delta^2}\sigma_X^2+\frac{1}{s}\left(\frac{1}{\Delta^2}\sigma_N^2+\sigma_q^2\right)\right]\right\}$$

and

$$V_2 \sim \mathcal{N}\left\{\frac{1}{\Delta}(\overline{x}-y_0)+\overline{q}, \left[\frac{1}{\Delta^2}\sigma_X^2+\frac{1}{k+s}\left(\frac{1}{\Delta^2}\sigma_N^2+\sigma_q^2\right)\right]\right\}.$$

Similar to the entropies of U_i $(i=1,\ldots,n)$ given in (3.7), the entropies of V_1 and V_2 are respectively given by:

$$\begin{aligned} H(V_1) &= \frac{1}{2}\log\left\{2\pi e\left[\frac{1}{\Delta^2}\sigma_X^2+\frac{1}{s}\left(\frac{1}{\Delta^2}\sigma_N^2+\sigma_q^2\right)\right]\right\}; \\ H(V_2) &= \frac{1}{2}\log\left\{2\pi e\left[\frac{1}{\Delta^2}\sigma_X^2+\frac{1}{k+s}\left(\frac{1}{\Delta^2}\sigma_N^2+\sigma_q^2\right)\right]\right\}. \end{aligned} \tag{3.21}$$

We now let:

$$\rho_u = \frac{\sigma_X^2}{\sigma_N^2+\Delta^2\sigma_q^2}, \quad f_s = \left[\frac{1}{1+\rho_u}\left(1+\frac{k}{s}\right)^{\frac{1}{k}}\right]^{\frac{1}{2}}. \tag{3.22}$$

Using (3.7), (3.21), and (3.22), the theoretical optimal random-binning coding rate R_{kc} in (3.13) can be rewritten as:

$$R_{kc} = \frac{1}{k}\left[\sum_{i=1}^{k} H(U_i)+H(V_2)-H(V_1)\right]+\log f_s. \tag{3.23}$$

Considering (3.23), since V_1, V_2 and U_i $(i=1,\ldots,k)$ are Gaussianly distributed with the same mean, and conditionally independent given the source samples, the sum of the entropies for any two of these random variables is equal to the entropy of the two variables' product. Similarly, the difference of the entropies for any two of these random variables is equal to the entropy of the two variables' division, and the algebraic mean of these variables' entropies is equal

to the entropy of the variables' geometric mean. Therefore, the side information for decoding the k indices, denoted by $\hat{U}_0$, can be approximated by the geometric mean of U_i $(i = 1, \ldots, k)$, scaled by $\left(\frac{V_2}{V_1}\right)^{\frac{1}{k}}$, i.e:

$$\hat{U}_0 = \left(\frac{V_2}{V_1} \cdot \prod_{i=1}^{k} U_i\right)^{\frac{1}{k}}, \tag{3.24}$$

which is close to the most desirable side information, U_0.

The side information constructed by (3.24), however, assumes that the k indices I_i have been correctly decoded to U_i $(i = 1, \ldots, k)$. To solve this problem, an iterative method is used to jointly construct $\hat{U}_0$ and decode I_i. In each iteration, U_i is estimated by a value in the sub-codebook $\mathcal{C}_{R_k,I_i}$ which is closest to the constructed side information $\hat{U}_0$, as illustrated in Figure 3-8.

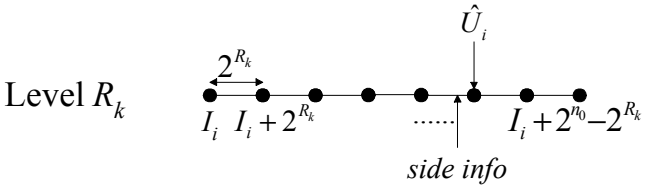

Figure 3-8: Decoding process of random-binning based DSC: recover U_i from the sub-codebook with the bin index I_i.

The decoding method is then described as follows:

1) Initially only the algebraic mean of the s uncoded readings, V_1, is used to approximate $\hat{U}_0$.

2) A value in the sub-codebook $\mathcal{C}_{R_k,I_i}$ $(i = 1, \ldots, k)$, which is closest to $\hat{U}_0$, is chosen to estimate U_i.

3) The estimated U_i are used to calculate V_2 (with (3.20)) and provide the new $\hat{U}_0$ (with (3.24)), which is closer to U_0.

4) Updating the old $\hat{U}_0$ with the newly calculated value, the above operations

are repeated, until $\hat{U}_0$ gradually converges to the optimal value. The convergence condition is set as either the update of $\hat{U}_0$ value being less than a predetermined threshold (e.g. 10^{-5}), or the maximum allowed number of iterations (e.g. 500) being reached.

5) After the iteration process finishes, the sink uses the finally calculated side information $\hat{U}_0$ to decode I_i $(i = 1, \ldots, k)$, by choosing the value in the sub-codebook $\mathcal{C}_{R_k,I_i}$ closest to $\hat{U}_0$ as the decoded value $\hat{U}_i$.

The source signal is then estimated with the s uncoded readings U_j $(j = n - s + 1, \ldots, n)$ and the k decoded readings $\hat{U}_i$ $(i = 1, \ldots, k)$.

3.4.4 Decoding Performance

The iterative method determines that the value of the initial $\hat{U}_0$, i.e. V_1, has a large impact on the performance of the decoding algorithm. In what follows, the probability of error in decoding of the proposed decoding method will be analyzed.

According to (3.17), due to the observation noise and the quantization noise of sensor data, for a particular operational coding rate R_k and a particular mean of quantized sensor readings U_0, the sink can only correctly decode sensor readings within $[U_0 - \delta, U_0 + \delta]$, where δ is the offset bound of $U_i (i = 1, \ldots, n)$ from U_0, determined by (3.19). The probability of error in decoding introduced by this offset is bounded by P_{err}, given by (3.18).

On the other hand, as in the first round of the iterative decoding, V_1 is used to approximate the side information $\hat{U}_0$ and estimate the quantized readings U_i for further iterations, the offset of V_1 from U_0 largely affects the correctness of the decoding result. According to (3.15), for a particular R_k and U_0, the estimated U_i in the first round of iteration is limited within $[V_1 - d, V_1 + d]$, where d is half

of the spacing distance of the representative values in the sub-codebook $\mathcal{C}_{R_k,I_i}$, given by:

$$d = 2^{R_k - 1}. \tag{3.25}$$

The probability that U_i in $[U_0 - \delta, U_0 + \delta]$ overlaps U_i in $[V_1 - d, V_1 + d]$, therefore, can be used to approximate the successful decoding probability.

Define an auxiliary probability function

$$\phi(u_1, u_2) = \frac{\int_{u_1}^{u_2} \frac{1}{\sqrt{2\pi}\sigma} e^{-\frac{(u-U_0)^2}{2\sigma^2}} du}{\int_{V_1-d}^{V_1+d} \frac{1}{\sqrt{2\pi}\sigma} e^{-\frac{(u-U_0)^2}{2\sigma^2}} du}, \text{ where } \sigma = \sqrt{\frac{1}{\Delta^2}\sigma_N^2 + \sigma_q^2} \tag{3.26}$$

showing the overlapping probability of U_i in $[u_1, u_2]$ with U_i in $[V_1 - d, V_1 + d]$. The successful decoding probability, denoted as P_{suc}, is determined by the following possible cases:

1. When $\begin{cases} V_1 - d \geq U_0 - \delta \\ V_1 + d \leq U_0 + \delta \end{cases}$, i.e. $\begin{cases} d \leq \delta \\ d - \delta \leq V_1 - U_0 \leq \delta - d \end{cases}$,

$$P_{suc} = 1; \tag{3.27}$$

2. When $\begin{cases} U_0 - \delta \leq V_1 - d \leq U_0 + \delta \\ V_1 + d \geq U_0 + \delta \end{cases}$,

i.e. $\begin{cases} d \leq \delta \\ \delta - d \leq V_1 - U_0 \leq \delta + d \end{cases}$ or $\begin{cases} d \geq \delta \\ d - \delta \leq V_1 - U_0 \leq \delta + d \end{cases}$,

$$P_{suc} = \phi(V_1 - d, U_0 + \delta); \tag{3.28}$$

3. When $\begin{cases} V_1 - d \leq U_0 - \delta \\ U_0 - \delta \leq V_1 + d \leq U_0 + \delta \end{cases}$,

i.e. $\begin{cases} d \leq \delta \\ -\delta - d \leq V_1 - U_0 \leq d - \delta \end{cases}$ or $\begin{cases} d \geq \delta \\ -\delta - d \leq V_1 - U_0 \leq \delta - d \end{cases}$,

$$P_{suc} = \phi(U_0 - \delta, V_1 + d); \tag{3.29}$$

4. When $\begin{cases} V_1 - d \leq U_0 - \delta \\ V_1 + d \geq U_0 + \delta \end{cases}$, i.e. $\begin{cases} d \geq \delta \\ \delta - d \leq V_1 - U_0 \leq d - \delta \end{cases}$,

$$P_{suc} = \phi(U_0 - \delta, U_0 + \delta); \tag{3.30}$$

5. When $V_1 + d \leq U_0 - \delta$ or $V_1 - d \geq U_0 + \delta$, i.e. $V_1 - U_0 \leq -\delta - d$ or $V_1 - U_0 \geq \delta + d$,

$$P_{suc} = 0. \tag{3.31}$$

Since the offset of V_1 from U_0 can be shown as

$$V_1 - U_0 = \frac{1}{s}\left(\frac{1}{\Delta}\sum_{j=n-s+1}^{n} N_j + \sum_{j=n-s+1}^{n} q_j\right) - \overline{q},$$

the distribution of $(V_1 - U_0)$ is given by $(V_1 - U_0) \sim \mathcal{N}(0, \sigma_v^2)$, where

$$\sigma_v = \sqrt{\frac{1}{s}\left(\frac{1}{\Delta^2}\sigma_N^2 + \sigma_q^2\right)}. \tag{3.32}$$

Now consider (3.26). Let $w = u - U_0$, (3.26) can be rewritten as:

$$\phi(u_1, u_2) = \frac{\int_{u_1-U_0}^{u_2-U_0} \frac{1}{\sqrt{2\pi}\sigma} e^{-\frac{w^2}{2\sigma^2}} dw}{\int_{V_1-U_0-d}^{V_1-U_0+d} \frac{1}{\sqrt{2\pi}\sigma} e^{-\frac{w^2}{2\sigma^2}} dw}, \text{ where } \sigma = \sqrt{\frac{1}{\Delta^2}\sigma_N^2 + \sigma_q^2}. \tag{3.33}$$

Let $v = V_1 - U_0$, and define another auxiliary function

$$\psi(w_1, w_2) = \frac{\int_{w_1}^{w_2} \frac{1}{\sqrt{2\pi}\sigma} e^{-\frac{w^2}{2\sigma^2}} dw}{\int_{v-d}^{v+d} \frac{1}{\sqrt{2\pi}\sigma} e^{-\frac{w^2}{2\sigma^2}} dw}, \text{ where } \sigma = \sqrt{\frac{1}{\Delta^2}\sigma_N^2 + \sigma_q^2}, \tag{3.34}$$

(3.33) can be further transformed, i.e.:

$$\phi(u_1, u_2) = \psi(u_1 - U_0, u_2 - U_0). \tag{3.35}$$

The successful decoding probability P_{suc} is then given as a function of v:

- When $d \leq \delta$, $P_{suc}(v) = \begin{cases} 1, & \text{when } d - \delta \leq v \leq \delta - d; \\ \psi(v - d, \delta), & \text{when } \delta - d \leq v \leq \delta + d; \\ \psi(-\delta, v + d), & \text{when } -\delta - d \leq v \leq d - \delta; \\ 0, & \text{when } v \leq -\delta - d \text{ or } v \geq \delta + d. \end{cases}$
- When $d \geq \delta$, $P_{suc}(v) = \begin{cases} \psi(v - d, \delta), & \text{when } d - \delta \leq v \leq \delta + d; \\ \psi(-\delta, v + d), & \text{when } -\delta - d \leq v \leq \delta - d; \\ \psi(-\delta, \delta), & \text{when } \delta - d \leq v \leq d - \delta; \\ 0, & \text{when } v \leq -\delta - d \text{ or } v \geq \delta + d. \end{cases}$

Considering the distribution of v, define another auxiliary function

$$F[P_{suc}(v), v_1, v_2] = \int_{v_1}^{v_2} P_{suc}(v) \cdot \frac{1}{\sqrt{2\pi}\sigma_v} e^{-\frac{v^2}{2\sigma_v^2}} dv. \tag{3.36}$$

showing the average P_{suc} when $v \in [v_1, v_2]$. The expectation of P_{suc} is then given by:

$$\begin{cases} \mathbb{E}[P_{suc}] &= F[1, d-\delta, \delta-d] + F[\psi(v-d, \delta), \delta-d, \delta+d] \\ & \quad + F[\psi(-\delta, v+d), -\delta-d, d-\delta], \qquad \text{when } d \leq \delta; \\ \mathbb{E}[P_{suc}] &= F[\psi(v-d, \delta), d-\delta, d+\delta] + F[\psi(-\delta, v+d), -\delta-d, \delta-d] \\ & \quad + F[\psi(-\delta, \delta), \delta-d, d-\delta], \qquad \text{when } d \geq \delta. \end{cases} \tag{3.37}$$

The total probability of error in decoding for the proposed random-binning decoding method, P_{rb}, is, therefore, approximated using P_{err} (given by (3.18)) and $\mathbb{E}[P_{suc}]$ (given by (3.37)), i.e.:

$$P_{rb} = 1 - (1 - P_{err})\mathbb{E}[P_{suc}]. \tag{3.38}$$

3.5 Simulation Results

3.5.1 Simulation Method and Parameters

This section will present some typical simulation results to illustrate the effectiveness of the proposed random-binning based DSC scheme. The random-binning decoding algorithm and the DSC estimation scheme were tested by running 2000 simulations to obtain the mean decoding error probability and estimation distortion. In each round, the source signal with Gaussian distribution is generated and observed by all the sensor nodes in the network with additive Gaussian noise.

It is simply assumed that all the nodes transmit their observations to the sink and there is no packet delivery loss.

The values of simulation parameters are summarized in Table 3.1, where n denotes the number of wireless sensor nodes transmitting sensor readings in the system, s denotes the number of uncoded readings as the condition of joint encoding, k denotes the number of joint encoding nodes. In order to compress the correlated sensor readings to the maximum extent, s is set as the minimum value 1. $\overline{x}$ denotes the mean of the source signal across time, σ_X^2 denotes the source signal's deviation, and σ_N^2 denotes the observation noise signal's deviation. The signal to observation noise ratio (SNR, dB), defined as

$$SNR = 10 \lg \frac{\overline{x}^2 + \sigma_X^2}{\sigma_N^2},$$

is set for a typical WSN. The quantization rate of the uniform quantizer for Gaussian signals, n_0, is set as 6. y_0 denotes the reference point for the uniform quantizer, and Δ denotes the quantization step. P_{err} denotes the prediction error probability. The total expected probability of error in decoding P_{rb} is set to 5.67×10^{-5}, which is tolerable in a typical WSN.

To evaluate the performance of the proposed decoding algorithm, a reference algorithm is used for comparison in which the mean of the quantized sensor readings U_0 is used as the side information to decode the random-binning indices. Although the quantized readings are normally unknown to the sink, the reference decoding algorithm provides a decoding performance benchmark.

3.5.2 Simulation Results

Using the parameters summarized in Table 3.1, the optimal joint encoding rate R_k^* is found to be 4. The mean probability of error in decoding achieved in the simulation is 5.26×10^{-5} for the proposed decoding algorithm and 2.63×10^{-5} for

Table 3.1: Parameters for simulation of DSC scheme

Variable	Description	Value
n	number of nodes transmitting sensor readings	20
s	number of uncoded readings as condition of joint encoding	1
k	number of joint encoding nodes	5
$\overline{x}$	mean of source signal across time	0
σ_X^2	deviation of source signal across time	200
σ_N^2	deviation of observation noise signal across time	30
SNR	signal to observation noise ratio	8.24 dB
n_0	quantization rate of uniform quantizer	6
y_0	reference point for the uniform quantizer	-91
Δ	quantization step	2.84
P_{err}	prediction error probability	4×10^{-5}
P_{rb}	total expected probability of error in decoding	5.67×10^{-5}

the reference decoding algorithm, when the operational coding rate $R_k = 4$. It is observed that the performance of the proposed decoding algorithm can approach to the performance benchmark given by the reference decoding algorithm, which is taken to be evidence that the proposed decoding algorithm can efficiently exploit the side information carried by the sensor readings. Similar simulation results and performance trends are observed when using other parameters not given here, which shows the scalability of the proposed decoding algorithm.

Figure 3-9 shows some intermediate quantities, including quantization values, random-binning indices and decoded quantization values, for one of the 2000 simulations. The decoded quantization values are denoted as "Decoded value" for the proposed decoding algorithm, and "Decoded value (reference)" for the reference decoding algorithm. The particular source value that generates Figure 3-9 is -0.082145, and it is seen that for this value there is no decoding error for either decoding algorithm. Similar decoding performance is observed for the simulation results generated by other source values.

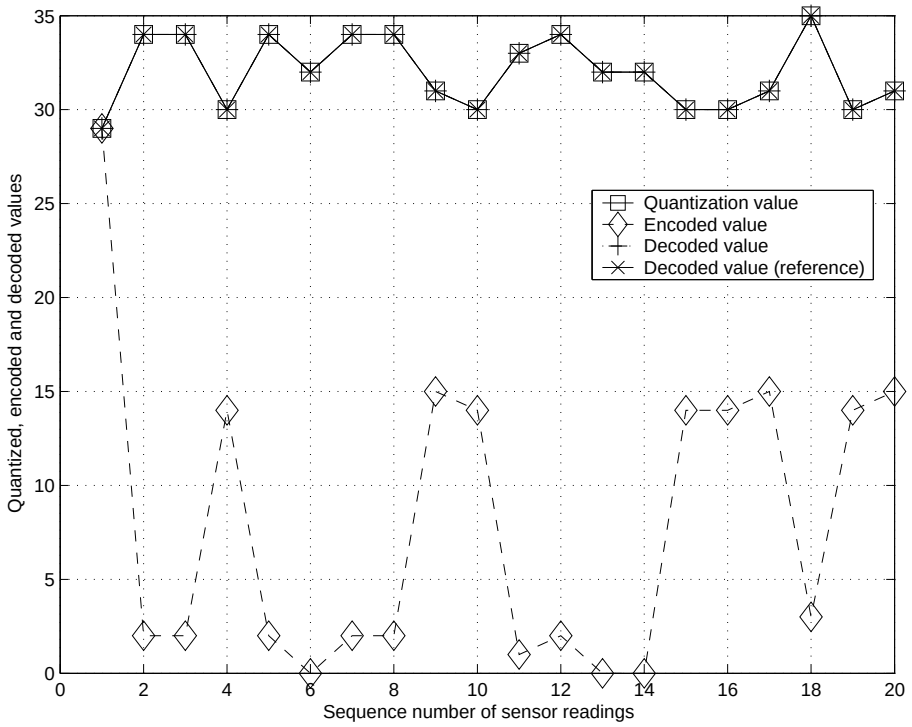

Figure 3-9: Comparison of the proposed decoding algorithm and the reference decoding algorithm. Generated source $x = -0.082145$, coding rate $R_k = 4$ bits.

The distortion of the DSC estimation scheme is quantified by the Signal to Distortion Ratio (SDR, dB), given by:

$$SDR(t) = 10 \lg \frac{X(t)^2}{[X(t) - \hat{X}(t)]^2},$$

where $X(t)$ and $\hat{X}(t)$ are the generated and the estimated source signal, respectively, in the t^{th} simulation round. Both DSC estimation schemes are compared to a simple quantization scheme, in which all quantized sensor readings are sent to the sink without random-binning coding. Figure 3-10 shows the source estimation results for the first 100 rounds of the 2000 simulations, including the estimated source by both the proposed DSC estimation scheme and the simple quantization scheme. With an operational coding rate $R_k = 4$, the mean SDR is 21.2936 dB for the proposed DSC scheme and 21.2948 dB for the reference DSC

scheme. The mean SDR of the quantization scheme is 21.3148 dB. Compared to the quantization scheme, the difference in SDR is negligible while the proposed DSC scheme saves 2 bit per sensor reading.

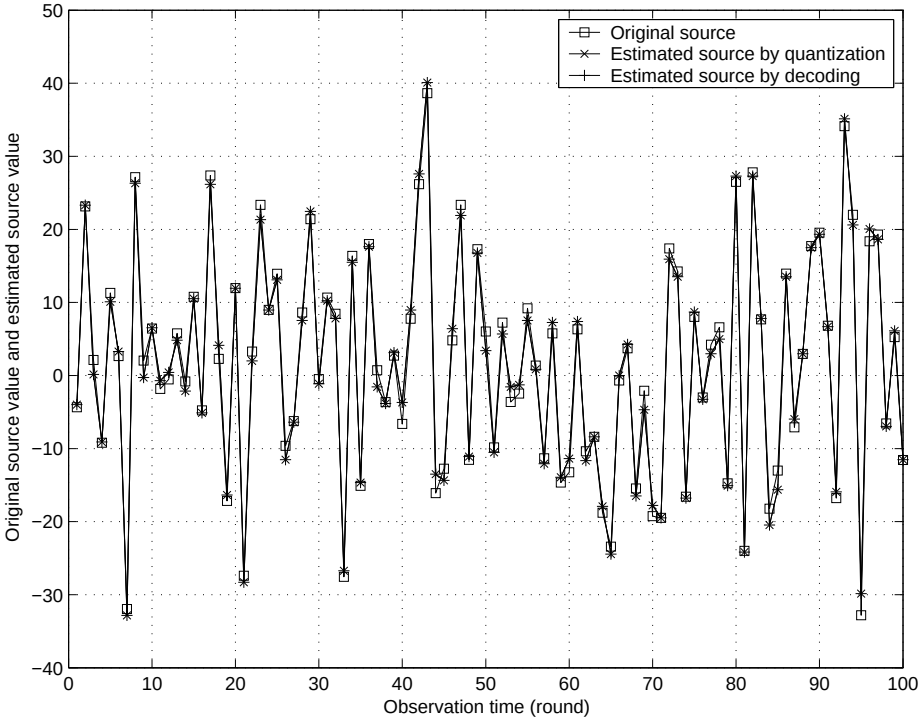

Figure 3-10: First 100 simulations of source estimation: comparison of the proposed DSC estimation scheme and the simple quantization scheme.

3.6 Summary

Due to its unique ability to exchange the computational complexity of the encoder and the decoder, DSC has been identified as an important approach to data compression in WSNs. Previous research work on the application of DSC in WSNs has focused on information-theoretic aspects such as achievable rate-distortion regions, although some existing work has addressed the construction of distributed source codes. Challenges remain, however, in the design of practical DSC schemes which can efficiently construct and utilize side information in order

to compress multiple sensor observations simultaneously.

This chapter has proposed a simple and efficient random-binning based DSC scheme for source estimation in WSNs. The encoding and decoding methods for the random-binning based algorithm are presented and an analytical model is developed to evaluate the decoding performance of the algorithm. Simulation is used to evaluate the algorithm's performance. Simulation results show that the proposed DSC scheme achieves high coding efficiency and reduces network bandwidth consumption while maintaining low signal distortion. By transmitting fewer data bits over the network, energy is also saved. The simplicity and energy efficiency of the DSC scheme makes it especially suitable for WSN applications.

Chapter 4

Energy Efficient Adaptive DSC Scheme

4.1 Introduction

In the last chapter, the problem of remote source estimation in WSNs was investigated. A practical random-binning based DSC scheme was proposed that compresses multiple quantized sensor readings in a distributed way without intercommunication between sensor nodes. By fully utilizing the correlation between the sensor readings, the proposed DSC scheme achieves high coding efficiency, reduces network bandwidth consumption, and shows the potential of saving energy, while maintaining low signal distortion.

Challenges remain, however, not only because of the possible packet losses in the wireless channels but also because the wireless bandwidth changes over time and the total network bandwidth is shared by a large number of remote sensor nodes. It is, therefore, necessary and beneficial to adapt the DSC scheme to the changing network conditions and solve the remote source estimation problem in an integrated coding and network environment.

On the other hand, as mentioned earlier, large scale and special application environments of WSNs require the sensor applications to be highly energy efficient. To improve the energy efficiency of WSNs, wide research has been carried out in diverse areas such as wireless communications, medium access control (MAC), network routing and transport. Energy efficiency is, of course, one of the most important metrics that should be taken into account in the design of DSC schemes. To the best of the author's knowledge, however, although energy consumption is critical for WSNs, the performance of energy consumption for DSC schemes has not been strictly analyzed for optimization in the existing literature. It is, therefore, necessary to analyze and optimize the energy performance of the DSC scheme for WSNs.

This chapter further develops the previously proposed DSC scheme for remote source estimation in WSNs, in three main aspects. Firstly, a random-binning based DSC scheme for a packet-loss-prone WSN is designed. Its estimated signal to distortion ratio (SDR) performance is analyzed, in which the observation noise, quantization noise, DSC decoding errors and network packet losses are all taken into account. Secondly, with the introduction of a detailed power consumption model for wireless sensor communications, the overall network energy consumption of the DSC scheme is quantitatively analyzed. Thirdly, a novel adaptive control mechanism for the DSC scheme is further proposed, which flexibly optimizes the DSC performance in terms of either SDR or energy consumption by adapting the source coding and transmission parameters to the network conditions. Simulations are carried out to validate the efficiency of the proposed DSC scheme and the adaptive control mechanism for both saving energy and improving the quality of source estimation.

The remainder of this chapter is organized as follows. Section 4.2 reviews some energy-efficient techniques for wireless communications and MAC for sen-

sor networks. Section 4.3 formulates the problem and introduces a multi-mode power consumption model for wireless sensor communications. To provide a performance benchmark to be compared to that of the adaptive DSC scheme, Section 4.4 proposes a basic transmission scheme. Its performances for source estimation quality and energy consumption are also analyzed. Section 4.5 proposes a novel adaptive DSC scheme. The SDR performance of the DSC scheme is analyzed and used to find the optimal coding and transmission parameters in the adaptive DSC scheme. In Section 4.6, the energy consumption performance of the DSC scheme is analyzed and used as a constraint in the SDR optimization process of the adaptive DSC scheme. Simulation results are presented and discussed in Section 4.7. Section 4.8 summarizes the chapter.

4.2 Related Work

4.2.1 Energy-efficient Wireless Communications

There has been much research effort on hardware designs and software protocols to improve the energy efficiency in WSNs. Since wireless communication accounts for a major portion of the total energy consumption in a sensor node, controlling the communication cost is fundamental to prolonging the lifetime of a WSN.

Poon proposed and implemented a reconfigurable baseband processor architecture for wireless communications with energy efficiency approaching the dedicated hardware implementations [87]. Hong et al. analyzed the power dissipation, performance and hardware complexity of the fast Fourier transform (FFT) demodulator and the channel equalizer, and proposed an optimum multi-carrier receiver design with minimum power consumption through the tradeoff between the FFT size and the equalizer length [88, 89]. By employing energy constrained design techniques for the radio frequency (RF) receiver and transmitter circuits,

Larson et al. presented several new approaches to the minimization of the energy usage of a mobile wireless transceiver without compromising system performance in a dynamic operating environment [90].

Unlike in traditional wireless links where the transmission distance is large so that the transmission energy is dominant in the total energy consumption, in WSNs where sensor nodes are densely deployed the transmission distance is relatively small. In this circumstance the energy consumed in the onboard circuit becomes comparable to the transmission energy or even dominates the total energy consumption. Cui et al. investigated energy-constrained modulation and transmission optimization by analyzing the tradeoff of the transmission energy, circuit energy, transmission time and constellation size [91]. The peak-power and delay constraints were taken into account when minimizing the overall energy consumption. They also used same transceiver circuitry to analyze the total energy consumption where individual single-antenna sensor nodes were considered cooperating to form multiple-antenna transmitters or receivers [92].

Since a power consumption model similar to the one proposed in [91] and [92] for wireless sensor communications will be used in the subsequent sections of this chapter, in what follows, the system model of the RF transceiver circuitry used in [91] will briefly introduced. According to [91], the transceiver circuitry in sensor nodes works on a multi-mode basis: all circuits work in active mode when there is a signal to transmit, in sleep mode when there is no signal to transmit, and in transient mode when switching from sleep mode to active mode. Before transmitting a signal to the wireless channel, the baseband signal is first converted by the digital-to-analog converter (DAC) to an analog signal, filtered by the low-pass filter and modulated by the mixer with local oscillator (LO), then filtered again by the band-pass filter and finally amplified by the power amplifier (PA). Upon receiving a signal from the wireless channel, the RF signal

is first filtered and amplified by the low noise amplifier (LNA), cleaned by the antialiasing filter and demodulated by the mixer, then filtered again by the low-pass filter before going through the intermediate frequency amplifier (IFA) and finally converted by the analog-to-digital converter (ADC) to a digital signal [91]. Figure 4-1 illustrates the circuit blocks in the sensor node transceiver.

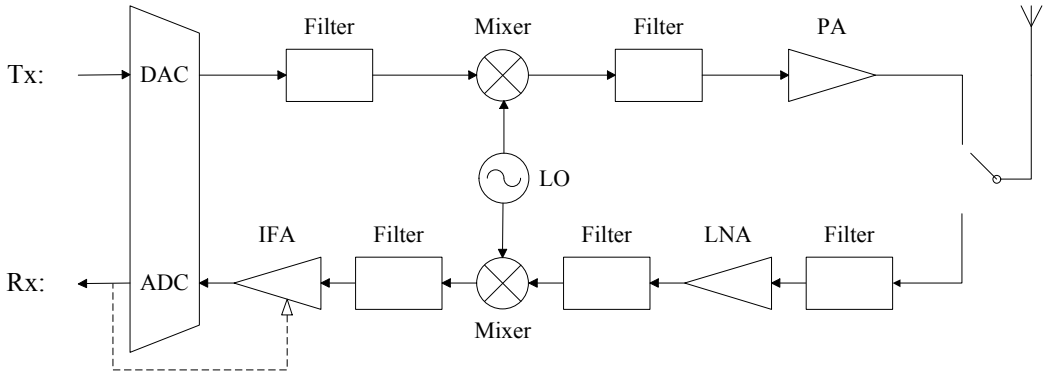

Figure 4-1: Transceiver circuit blocks in wireless sensor node. Dotted arrowheaded line means the adjustable gain of the IFA.

4.2.2 Energy-efficient MAC Protocols

Since the wireless channel is shared by all sensor nodes in the network, MAC is necessary to resolve contention when multiple sensor nodes require access to the channel. In addition, since WSNs are event-driven and events usually occur with a low frequency, sensor nodes normally remain idle. Idle listening is, therefore, the major source of energy waste in MAC for WSNs. Other energy inefficiencies come from collisions, overhearing, and control packet overhead. Waking up sensor nodes from a low-power mode such as sleep also affects the energy efficiency of MAC for WSNs.

Existing MAC protocols can be generally divided into two categories: contention-based (or CSMA-based) and TDMA-based (or collision-free) protocols. TDMA-based protocols conserve energy by reducing radio's duty cycle and eliminat-

ing collisions and contention-introduced overhead, especially for high traffic load conditions. Their major drawbacks are, however, the expensive cost to maintain a contention-free scheduling and clock synchronization in a distributed environment and lack of scalability and adaptability to dynamic network topology changes. There is some prior work on energy-efficient TDMA for WSNs, such as the TRAMA protocol [94] and the BMA protocol [95], although most recent work is on contention-based protocols including the best-known S-MAC [96], T-MAC [97], and B-MAC [98].

Compared with TDMA-based protocols, contention-based protocols for WSNs are normally simple to implement, flexible and robust to network changes, but they suffer from the energy inefficiency due to idle listening, collisions and overhearing. During low contention periods, however, contention-based protocols can give higher channel utilization, lower network delays, and even better energy efficiency than TDMA-based protocols. There have been some attempts to combine both CSMA and TDMA schemes to utilize their advantages, for example, the Z-MAC protocol [99], the HMAC protocol [100], and the pre-schedule scheme for hybrid MAC [101]. Various wake-up schemes have also been investigated for energy-efficient MAC for WSNs [102–105].

4.3 Problem Formulation

4.3.1 Problem Assumption

In this section, it is assumed that a WSN is designed to monitor remote targets. To save the energy consumption, multi-hop communication and clustering techniques are used in the WSN. Similar to Chapter 3, for simplicity, it is assumed that there is at most one active target at any time. Once the target becomes active, it is observed by the surrounding wireless sensor nodes clustered

in a sensing cell. The surrounding sensor nodes generate observation signals and transmit the signals via other sensor nodes to an information sink for further processing and taking corresponding actions. Since the focus of this chapter is on the energy efficiency and adaptive control of DSC, the routing problem for WSNs is not considered. Instead, for each active target, all the traffic generated from the surrounding sensor nodes is assumed to follow a predefined route to the sink. The route consists of n_r relay sensor nodes, which are numbered as 1 to n_r, towards the sink. Each sensor node in the sensing cell is one hop from the 1^{st} relay node. Since the duration of an active event in a WSN is generally short, this assumption is reasonable. In addition, as what will be presented in Section 4.5.1, the proposed DSC scheme operates in rounds, which can adapt to route changes.

For each active target, it is assumed that N individual sensor nodes in the sensing cell make synchronous, correlated and noisy measurements of the signal generated by the target (represented by a source process X). The N noisy observations $Y_1, \ldots, Y_N$ are quantized yielding $U_1, \ldots, U_N$. Basically, these quantized signals can be directly transmitted to the sink for further processing. This simple remote source estimation scheme is denoted as the basic transmission scheme and will be discussed in more detail in Section 4.4. To improve network performance by fully utilizing the correlations between sensor readings and also compress sensor data in one step, a random-binning based DSC scheme is used. The basic DSC scheme has been investigated in Chapter 3. Next will describe the adaptive DSC scheme which is illustrated in Figure 4-2.

Similar to the basic DSC scheme, the operation of the adaptive DSC scheme can be divided into *rounds*. In order to save the energy consumption, however, unlike the basic DSC scheme, not all the N noisy sensor readings are transmitted. In each round, $u(\geq 1)$ quantized readings are selected to be sent uncoded to

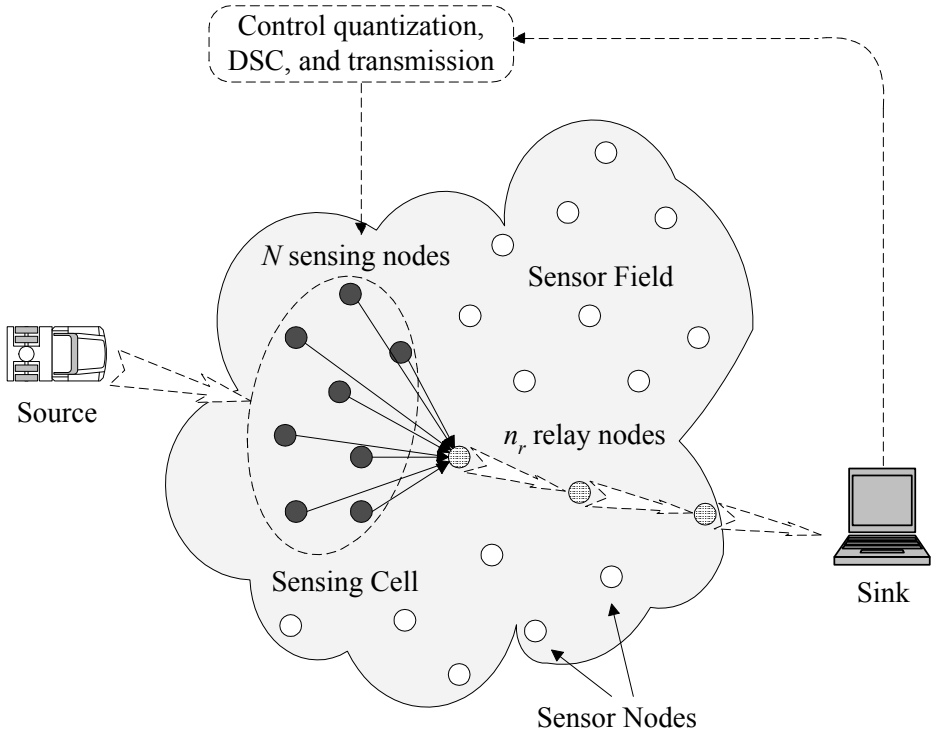

Figure 4-2: An adaptive DSC scheme for remote source estimation in a multi-hop WSN.

achieve a certain level of signal estimation reliability, among which s ($1 \leq s \leq u$) uncoded readings are selected as the condition of joint encoding. The other r ($\leq N - u$) quantized readings are randomly divided into groups of k ($1 \leq k \leq r$) readings and jointly encoded by the basic DSC scheme proposed in Section 3.4, yielding r indices $I_1, \ldots, I_r$. The r indices are then sent through the n_r relay nodes to the sink with the u uncoded readings $U_{r+1}, \ldots, U_{r+u}$ for joint decoding.

Furthermore, similar to the signal assumption made in Section 3.3, it is assumed that the source process $\{X(t)\}_{t=1}^{\infty} \sim \mathcal{N}(\overline{x}, \sigma_X^2)$ is an i.i.d. Gaussian source across time and the observation noise processes $\{N_i(t)\}_{t=1}^{\infty} \sim \mathcal{N}(0, \sigma_N^2)$ are i.i.d. Gaussian and independent of the source process. For the noisy sensor observations, let y_0 be the reference point for the uniform quantizer, Δ be the quantization step, and $\{q_i(t)\}_{t=1}^{\infty}$ be the quantization noise process with mean $\overline{q}$ and variance σ_q^2. With an appropriate choice of y_0 and Δ, the quantized sensor read-

ings are assumed to be Gaussianly-distributed, i.e.

$$\{U_i(t)\}_{t=1}^{\infty} \sim \mathcal{N}\left[\frac{1}{\Delta}(\overline{x} - y_0) + \overline{q}, \frac{1}{\Delta^2}(\sigma_X^2 + \sigma_N^2) + \sigma_q^2\right],$$

and are also conditionally independent and symmetrically correlated given the $X(t)$ samples. More details on the signal assumption have been give in equation (3.1) and (3.2). For concision of description, t will be omitted from the arguments of variables such as $X(t)$, $N_i(t)$ and $U_i(t)$, $i = 1, \ldots, n$, in the subsequent description. Note that the work presented in this chapter, however, can be extended to the case with general signal and noise distributions.

The transmitted sensor readings are subject to packet losses in the WSN. Suppose that the sink successfully receives j uncoded readings and m encoded indices. According to the property of the theoretic DSC proposed in Chapter 3, if $j = 0$, i.e. no uncoded reading is received, the sink can neither decode the received indices nor estimate the source signal X. If $j \geq 1$ uncoded readings are received, but m is less than k, the sink can estimate the source signal X only with the j received uncoded readings. Otherwise, the sink can decode the m received indices, and estimate the source signal X by first averaging the j received uncoded readings and m decoded readings and then dequantizing the averaged quantization value. The quality of source estimation, therefore, changes with different values of j and m. Figure 4-3 shows the above-described DSC scheme.

Since WSNs are generally characterized by limited network bandwidth and energy, the overall transmission rate of all transmitted sensor readings is constrained to the available network bandwidth. For simplicity, the available bandwidth is assumed known a priori. In practice, various methods can be used to measure the available network bandwidth, such as probing methods [93]. What needs to design then becomes high efficiency adaptive DSC schemes for WSNs, which achieve good quality of remote source estimation while satisfying network band-

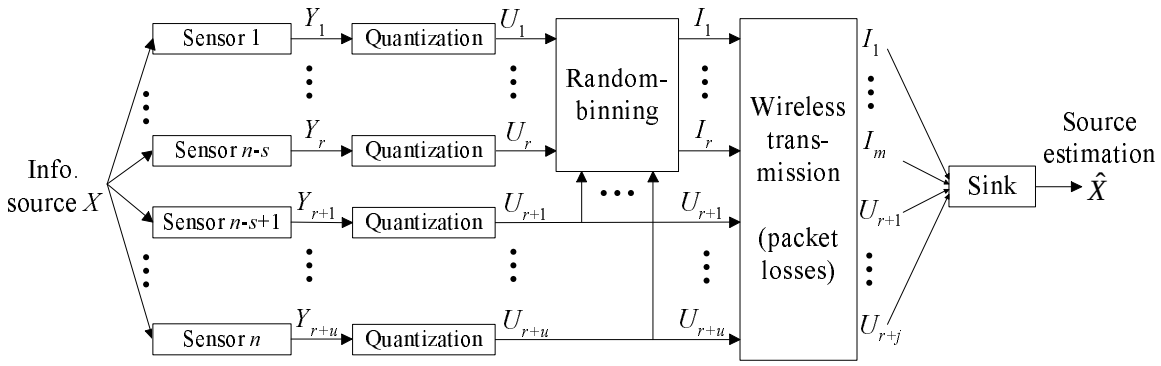

Figure 4-3: General DSC scheme for wireless sensor networks with possible packet losses. j out of u uncoded readings and m out of r encoded indices are successfully received by the sink.

width and energy conditions. In this chapter, the SDR is chosen as the metric of the estimation quality, where the distortion is calculated by the mean square error (MSE) of the estimated signal $\hat{X}$. The problems to be solved in the adaptive DSC scheme, therefore, become how to control the quantization processes, DSC and transmission parameters, and how sensor nodes communicate with the sink, to maximize the SDR under the constraints of decoding errors, available network bandwidth, and network energy consumption, or to minimize the network energy consumption, under the constraints of decoding errors, available network bandwidth, and SDR.

4.3.2 Multi-mode Power Consumption

In this chapter, a model similar to the power consumption model for wireless sensor communications proposed in [91] is used to analyze the energy consumption of both the basic transmission scheme and the DSC scheme. The difference from the model proposed in [91] is, however, that it is assumed when a sensor node is transmitting a signal only the transmitter circuit works in active mode, the receiver circuit works in sleep mode to save energy. Similarly, when a sensor node is receiving a signal, only the receiver circuit works in active mode while

the transmitter circuit works in sleep mode. To save energy, the transceiver circuit switches to sleep mode as soon as the signal transmission is finished, until the next signal transmission wakes it up. The transient mode is then for either the transmitter or the receiver circuit instead of both to switch from sleep mode to active mode.

For simplicity, it is assumed that the signal is modulated by uncoded M-order Quadrature Amplitude Modulation ($MQAM$). Let b denote the number of bits per symbol, B denote the bandwidth (in Hz), and P_b denote the bound of bit error probability. The transmission power is given by:

$$P_t = \frac{4}{3} B\sigma^2 N_f G_d (2^b - 1) \ln \frac{4\left(1 - 2^{-\frac{b}{2}}\right)}{bP_b}, \tag{4.1}$$

where σ^2 is the power spectral density of the additive white Gaussian noise (AWGN), N_f is the receiver noise figure, G_d is the power gain factor determined by link margin compensation M_l, gain factor G_1, transmission range d and pass loss exponent κ:

$$G_d = G_1 d^{\kappa} M_l. \tag{4.2}$$

The circuit power consumption in active mode at the transmitter and the receiver, are the same as those in [91], and are given by:

$$P_{ct} = P_{syn} + P_{filt} + P_{mix} + P_{DAC}; \tag{4.3}$$

and

$$P_{cr} = P_{mix} + P_{syn} + P_{LNA} + P_{filr} + P_{IFA} + P_{ADC}, \tag{4.4}$$

respectively, where P_{syn}, P_{mix}, P_{LNA}, P_{IFA}, P_{filt}, P_{filr}, P_{DAC} and P_{ADC} are the power consumption of frequency synthesizer, mixer, low noise amplifier (LNA), intermediate frequency amplifier (IFA), filter at the transmitter and the receiver,

digital-to-analog converter (DAC) and analog-to-digital converter (ADC), respectively.

The active mode power for a sensor transmitting a signal consists of P_t, P_{ct} and the power amplifier power P_{amp}, given by:

$$P_{on} = P_t + P_{ct} + P_{amp} = (1 + \alpha)P_t + P_{ct}, \tag{4.5}$$

where

$$\alpha = \frac{\xi}{\eta} - 1, \tag{4.6}$$

η is the drain efficiency of the power amplifier, ξ is the peak to average ratio (PAR):

$$\xi = 3\frac{\sqrt{M} - 1}{\sqrt{M} + 1}, \text{ and } M = 2^b. \tag{4.7}$$

The power consumption for the sleep mode is assumed to be zero. Since the transient mode is assumed to be for either the transmitter or the receiver circuit instead of both, the power consumption for the transient mode is half of that in [91], given by:

$$P_{tr} = P_{syn}. \tag{4.8}$$

4.4 Basic Transmission Scheme

4.4.1 Basic Transmission Scheme

As discussed in Section 4.3, in the basic transmission scheme the quantized sensor readings are directly transmitted to the sink without DSC encoding. Unlike the adaptive DSC scheme, which finds the optimal DSC and transmission parameters by interactions between the sink and sensor nodes, in the basic transmission scheme, it is assumed that the sink and the sensor nodes always know the best quantization and transmission parameters in order to achieve the maximum SDR

or the minimum energy consumption without any interaction. This assumption, therefore, minimizes the network overhead and results in better network performance, which provides a performance benchmark to be compared to that of the adaptive DSC scheme.

This section considers maximizing the SDR of the basic transmission scheme without the energy consumption constraint, as the primary concern of the basic transmission scheme is to ensure the SDR performance. However, the work can be extended to maximizing the SDR with an energy consumption constraint or minimizing the energy consumption with the network bandwidth and SDR constraints. Actually, this extension will be made in the design of the adaptive DSC scheme in the next section, by using the SDR or energy consumption of the basic transmission scheme as the constraint for the DSC scheme. Suppose that the quantization rate is n_0 and the available network bandwidth is B_w (in bps). To maximize the SDR under the network bandwidth constraint, the maximum allowed number of quantized sensor readings should be transmitted to the sink.

Figure 4-4 shows the time sequence process and packet format used by the basic transmission scheme. To improve the transmission efficiency, multiple readings of a sensor node in the sensing cell are put into one packet and sent to the sink. With every N_{sa} available samples of the source signal, each sensor node aggregates its N_{sa} quantized readings into one data packet (denoted by Data_uc) and transmits the data packet through the n_r relay nodes to the sink. The N_{sa} quantized readings are encapsulated with a packet header comprising L_{hd} bits flag ("00" for data packets), L_{pos} bits information of sensor node position, and L_{pk} bits information of quantization rate n_0.

For simplicity, the propagation delay is assumed to be zero. The sampling interval is denoted by T_{sa}. To enhance the network efficiency, the sensor nodes in the sensing cell are required to send their data through one hop to the 1^{st} relay

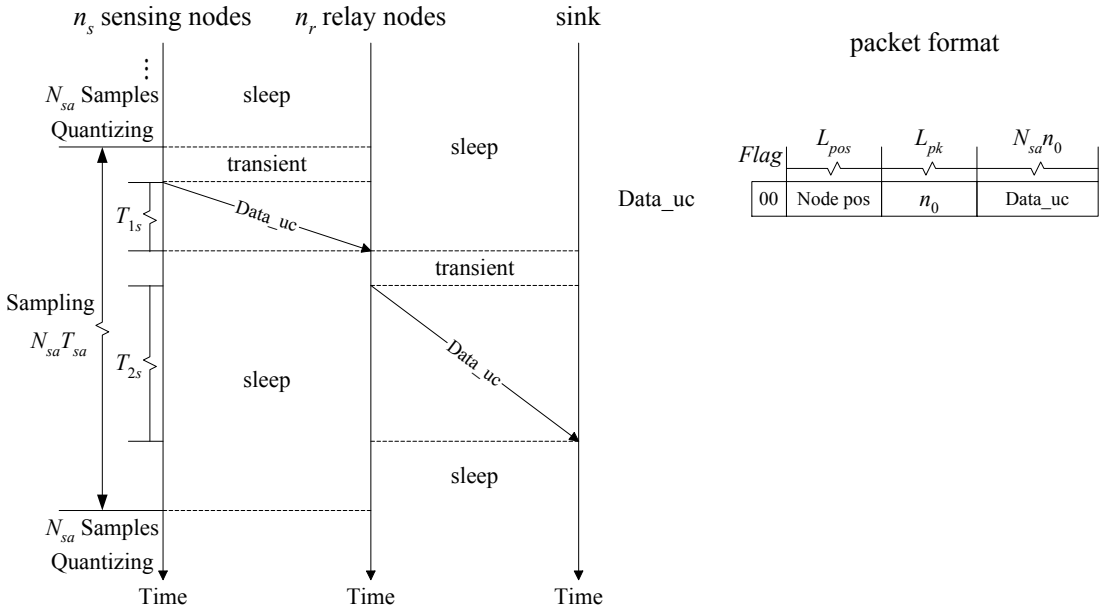

Figure 4-4: Time sequence process and packet format for the basic transmission scheme. The quantized readings are encapsulated in Data_uc packets and sent through relay nodes to the sink.

node within a deadline T, which is set as $T < N_{sa}T_{sa}$. Suppose in time T there are n_s sensor nodes in the sensing cell that can send their quantized readings to the 1^{st} relay node. In order to reduce the energy consumption, the 1^{st} relay node waits for time T to receive the data packets from the n_s sensor nodes before forwarding them to the 2^{nd} relay node. The maximum value of n_s, determined by the constraint of the consumed bandwidth being no larger than the available network bandwidth, is given by:

$$n_s \leq \frac{B_w T}{L_{hd} + L_{pos} + L_{pk} + N_{sa} n_0}. \tag{4.9}$$

The task of the basic transmission scheme is to control the parameters of the quantization rate (n_0) and the number of the transmitted quantized readings (n_s), in order to maximize the SDR under the constraint of (4.9).

4.4.2 SDR Calculation for Basic Transmission Scheme

This subsection calculates the SDR of the basic transmission scheme under the network bandwidth constraint. Since the transmitted quantized readings are subject to packet losses in the WSN, without loss of generality, it is assumed that v among n_s quantized readings are received by the sink. Combining equation (3.1) and (3.2), the v received quantized readings are expressed by:

$$U_i = \frac{1}{\Delta}(X + N_i - y_0) + q_i,\ i = 1, \ldots, v, \tag{4.10}$$

and their average, denoted by $\overline{U}$, is given by:

$$\begin{aligned} \overline{U} &= \frac{1}{v}\sum_{i=1}^{v} U_i \\ &= \frac{1}{\Delta}\left(X + \frac{1}{v}\sum_{i=1}^{v} N_i - y_0\right) + \frac{1}{v}\sum_{i=1}^{v} q_i. \end{aligned} \tag{4.11}$$

$\overline{U}$ is then dequantized to give the reconstructed source signal $\hat{X}$:

$$\begin{aligned} \hat{X} &= \Delta\overline{U} + y_0 \\ &= X + \frac{1}{v}\sum_{i=1}^{v} N_i + \Delta\frac{1}{v}\sum_{i=1}^{v} q_i. \end{aligned} \tag{4.12}$$

Since the $2nd$ moment of $\hat{X}$ is

$$\begin{aligned} \mathbb{E}\left[\hat{X}^2\right] &= \overline{x}^2 + \sigma_X^2 + \frac{1}{v^2}\cdot v\sigma_N^2 + \Delta^2\frac{1}{v^2}\left[v\left(\sigma_q^2 + \overline{q}^2\right) + v\left(v-1\right)\overline{q}^2\right] \\ &= \overline{x}^2 + \sigma_X^2 + \frac{1}{v}\sigma_N^2 + \frac{1}{v}\Delta^2\sigma_q^2 + \Delta^2\overline{q}^2, \end{aligned} \tag{4.13}$$

the signal to distortion ratio of the basic transmission scheme, denoted by SDR_s, is then given by:

$$SDR_s = \frac{v\left(\overline{x}^2 + \sigma_X^2\right)}{\sigma_N^2 + \Delta^2\sigma_q^2 + v\Delta^2\overline{q}^2}. \tag{4.14}$$

The packet loss rate per hop in the wireless channels is assumed to be uniformly distributed with mean of p_l. The probability of receiving v among n_s quantized readings is then given by:

$$P_v = C_{n_s}^{v}(1-p_p)^v p_p^{n_s-v}, \tag{4.15}$$

where p_p denotes the end-to-end packet loss rate from the sensor nodes in the sensing cell to the sink and is:

$$p_p = 1-(1-p_l)^{n_r+1}. \tag{4.16}$$

The expectation of SDR_s is, therefore, given by:

$$\mathbb{E}[SDR_s] = \sum_{v=1}^{n_s}\left[P_v \cdot \frac{v(\overline{x}^2+\sigma_X^2)}{\sigma_N^2+\Delta^2\sigma_q^2+v\Delta^2\overline{q}^2}\right]. \tag{4.17}$$

The optimal quantization rate n_0 and number of the transmitted quantized readings n_s are obtained by maximizing $\mathbb{E}[SDR_s]$ given in (4.17) for a given network condition (available network bandwidth B_w and packet loss rate per hop p_l).

4.4.3 Energy Consumption of Basic Transmission Scheme

In addition to the SDR, the network energy consumption is another critical performance metric for remote source estimation in WSNs. Although the network energy consumption is not put as a constraint for optimizing the SDR of the basic transmission scheme, it is used as the energy consumption constraint for the DSC scheme proposed in the next section. Therefore in this subsection the energy consumption of the basic transmission scheme is analyzed.

In the current design, only the energy consumed in the sensing cell and the n_r relay nodes for the active and transient modes are considered. The energy

consumed at the sink is not considered because the sink is assumed to have a high signal processing capability and an unlimited energy supply. Since sampling and quantization are indispensable operations for any source estimation scheme, the energy required by these operations is not considered here. The total energy consumption, therefore, focuses on the energy required to transmit and receive data packets in active mode and the energy consumed in transient mode.

As shown in Figure 4-4, T_{1s} denotes the time for one hop transmission of n_s Data_uc packets from the sensing cell to the 1^{st} relay node. Let T_{Data_uc} denote the transmission time of a Data_uc packet,

$$T_{Data\_uc} = \frac{L_{hd} + L_{pos} + L_{pk} + N_{sa} n_0}{B_w}. \tag{4.18}$$

T_{1s} is then given by:

$$T_{1s} = n_s \cdot T_{Data\_uc}. \tag{4.19}$$

T_{2s} denotes the time for transmission of all the received uncoded data packets from the 1^{st} relay node to the sink. Since the transmitted data packets are subject to packet losses in the WSN, only $(1 - p_l)$ part of the received packets at each relay node are sent to the next node. T_{2s} is then given by:

$$\begin{aligned} T_{2s} &= \sum_{i=1}^{n_r} (1 - p_l)^i \cdot T_{1s} \\ &= \frac{1 - p_l}{p_l} \left[1 - (1 - p_l)^{n_r}\right] T_{1s}. \end{aligned} \tag{4.20}$$

Due to the packet losses in the WSN, the time spent at the n_r relay nodes for receiving the uncoded data packets, denoted by T_{7s}, is given by:

$$T_{7s} = \sum_{i=0}^{n_r - 1} (1 - p_l)^i \cdot T_{1s}$$

$$= \frac{1-(1-p_l)^{n_r}}{p_l} T_{1s}. \tag{4.21}$$

Since when relaying a packet each relay node works in transient mode twice to successively switch on the receiver and transmitter circuits, the total transient time for transmitting the uncoded data packets is:

$$T_{10s} = (n_s + 2n_r)T_{tr}, \tag{4.22}$$

where T_{tr} is the transient mode duration. The overall network energy consumption of the basic transmission scheme in an operation round, denoted by E_s, is then given by:

$$E_s = P_{on}(T_{1s} + T_{2s}) + P_{cr}T_{7s} + P_{tr}T_{10s}, \tag{4.23}$$

where P_{cr}, P_{on}, and P_{tr} are given by (4.4), (4.5), and (4.8), respectively.

4.5 Adaptive DSC scheme

4.5.1 Adaptive DSC scheme

The objective of the adaptive DSC scheme is, similar to that of the basic transmission scheme, to optimize the source estimation quality under the constraints of available network bandwidth B_w and energy consumption. The SDR is chosen as the metric for the estimation quality. Figure 4-5 shows the time sequence process and packet format of the adaptive DSC control scheme.

Suppose that the quantization rate is n_0, the number of uncoded readings as the condition of joint encoding is s, and the number of joint encoding nodes is k. According to Section 3.4, the random binning encoding rate R_k should be no less than $R_{kc}(s,k)$ (given by (3.13)) and should be larger than a value (denoted by R_{rb}) determined by the expected decoding error probability, P_{rb} (given by

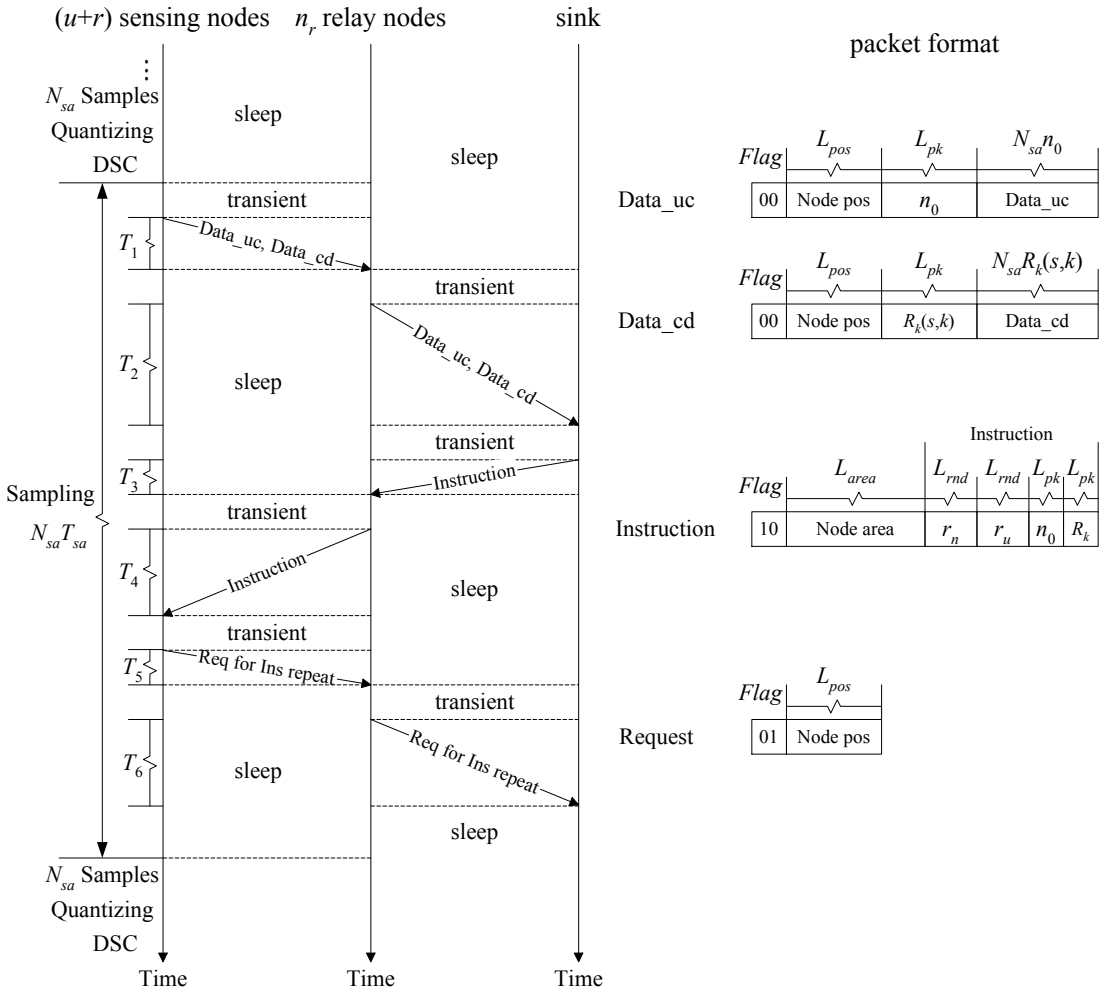

Figure 4-5: Time sequence process and packet format of the adaptive DSC scheme. The uncoded readings and encoded indices are encapsulated in Data_uc and Data_cd packets, respectively. The optimal parameters determined by the sink are encapsulated in Instruction packet and sent to the sensing cell.

(3.38)). The threshold of coding rate is, therefore, given by:

$$R_{th}(s,k) = max(R_{kc}(s,k), R_{rb}), \tag{4.24}$$

where $max()$ is a choosing of the largest value from the value set. The practical random-binning coding rate R_k is required to satisfy:

$$R_k(s,k) \in (R_{th}(s,k), n_0 - 1]. \tag{4.25}$$

Suppose the number of transmitted uncoded quantized readings is u, and the number of transmitted encoded indices is r. To improve the transmission efficiency, with every N_{sa} available samples of the source signal, each sensor node aggregates its N_{sa} observation readings into one data packet (denoted by Data_uc or Data_cd, depending on being uncoded or encoded with random-binning) and transmits the data packet through the n_r relay nodes to the sink. Both the uncoded readings and encoded indices are encapsulated with a packet header comprising L_{hd} bits flag ("00" for data), L_{pos} bits information of sensor node position, and L_{pk} bits information of sensor reading size (n_0 or R_k).

Similar to the basic transmission scheme, the propagation delay is assumed to be zero, and the sampling interval is denoted by T_{sa}. Suppose the deadline for the $u + r$ sensor nodes in the sensing cell to send their data through one hop to the 1^{st} relay node is set as T. In order to reduce the energy consumption, the 1^{st} relay node waits for time T to receive the data packets from the $u + r$ sensors before forwarding them to the 2^{nd} relay node. The constraint of the consumed bandwidth (denoted by B_c, in bps) being no larger than the available network bandwidth is then given by:

$$B_c = \frac{u(L_{hd} + L_{pos} + L_{pk} + N_{sa}n_0) + r[L_{hd} + L_{pos} + L_{pk} + N_{sa}R_k(s,k)]}{T}$$

$$\leq \quad B_w. \tag{4.26}$$

The task of the adaptive DSC scheme is to control the parameters of u, r, s, k, and n_0, in order to optimize the SDR under the constraint of (4.26) while keeping the network energy consumption low.

To implement the adaptive DSC scheme, the sensor nodes and the sink operate as follows:

- Sink:

  1) The sink first collects the information of the detected source signal ($\overline{x}$, σ_X, σ_N).

  2) After receiving the sensor readings from the n_r^{th} relay node, the sink reconstructs the source signal from the received readings, estimates the available network bandwidth (B_w) and the packet loss rate per hop (denoted by p_l), then determines the optimal source coding (n_0, s, k, R_k) and transmission (u, r) parameters for the sensor nodes' next round of operation, based on the analysis described in the next subsection.

  3) To balance the energy consumption of the sensor nodes in the sensing cell, and to control the number of uncoded and coded readings sent to the sink in a distributed way, two variables r_u and r_n are used, which are defined as:

$$r_u = \frac{u}{N}; \tag{4.27}$$

$$r_n = \frac{u+r}{N}. \tag{4.28}$$

  The sink calculates r_u and r_n, and then sends the instruction (r_n, r_u, n_0, R_k) back to the sensing cell through the n_r relay nodes. The instruction is encapsulated with a packet header comprising L_{hd} bits flag ("10" for

instruction) and L_{area} bits information of sensing cell area's position which is used for multicast from the 1^{st} relay node to the sensing cell.

- Sensor nodes in the sensing cell:

  1. It is assumed that all sensor nodes in the sensing cell are well-scheduled to wake up to receive the instruction from the sink for the next round of operation.
  2. However, the transmitted instructions are subject to packet losses in the WSN. If a sensor node has not received the instruction by a predetermined time period, it sends a request through the n_r relay nodes to the sink and asks the sink to resend the instruction. The request packet consists of L_{hd} bits flag ("01" for request) and L_{pos} bits information of sensor node position.
  3. If there are multiple sensor nodes not receiving the instruction, only one request is sent, since the other sensors will know about the transmission of request by sensing the channel after the predetermined time period.

- Sink:

  4) Upon receiving a request, the sink extracts the information of the sensor node position, finds the sensing cell which the sensor node belongs to, then sends the instruction again to the sensing cell through the relay nodes.
  5) The operations of sending a request and instruction are repeated until all the sensor nodes in the sensing cell receive the sink's instruction before the next round of operation begins.

- Sensor nodes in the sensing cell:

4. Each sensor node receiving the instruction creates a random number uniformly distributed in $[0, 1]$, and compares the random number with r_n and r_u given in the instruction.

5. If the random number is larger than r_n, the sensor node turns to sleep, otherwise it turns to sample the source signal and quantize its readings with quantization rate n_0 in the next round of operation.

6. If the random number of a sensor node is larger than r_u, the sensor node is also selected to encode its quantized readings with random-binning rate R_k and sends its random-binning indices to the sink. Otherwise the sensor node only sends its quantized readings to the sink.

- Sink:

6) After the sink collects the sensor readings and reconstructs the source signal, it updates the information of $\bar{x}$, σ_X, σ_N, B_w and p_l, and determines a set of optimal source coding and transmission parameters. A new round of operation then begins.

4.5.2 SDR Calculation for Adaptive DSC scheme

This subsection calculates the SDR of the adaptive DSC scheme. The coding and transmission parameters achieving the best source estimation are determined by analyzing the impact of the parameters on the SDR.

Since the coding rate bound $R_{th}(s, k)$ (given by (4.24)) may be nonintegral while the practical coding rate $R_k(s, k)$ (given by (4.25)) is required to be integral, the random-binning decoding requirement is looser-bounded than that mentioned in Section 4.3.1, i.e. when $j \geq 1$ uncoded readings are received, as long as the average entropy of the j readings and m indices is larger than $R_{th}(j, m)$, the sink can decode the m indices, and estimate the source signal X with the j uncoded

readings and m decoded readings. Otherwise the sink can not decode the m indices, and the source signal is estimated only with the j uncoded readings. The threshold value of the number of received indices, denoted by m_{th}, is, therefore, determined by:

$$j \cdot n_0 + m \cdot R_k(s,k) \geq (m+j) \cdot R_{th}(j,m). \tag{4.29}$$

Without loss of generality, it is assumed that j uncoded readings and m indices are received by the sink, and l among m indices are not correctly decoded. Let $D_{rb}(l)$ denote the total decoding deviation produced by l incorrectly decoded readings, similar to the SDR calculation for the basic transmission scheme (Section 4.4.2), the SDR of the adaptive DSC scheme is given by the following three possible cases:

1) $SDR = 0$, when $j = 0$;

2) $SDR = \dfrac{j(\overline{x}^2 + \sigma_X^2)}{\sigma_N^2 + \Delta^2\sigma_q^2 + j\Delta^2\overline{q}^2}$, when $1 \leq j \leq s$, $0 \leq m < m_{th}$;

3) $SDR = \dfrac{(m+j)(\overline{x}^2 + \sigma_X^2)}{\sigma_N^2 + \Delta^2\sigma_q^2 + (m+j)\left[\Delta\overline{q} + \dfrac{1}{m+j}\Delta D_{rb}(l)\right]^2}$, when $1 \leq j \leq s$, $m_{th} \leq m \leq r$.

According to Section 3.4.3, one decoding error usually provides a decoded quantization value with a deviation within 2^{R_k} from the original value. Due to the symmetry of the deviation, the total deviation for the l incorrectly decoded readings is modeled as:

$$D_{rb}(l) = \rho l 2^{R_k}, \tag{4.30}$$

where ρ is a distortion coefficient within $[0,1]$.

Assuming that the packet loss rate per hop in the wireless channels is uniformly distributed with mean of p_l, the end-to-end packet loss rate from the

sensing cell to the sink is p_p given by (4.16). The probabilities of receiving j uncoded readings and m indices are, therefore, given by

$$P_j = C_u^j (1-p_p)^j p_p^{u-j} \tag{4.31}$$

and

$$P_m = C_r^m (1-p_p)^m p_p^{r-m}, \tag{4.32}$$

respectively. Similarly, the probability of incorrectly decoding l of m indices is given by

$$P_l = C_m^l (1-P_{rb})^{m-l} P_{rb}^l. \tag{4.33}$$

Considering the joint distribution of P_j, P_m and P_l, the source estimation quality is found by calculating the expectation of the SDR, given by:

$$\begin{aligned}\mathbb{E}[SDR] = &\sum_{j=1}^{u} \sum_{m=0}^{[m_{th}]-1} \left[P_j P_m \cdot \frac{j(\overline{x}^2 + \sigma_X^2)}{\sigma_N^2 + \Delta^2 \sigma_q^2 + j\Delta^2 \overline{q}^2} \right] \\ &+ \sum_{j=1}^{u} \sum_{m=[m_{th}]}^{r} \sum_{l=0}^{m} \left[P_j P_m P_l \cdot \frac{(m+j)(\overline{x}^2 + \sigma_X^2)}{\sigma_N^2 + \Delta^2 \sigma_q^2 + (m+j)\left(\Delta \overline{q} + \frac{1}{m+j} \rho l 2^{R_k} \Delta\right)^2} \right], \end{aligned} \tag{4.34}$$

where $[m_{th}]$ denotes the value of the smallest integer no less than m_{th}.

The optimal coding and transmission parameters are obtained by maximizing $\mathbb{E}[SDR]$ given in (4.34) for a given network condition (available network bandwidth B_w and packet loss rate per hop p_l) under the energy consumption constraint.

4.6 Energy Consumption of Adaptive DSC Scheme

In this section the energy consumption of the adaptive DSC scheme is analyzed. Similar to Section 4.4.3, in the current design, only the energy consumed in

the sensing cell and the n_r relay nodes for the active and transient modes are considered. The energy consumed at the sink and at the sensor nodes for sampling and quantization is not considered. Furthermore, the energy consumption for DSC encoding in the sensing cell is also neglected because of the low complexity of modulo operation [86]. The total energy consumption of the adaptive DSC control scheme, therefore, focuses on the energy required to transmit and receive data, instruction and request packets in active mode and the energy consumed in transient mode.

As shown in Figure 4-5, T_1 denotes the time for one hop transmission of u Data_uc packets and r Data_cd packets from the sensing cell to the 1^{st} relay node. Let T_{Data_cd} denote the transmission time of a Data_cd packet, given by:

$$T_{Data\_cd} = \frac{L_{hd} + L_{pos} + L_{pk} + N_{sa}R_k(s,k)}{B_w}. \tag{4.35}$$

T_1 is, therefore, given by:

$$T_1 = u \cdot T_{Data\_uc} + r \cdot T_{Data\_cd}, \tag{4.36}$$

where T_{Data_uc} is given by (4.18). T_2 denotes the time for transmission of all the received data packets from the 1^{st} relay node to the sink. Similar to T_{2s} in the basic transmission scheme, T_2 is given by:

$$\begin{aligned} T_2 &= \sum_{i=1}^{n_r} (1-p_l)^i \cdot T_1 \\ &= \frac{1-p_l}{p_l}\left[1-(1-p_l)^{n_r}\right] T_1. \end{aligned} \tag{4.37}$$

Let T_{Ins} and T_{Req} denote the transmission time of an instruction and request

packet respectively, given by:

$$T_{Ins} = \frac{L_{hd} + L_{area} + 2L_{rnd} + 2L_{pk}}{B_w}; \tag{4.38}$$

and

$$T_{Req} = \frac{L_{hd} + L_{pos}}{B_w}. \tag{4.39}$$

Since the transmission of instruction and request packets is to ensure all the sensor nodes in the sensing cell receive the instruction, the average number of instruction packets sent by the sink in an operation round is determined by the following analysis:

- Consider the probability that after i multicasts the instruction packet sent from the 1^{st} relay node has been successfully received by all the N nodes in the sensing cell, which is given by $(1 - p_l^i)^N$. The probability that the instruction packet is successfully received by all the N nodes after exactly i multicasts, denoted by P_i, is then given by:

$$P_i = (1 - p_l^i)^N - (1 - p_l^{i-1})^N. \tag{4.40}$$

- It is assumed that after the sink sends exactly n ($n \geq i$) instruction packets, all the N nodes successfully receive the instruction. This means the last transmission of instruction packet from the sink (through n_r hops) to the 1^{st} relay node is successful and the nodes in the sensing cell which are waiting for the instruction finally receive it. Let $P_I(n, i)$ denote the probability that i transmissions (including the last successful transmission) among the n transmissions to the 1^{st} relay node are successful. $P_I(n, i)$ is, therefore,

given by:

$$\begin{aligned} P_I(n,i) &= C_{n-1}^{i-1} \cdot [1-(1-p_l)^{n_r}]^{n-i} \cdot [(1-p_l)^{n_r}]^{i-1} \cdot (1-p_l)^{n_r} \\ &= C_{n-1}^{i-1} [1-(1-p_l)^{n_r}]^{n-i} (1-p_l)^{in_r}. \end{aligned} \tag{4.41}$$

- Considering the joint distribution of P_i and $P_I(n,i)$, the probability that all the N nodes receive the instruction after the sink sends exactly n instruction packets is given by:

$$\begin{aligned} P_I(n) &= \sum_{i=1}^{n} P_I(n,i) \cdot P_i \\ &= \sum_{i=1}^{n} C_{n-1}^{i-1} [1-(1-p_l)^{n_r}]^{n-i} (1-p_l)^{in_r} \left[(1-p_l^i)^N - (1-p_l^{i-1})^N\right] \end{aligned} \tag{4.42}$$

  The average number of instruction packets sent by the sink, denoted by N_I, is then given by:

$$N_I = \sum_{n=1}^{\infty} n \cdot P_I(n). \tag{4.43}$$

Since a request packet is sent from the sensing cell to the 1^{st} relay node if there is at least one node that does not receive the instruction, the fact that there are n instruction packets sent by the sink means there are $(n-1)$ request packets sent from the sensing cell. The average number of request packets sent from the sensing cell, denoted by N_R, is, therefore, determined by:

$$N_R = N_I - 1. \tag{4.44}$$

As shown in Figure 4-5, T_3 denotes the average transmission time of the instruction packets from the sink to the n_r^{th} relay node, which is

$$T_3 = N_I \cdot T_{Ins}. \tag{4.45}$$

The average transmission time of the instruction packets from the n_r^{th} relay node to the sensing cell, denoted by T_4, is given by:

$$\begin{aligned} T_4 &= \sum_{i=1}^{n_r}(1-p_l)^i \cdot T_3 \\ &= \frac{1-p_l}{p_l}\left[1-(1-p_l)^{n_r}\right]T_3. \end{aligned} \tag{4.46}$$

T_5 denotes the average transmission time of the request packets from the sensing cell to the 1^{st} relay node, which is

$$T_5 = N_R \cdot T_{Req}. \tag{4.47}$$

The average transmission time of the request packets from the 1^{st} relay node to the sink, denoted by T_6, is given by:

$$\begin{aligned} T_6 &= \sum_{i=1}^{n_r}(1-p_l)^i \cdot T_5 \\ &= \frac{1-p_l}{p_l}\left[1-(1-p_l)^{n_r}\right]T_5. \end{aligned} \tag{4.48}$$

Due to the packet losses in the WSN, the time spent at the n_r relay nodes for receiving the data packets is:

$$\begin{aligned} T_7 &= \sum_{i=0}^{n_r-1}(1-p_l)^i \cdot T_1 \\ &= \frac{1-(1-p_l)^{n_r}}{p_l}T_1. \end{aligned} \tag{4.49}$$

Similarly, the average time spent at the n_r relay nodes and the N nodes in the sensing cell for receiving the sink's instruction is:

$$T_8 = \sum_{i=0}^{n_r-1}(1-p_l)^i \cdot T_3 + N \cdot (1-p_l)^{n_r} \cdot T_3$$

$$= \left[\frac{1}{p_l} + \left(N - \frac{1}{p_l}\right)(1-p_l)^{n_r}\right] T_3, \tag{4.50}$$

and the average time spent at the n_r relay nodes for receiving the request sent from the sensing cell is given by:

$$\begin{aligned} T_9 &= \sum_{i=0}^{n_r-1} (1-p_l)^i \cdot T_5 \\ &= \frac{1-(1-p_l)^{n_r}}{p_l} T_5. \end{aligned} \tag{4.51}$$

The total transient time in the adaptive DSC scheme for transmitting data, instruction and request packets is given by:

$$\begin{aligned} T_{10} &= (u + r + 2n_r)T_{tr} + N_I(2n_r + N)T_{tr} + N_R(1 + 2n_r)T_{tr} \\ &= [u + r + N_I N + N_R + 2n_r(N_I + N_R + 1)]T_{tr}, \end{aligned} \tag{4.52}$$

where T_{tr} is the transient mode duration.

Considering the operations in active mode and transient mode, the overall network energy consumption of the adaptive DSC scheme in an operation round, denoted by E, is given by:

$$E = P_{on}(T_1 + T_2 + T_4 + T_5 + T_6) + P_{cr}(T_7 + T_8 + T_9) + P_{tr}T_{10}. \tag{4.53}$$

Using the network energy consumption as an extra constraint for optimizing the SDR performance of the adaptive DSC scheme, the task of the adaptive DSC scheme then becomes that of controling the parameters of u, r, s, k and n_0 under the constraint of (4.26), in order to maximize $\mathbb{E}[SDR]$ while keeping E less than E_s (denoted by the *SDR criterion*), or to minimize E while keeping $\mathbb{E}[SDR]$ larger than $\mathbb{E}[SDR_s]$ (denoted by the *energy criterion*). Since the size of the parameter space is small, a simple method is used to exhaustively search over the parameter

space to compute the optimal source coding and transmission parameters with equation (4.34). It is computation-efficient to find the best parameters.

4.7 Simulation Results

4.7.1 Simulation Method and Parameters

In this section, some typical simulation results will be presented to illustrate the effectiveness of the proposed adaptive DSC scheme. The simulation is implemented in Matlab and used to evaluate the performance of the scheme. For the reported results, each value is obtained by averaging over 30 simulations. For each simulation, the network is simulated for 30 minutes. Since the basic transmission scheme is simple and robust, it is used as a benchmark to evaluate the proposed adaptive DSC scheme against. The values of simulation parameters, used to obtain the simulation results, are summarized in Table 4.1.

In the simulations, the mean of the Gaussian source $\overline{x} = 0$, the variance of the source and the observation noise are $\sigma_X^2 = 200$ and $\sigma_N^2 = 30$, respectively. A uniform quantizer for Gaussian signals is used with the quantization rate $n_0 \in \{6, 7, 8\}$. The expected decoding error probability $P_{rb} = 0.015$. The distortion coefficient is set as an empirical value $\rho = 0.25$. The number of active sensor nodes in the sensing cell is set to 10. The number of relay nodes is set to 3. The network bandwidth $B_w \in [30, 60]$ Kbps and the packet loss rate $p_l \in \{0.025, 0.05, 0.1, 0.2\}$. The number of samples in each data packet $N_{sa} = 100$. The sampling interval $T_{sa} = 10$ ms. The deadline T to transmit all data packets through one hop is set to 100 ms. For the data packet encapsulation, L_{hd}, L_{pk}, L_{pos}, L_{area} and L_{rnd} are set to 2, 4, 16, 32 and 8, respectively. The bandwidth is 50 KHz. The number of bits per symbol for uncoded $MQAM$ is set to 4, and the bound of bit error probability is set to 10^{-4}. The transmission range is set as an average value of

Table 4.1: Parameters for simulation of adaptive DSC scheme

Variable	Value	Variable	Value
$\bar{x}$	0	B	50 KHz
σ_X^2	200	b	4
σ_N^2	30	P_b	10^{-4}
n_0	{6,7,8}	d	50 m
P_{rb}	0.015	T_{tr}	5 μs
ρ	0.25	N_f	10 dB
N	10	M_l	40 dB
n_r	3	G_1	30 dB
B_w	[30,60] Kbps	κ	3.5
p_l	{0.025,0.05,0.1,0.2}	P_{syn}	50 mW
N_{sa}	100	P_{mix}	30.3 mW
T_{sa}	10 ms	P_{filt}	2.5 mW
T	100 ms	P_{filr}	2.5 mW
L_{hd}	2	P_{LNA}	20 mW
L_{pk}	4	P_{IFA}	3 mW
L_{pos}	16	η	0.35
L_{area}	32	σ^2	-174 dBm/Hz
L_{rnd}	8		

$d = 50$ m. The values of all other parameters for power calculation are the same as those specified in [91]. With the above settings, the DSC scheme adaptively searches for the optimal source coding and transmission parameters, while the basic transmission scheme only searches for the maximum allowed number of transmitted quantized readings.

4.7.2 Simulation Results

Typical simulation results for the optimal SDR performance are plotted in Figure 4-6 for different network bandwidth and packet loss rate. Figure 4-6(a) shows the optimal SDR using the *SDR criterion*, and Figure 4-6(b) shows the optimal SDR using the *energy criterion*, both for the adaptive DSC scheme and the

basic transmission scheme. It is observed that in the investigated scenarios, the adaptive DSC scheme using the *SDR criterion* generally achieves up to 1.5 dB SDR improvement compared to the basic transmission scheme without increasing the energy consumption. This shows the effectiveness of improving the signal estimation performance. Although the absolute SDR improvement is not so high, in the case of $p_1 = 0.025$, increasing the network bandwidth from 30 Kbps to 60 Kbps only results in a SDR increase of 2.5 dB for the adaptive DSC scheme using the *SDR criterion*. A 1.5 dB improvement of SDR is, therefore, not negligible. The evaluation consideration can be changed to the bandwidth consumption: for the network scenario of $p_1 = 0.0025$, if the received SDR performance is required to be 17 dB, the adaptive DSC scheme using the *SDR criterion* consumes 40 Kbps, while the basic transmission scheme consumes nearly 50% more bandwidth.

The average energy consumption of the adaptive DSC scheme (using the *SDR criterion* and the *energy criterion*) and the basic transmission scheme in one operation round, associated with the optimal SDR performance in Figure 4-6, are plotted in Figure 4-7 and denoted by DSC, DSC (E) and Basic, respectively, for different network bandwidth and packet loss rate. It is observed that the adaptive DSC scheme using the *energy criterion* generally saves up to 31.6% energy consumption compared to the basic transmission scheme without decreasing the estimation performance. Even using the *SDR criterion* the adaptive DSC scheme saves up to 9.4% energy consumption compared to the basic transmission scheme. This shows the energy efficiency of the proposed adaptive DSC schem for signal estimation.

Figure 4-8 shows the obtained source coding parameters (quantization rate n_0, random-binning coding rate R_k, number of uncoded readings as the condition of joint encoding s, and number of joint encoding nodes k), which are associated with the optimal SDR performance presented in Figure 4-6. Figure 4-8(a) and

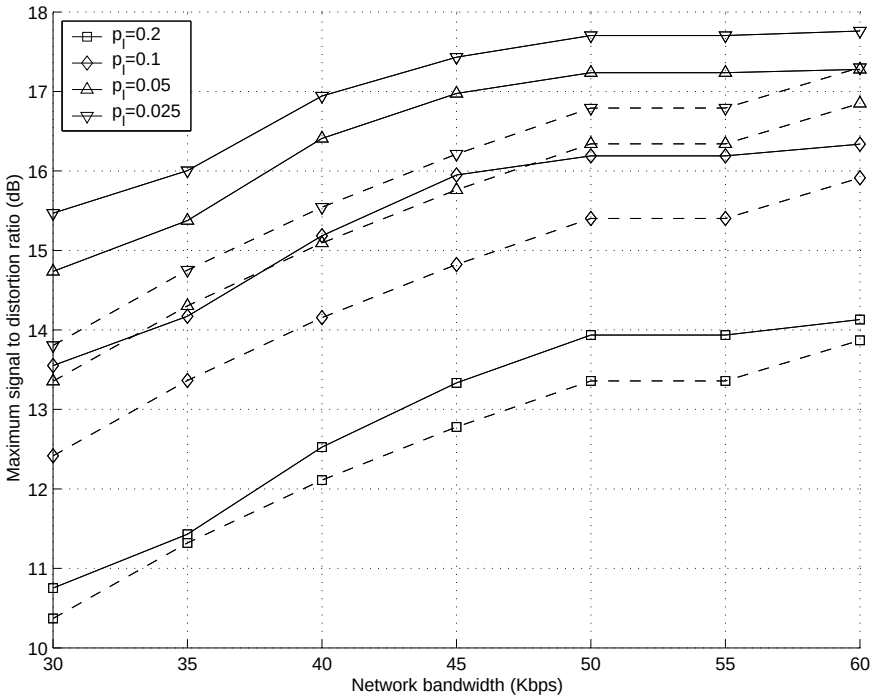

(a) By *SDR criterion*

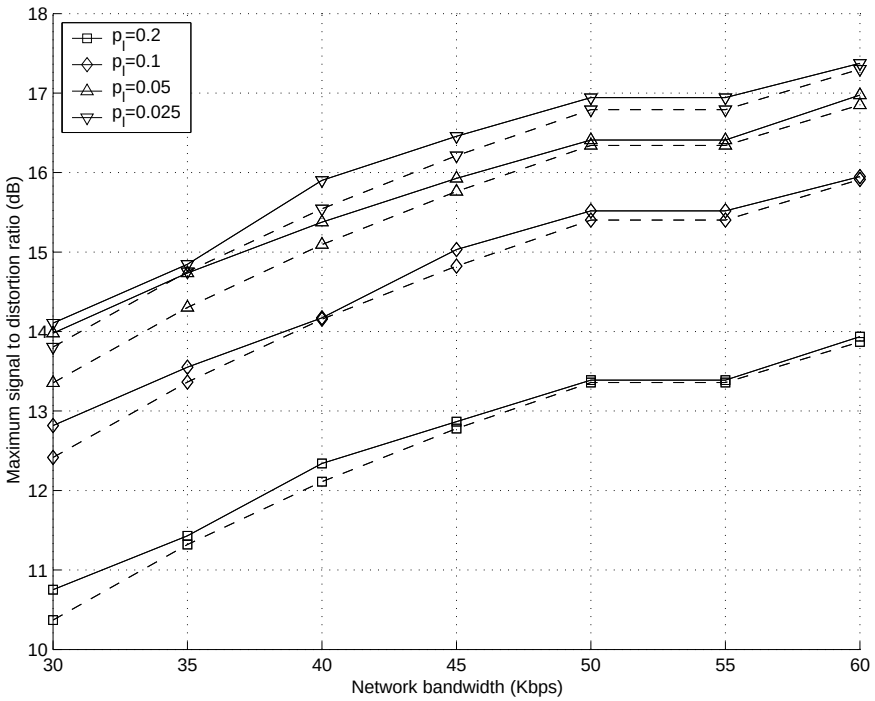

(b) By *energy criterion*

Figure 4-6: Optimal estimation performance (SDR) for the adaptive DSC scheme (solid) and the basic transmission scheme (dashed), versus network bandwidth B_w and packet loss rate p_l.

Figure 4-8(b) show the results using the *SDR criterion* and the *energy criterion*, respectively. Figure 4-9 shows the obtained optimal transmission parameters (number of transmitted uncoded readings u and number of transmitted encoded indices r) using the *SDR criterion* and the *energy criterion* (denoted by (E)).

Note that although the optimal parameters and the signal estimation performance are different for the two criteria, they can be adopted separately or jointly in the adaptive DSC scheme, to fully utilize the tradeoff between the source estimation quality and the energy efficiency.

4.8 Summary

This chapter has studied the problem of remote source estimation in WSNs with application of a random-binning based DSC scheme. Compared to a basic transmission scheme, in the DSC scheme the correlated sensor readings are jointly encoded in a distributed way and sent to the sink for decoding and further processing. The SDR performance of both the basic transmission scheme and the DSC scheme is modeled as a function of observation noise, quantization, network bandwidth constraint and network packet losses. Based on the SDR model, an adaptive DSC scheme is proposed and the packet format for the scheme is designed, with which the SDR performance can be optimized by adapting the source coding and transmission parameters to the changing network conditions (available network bandwidth and packet loss rate). With the introduction of a multi-mode power model for wireless sensor communications, the network energy consumption of the basic transmission scheme and the DSC scheme is also quantitatively analyzed. The energy consumption is then used as an extra constraint for SDR performance optimization of the adaptive DSC scheme to find the optimal source coding and transmission parameters. Simulation results show the proposed adaptive DSC scheme either consumes up to 31.6% less energy without

decreasing the SDR or maximizes the SDR with up to 9.4% energy saving.

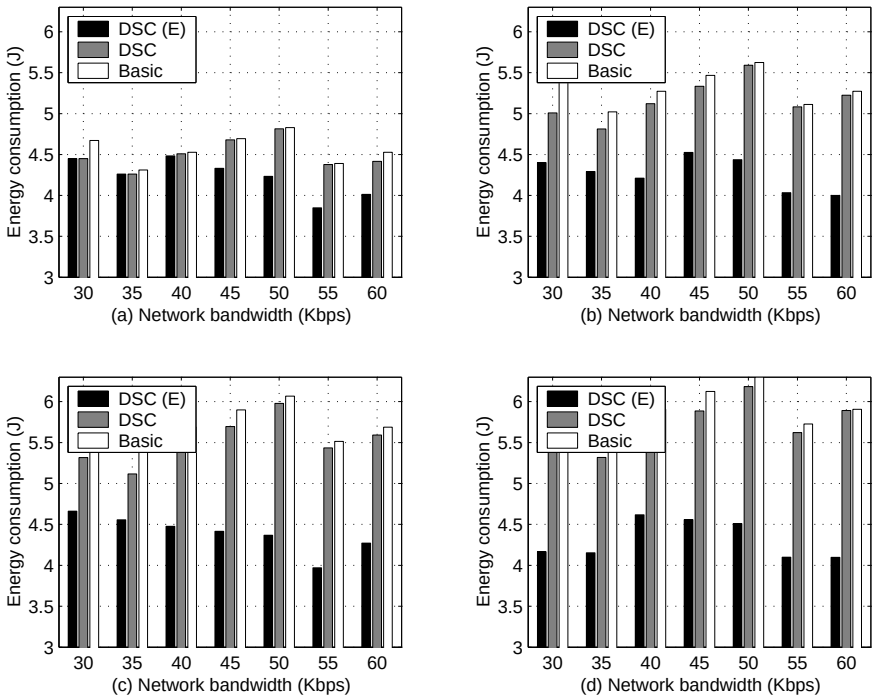

Figure 4-7: Energy consumption performance associated with the optimal SDR performance: (a) $p_l = 0.2$, (b) $p_l = 0.1$, (c) $p_l = 0.05$, (d) $p_l = 0.025$.

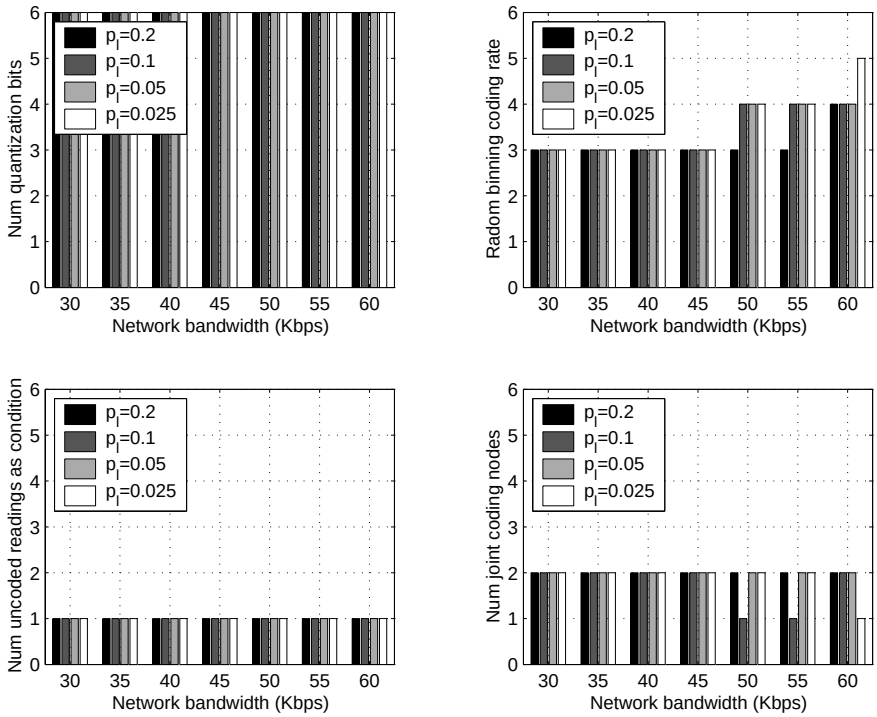

(a) Using the *SDR criterion*

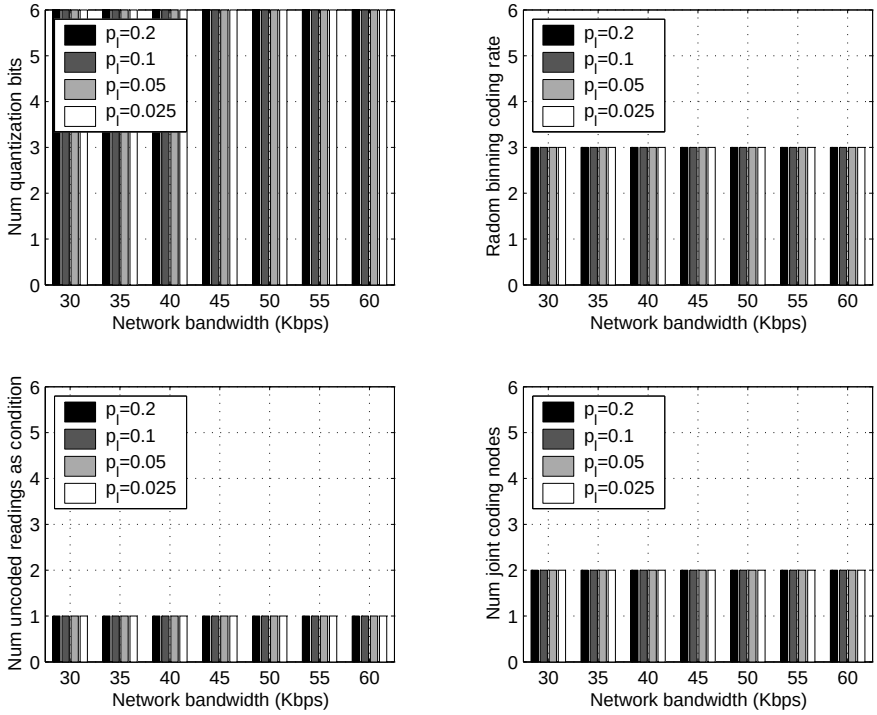

(b) Using the *energy criterion*

Figure 4-8: Optimal source coding parameters (n_0, R_k, s, k) associated with the optimal SDR performance, versus network bandwidth B_w and packet loss rate p_l.

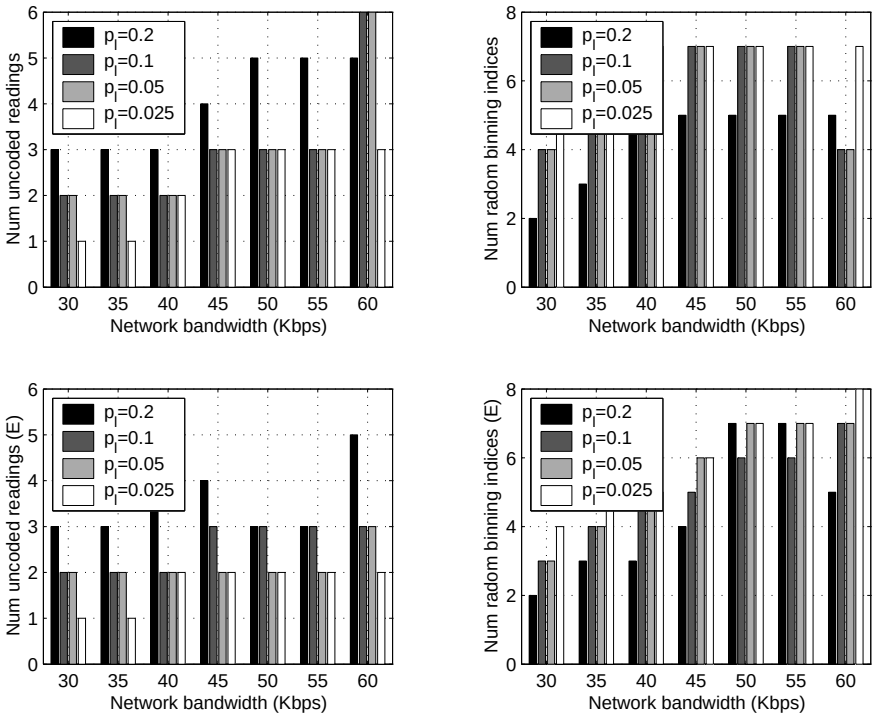

Figure 4-9: Optimal transmission parameters (u, r) associated with the optimal SDR performance, using the *SDR criterion* and the *energy criterion* (denoted by (E)), respectively.

Chapter 5

Localization in Wireless Sensor Networks

5.1 Introduction

WSNs can be used to realize a large number of parallel-distributed systems that interact with the physical world [2,106]. In many of these applications, including source detection and tracking, location estimation is a vital component. Without information about node location, the origin of data received at the sink node can not be identified, and may become meaningless in some applications (e.g. source tracking). Location information is also useful in the design and operation of efficient networking and management protocols. Geographically based network routing and network-sensor node coordination for target tracking [107] are examples.

Due to the importance and utilization of location information, numerous localization algorithms have been proposed for WSNs [108–110]. The large scale and difficulty of re-deploying a WSN make planning and pre-evaluation of the localization algorithms important. The large number of sensor nodes, however, makes

discrete-event sensor network simulations (e.g. the network simulator (NS-2) and OPNET [111, 112]) and field tests challenging. Diverse application requirements and network environments make the localization problems difficult. Efficient, convenient, and adaptive evaluation tools for different localization algorithms, which can be applied to various application and network scenarios, would be useful. Using evaluation results (e.g. location accuracy, computation complexity, energy and bandwidth overheads), sensor networks can be dimensioned, deployed and controlled using appropriate localization algorithms and configuration parameters. For example, the number and placement of anchor nodes and the best localization algorithm for a specific network application and environment can be determined. The location accuracy can be traded-off for lower energy consumption and less bandwidth. Much effort has been expended on the development and evaluation of sensor localization algorithms. Theoretical analysis and scalable evaluation of multi-hop localization algorithms, however, still need further research.

In this chapter, theoretical analysis of two general localization algorithms is carried out for large-scale WSNs. Cramer-Rao bound (CRB) analysis is applied to determine the lower bound of the variance of unbiased location estimations for multi-hop sensor networks. The statistical lower bound can be viewed as the best estimation accuracy that can be achieved for different kinds of location algorithms, and can be used as a tool for the evaluation and optimization of localization algorithms for WSNs. CRB analysis is not only quick and efficient but also scalable for large-scale WSNs. Such large-scale networks may present a extreme challenge for simulation-based approaches. To underline the efficiency of CRB analysis, simulation has been used to evaluate the means and variances of several distributed localization algorithms. Using both analytical and simulation approaches, insights can be got into not only the accuracy sensitivity of the

estimation to ranging errors but also the impacts of available anchor nodes and their locations on estimation performance. These insights can help to compare, select and configure different distributed and centralized localization algorithms for large-scale WSNs.

In the remainder of this chapter, related work is surveyed in Section 5.2. The localization algorithms are presented in Section 5.3. The Cramer-Rao bound problem is formulated in Section 5.4. A CRB-based analytical approach is developed in Section 5.5. Typical simulation results and discussions are presented in Section 5.6 and Section 5.7, respectively, and the chapter is summarized in Section 5.8.

5.2 Related Work

CRB-based analysis has received much research attention in the context of WSNs [113–115]. It is used to provide a lower bound for the positioning error of location algorithms, achievable for a given sensor network setup. Larsson proposed a CRB analysis for a collaborative and a non-collaborative location algorithm for single-hop WSNs [113]. (Collaborative means that all distance measurements among anchor nodes and non-anchor sensor nodes are exploited to determine a node's location, whilst non-collaborative means that only the distance measurements between anchor nodes and an unknown node is used to determine this node's location.) Both collaborative and non-collaborative algorithms were implemented in a centralized way. It was demonstrated analytically that collaborative location algorithm can improve location accuracy. Catovic and Sahinoglu analyzed the CRB of a hybrid time-of-arrival (TOA) and received signal strength (RSS) based location estimation scheme, and also a time-difference-of-arrival (TDOA) and RSS based scheme [114]. The impacts of different ranging measurements on the estimation accuracy were investigated. Their analysis, however, is also

focused on single-hop sensor networks and is not appropriate for the multi-hop location problem. A CRB analysis for multi-hop WSNs was presented in [115], in which it was assumed that the distances between any two sensor nodes are available to determine the locations of the nodes with unknown locations. This assumption, however, is ideal. It is not practical for a localization algorithm to obtain and report the information of all the distances in a large-scale WSN. Such CRB analysis cannot, therefore, provide insights to the evaluation of practical localization algorithms.

The benefit (better accuracy) of centralized implementations of localization needs to be justified in terms of the consequent communication overhead. Niculescu and Nath proposed a lower bound for positioning error in a multi-hop network for a distributed range/angle free algorithm [116]. The theoretical analysis does not work for range-based algorithms and cannot be used for comparison with centralized algorithms. A quantitative comparison of distributed localization algorithms was presented in [117]. Three distributed localization algorithms (Ad-hoc positioning [108], Robust positioning [109], and N-hop multilateration [110]) were compared on a single simulation platform. A common three-phase structure was identified for the distributed localization algorithms [117]. Detailed comparison showed that no algorithm performs best and there exists room for improvement in most cases. Simulation-based evaluation, however, is not scalable to evaluate localization algorithms for large-scale sensor networks.

5.3 Distributed Localization Algorithms

In WSNs, sensor nodes with known, either absolute or relative, locations, are called anchor nodes. The primary purpose of a localization algorithm is to estimate the (absolute or relative) locations of unknown sensor nodes, using the available anchor nodes. This chapter will consider only localization problems for

absolute location estimations.

Localization algorithms can be divided into two major categories: range-based and range-free. In range-based location algorithms, distance or angle estimations between neighboring nodes are used to calculate node locations. Typical range-based algorithms include the sum-distance algorithm [110, 117]. In range-free algorithms, the distance or angle information between neighboring nodes is assumed to be unavailable for localization due to cost and hardware limitations. DV-hop (distance-vector, in hops) algorithm is a typical range-free location algorithm [108, 109].

Location algorithms may be implemented in either centralized or distributed forms to trade off accuracy, communication and computation overhead. Here, centralized algorithms are taken to be those that incorporate a sink. The sink collects all the available information, such as measured distances between sensor nodes (within communication range) and estimated distances from unknown sensor nodes to anchor nodes. It then determines the locations for unknown sensor nodes in a centralized way. After the sink determines the locations, it sends the location information back to the sensor nodes. In a distributed localization algorithm, the function of determining the locations is distributed over sensor nodes themselves, instead of implemented at a (privileged) sink.

Since more information is gathered and utilized to determine the nodes' locations in centralized algorithms, they may have better location accuracy compared to that of distributed localization algorithms. Centralized algorithms, however, have big communication and computational challenges. In addition, as sensor nodes normally have no identification, it is very difficult for the sink to send location information back to sensor nodes. Centralized localization algorithms are, therefore, normally limited to use in small-scale sensor networks or for understanding the upper performance bounds of distributed localization algorithms.

In this chapter, CRB analysis is used to study the lower bounds of estimation variances for two centralized localization algorithms, whilst simulation will be used to investigate four distributed localization algorithms. The algorithm structure proposed in [117] is used. There are three-phases:

(1) to determine the distances from the unknown nodes to the anchor nodes;

(2) to compute the nodes' locations;

(3) to optionally refine locations using an iterative procedure.

The investigated distributed localization algorithms consist of only the first two phases. It is intended that the third phase will be considered in the future work. The methods of determining node distances and computing node positions is now addressed.

5.3.1 Determination of Distances to Anchor Nodes

In this phase, sensor nodes share information to collectively determine the distances between individual unknown nodes within communication range, and between nodes and anchor nodes. Simple calculation methods can be used for this purpose. A common routing method used is flooding, which is initiated from the anchor nodes. Since a network-wide flood by an anchor node will be too expensive for large networks, flooding is controlled in practical localization algorithms. Specifically, as it is possible to derive a good estimation on a node's location with the knowledge of the location of, and distance from, a limited number of anchor nodes, forwarding information can be stopped when enough anchor nodes have been found [117]. The flooding control presented in [109] was shown to be highly effective in reducing the amount of communication overhead. For simplicity, however, in this chapter network-wide flooding will be assumed such

that the maximum possible anchor information is gathered thereby maximizing estimation accuracy.

Three methods to determine distances to anchor nodes are summarized in [117]. These are:

- Sum-dist:

  Sum-dist (sum of distance) is a simple solution to determining the distance from unknown nodes to anchor nodes, where the ranges encountered at each hop during network-wide flooding are simply summed [110, 117]. It resembles minimal-distance routing protocols for wireless ad hoc networks.

  Anchor nodes start the network-wide flooding by sending a message, including their identity, position, and a path length set to 0, to sensor nodes one hop from them. Each node receiving a message from an anchor node updates the path length using the measured range from the anchor node to it, records the distance to the anchor node, and forwards the message to other sensor nodes one hop from it. When a node receives a forwarded message, it updates the path length in the received message by adding the measured range from the forwarding node to the path length, and estimates the distance to the initiating anchor node using the updated path length. If a node receives more than one message initiated from the same anchor node, only the minimum distance to the initiating anchor node will be recorded, and only the message resulting in the minimum distance will be forwarded to other sensor nodes.

- DV-hop:

  A drawback of Sum-dist is the accumulation of range measurement errors when path length information is propagated over multiple hops. The cumulative error may become significant for large networks with poor ranging

performance. An alternative is to count the number of the hops to the anchor nodes instead of summing up the ranges [108, 109].

DV-hop essentially consists of two network-wide flooding waves. The first wave is similar to that in Sum-dist, in which sensor nodes obtain the position of, and the minimum hop count to, anchor nodes. The difference is that during this wave each anchor node also estimates the average hop distance to it, by dividing the cumulative distances to other anchor nodes by the cumulative hop counts to other anchor nodes. The estimated average hop distances are also propagated from anchor nodes to unknown nodes by controlled flooding. In the second wave, each hop count at an unknown node is converted to a distance to an anchor node, by multiplying the hop count by the estimated average hop distance updated at the unknown node.

- Euclidean:

  Euclidean is another method based on the local geometry of the nodes around an anchor node [117]. Similar to Sum-dist, flooding is initiated by anchor nodes, to forward the information about the position of, and the distance to, anchor nodes. The computation and forwarding of the distances to anchor nodes are, however, more complicated. A node receiving messages from two neighbors, with information of their distances to an anchor node and to each other, can calculate the Euclidean distance to the anchor node. Two methods, called *neighbor vote* and *common neighbor*, respectively, are applied to reduce or eliminate the uncertainty of the choice between two possible distances. The computed Euclidean distances, instead of the summed range measurements in the Sum-dist method, are forwarded over the multiple-hop network. More details can be found in [117].

5.3.2 Computation of Node Locations

In the second phase, unknown nodes determine their locations based on the estimated distances to anchor nodes provided by the methods in the first phase [117]. Trilateration was used for this purpose in [108, 109]. A much simpler method, called Min-max, was used in [110]. In both cases no additional communication is need to determine the node locations.

- Trilateration:

  Trilateration is a form of triangulation. It is the most common method for deriving a location. For example, assume that there are n anchor nodes. For a node with the estimated distances (d_i) to, and the location (x_i, y_i) of, the anchor node i, $i \in [1, n]$, the following system of equations are derived as shown in [117] for the unknown node location (x, y):

$$\begin{cases} (x_1 - x)^2 + (y_1 - y)^2 = d_1^2, \\ (x_2 - x)^2 + (y_2 - y)^2 = d_2^2, \\ \vdots \\ (x_{n-1} - x)^2 + (y_{n-1} - y)^2 = d_{n-1}^2, \\ (x_n - x)^2 + (y_n - y)^2 = d_n^2. \end{cases} \tag{5.1}$$

  By subtracting the last equation from the first $n - 1$ equations, the system of equations can be linearized and written in the form

$$A\mathbf{x} = b, \tag{5.2}$$

where

$$A = \begin{bmatrix} 2(x_1 - x_n) & 2(y_1 - y_n) \\ 2(x_2 - x_n) & 2(y_2 - y_n) \\ \vdots & \vdots \\ 2(x_{n-1} - x_n) & 2(y_{n-1} - y_n) \end{bmatrix}, \tag{5.3}$$

$$b = \begin{bmatrix} x_1^2 - x_n^2 + y_1^2 - y_n^2 + d_n^2 - d_1^2 \\ x_2^2 - x_n^2 + y_2^2 - y_n^2 + d_n^2 - d_2^2 \\ \vdots \\ x_{n-1}^2 - x_n^2 + y_{n-1}^2 - y_n^2 + d_n^2 - d_{n-1}^2 \end{bmatrix}, \tag{5.4}$$

and

$$\mathbf{x} = \begin{bmatrix} x \\ y \end{bmatrix}. \tag{5.5}$$

The equations can be solved by a standard least squares approach [117]:

$$\hat{\mathbf{x}} = (A^T A)^{-1} A^T b \tag{5.6}$$

.

- Min-max:

  Since trilateration is costly in terms of the number of required floating point computations, a simpler method, called Min-max (minimum and maximum), was proposed by Savvides et al. in [110]. For each unknown sensor node, this method first constructs a bounding box for each anchor node using the location of, and the estimated distances to, the anchor node. The

middle position of the intersection of these boxes is then determined as the estimated location of the unknown sensor node [117].

Consider, for example, determining the location of node k. The bounding box of an anchor node i for node k is created by adding and subtracting the estimated distance ($d_{k,i}$) from the anchor node's location (x_i, y_i). The lower left and the upper right corner coordinates of this box are $(x_i - d_{k,i}, y_i - d_{k,i})$ and $(x_i + d_{k,i}, y_i + d_{k,i})$, respectively. The intersection of the bounding boxes is a smaller box, with the lower left and the upper right corner coordinates computed by taking the maximum of all coordinate minimums, and the minimum of all coordinate maximums, as $(max(x_i - d_{k,i}), max(y_i - d_{k,i}))$ and $(min(x_i + d_{k,i}), min(y_i + d_{k,i}))$, respectively. The final location is obtained by averaging both corner coordinates [117].

5.4 Problem Formulation

For simplicity, this chapter focuses on range-based localization protocols. However, it is noted that the work presented here can be extended to range-free protocols.

Assume N nodes, among which N_k nodes are known anchors. Generally, a range-based localization problem in WSNs can be stated as follows:

With absolute location information of several anchor nodes and distance measurements (or estimates) of some pairs of nodes available, how to produce a set of coordinate assignments for each unknown node, such that the estimated distances between the node pairs are as close as to the measured or estimated distances.

In this section, besides the N_k anchor nodes with known locations, the location estimation of the remaining N_u ($N_u = N - N_k$) nodes will be considered. The unknown nodes are numbered as 1 to N_u, while the anchor nodes are numbered

as $N_u + 1$ to N. Let

$$\mathbf{x} = [x_1, \ldots, x_{N_u}]^T, \text{ and } \mathbf{y} = [y_1, \ldots, y_{N_u}]^T \tag{5.7}$$

be the vectors containing the coordinates of the N_u unknown nodes, where $(\cdot)^T$ denotes the transpose. Define $\mathbf{\Theta}$ as a vector given by:

$$\mathbf{\Theta} = [\theta_1, \ldots, \theta_{N_u}, \theta_{N+1}, \ldots, \theta_{N+N_u}]^T = \left[\mathbf{x}^T, \mathbf{y}^T\right]^T, \tag{5.8}$$

where θ_i ($i \in \{[1, N_u] \bigcup [N+1, N+N_u]\}$) represents one of $(x_1, \ldots, x_{N_u}, y_1, \ldots, y_{N_u})$. $\mathbf{\Theta}$ is then the parameter vector to be estimated for locating the unknown nodes.

Denote the one-hop distance between node k and node l by

$$d_{k,l} = \sqrt{(x_k - x_l)^2 + (y_k - y_l)^2}, \text{ where } k, l \in [1, N] \text{ and } k \neq l; \tag{5.9}$$

and let

$$t_{k,l} = \frac{d_{k,l}}{c} \tag{5.10}$$

be the one-hop propagation delay between node k and node l, where c is the speed of light. For simplicity, all the sensor nodes are assumed to be synchronized. Clock bias of sensor nodes is not considered here. It can be taken into account, however, by a method similar to that used in [113]. The ranging measurements are assumed to be estimates based on the noisy TOA. The measured propagation delay between any two directly connected nodes is assumed to be subject to independent additive white Gaussian noise (AWGN). The measured one-hop propagation delay between node k and node l is modeled as:

$$\hat{t}_{k,l} = t_{k,l} + e_{k,l}, \tag{5.11}$$

where $e_{k,l}$ is zero-mean, Gaussian noise with variance $\sigma_{k,l}^2$. The measured one-hop propagation delay is then Gaussianly-distributed:

$$\hat{t}_{k,l} \sim \mathcal{N}\left(t_{k,l}, \sigma_{k,l}^2\right).$$

The multidimensional criterion to determine the positions of all unknown nodes is, therefore, given by a minimum square error (MSE) form with respect to all elements in Θ:

$$min \sum_{k=1}^{N} \sum_{l=1, l\neq k}^{N} \frac{1}{\sigma_{k,l}^2} \left(\hat{t}_{k,l} - t_{k,l}\right)^2,$$

i.e.:

$$min \sum_{k=1}^{N} \sum_{l=1, l\neq k}^{N} \frac{1}{c^2\sigma_{k,l}^2} \left[\sqrt{\left(\hat{x}_k - \hat{x}_l\right)^2 + \left(\hat{y}_k - \hat{y}_l\right)^2} - \sqrt{\left(x_k - x_l\right)^2 + \left(y_k - y_l\right)^2}\right]^2.$$

5.5 Cramer-Rao Bound Analysis

With regard to the the localization problem formulated in Section 5.4, it is possible to use both centralized and distributed localization algorithms to determine the unknown nodes' locations. CRB analysis can be applied to both centralized and distributed localization algorithms. In this section, only the CRB analysis for two centralized algorithms is presented. It can be easily extended, however, to the four distributed location algorithms investigated in this chapter. As centralized localization algorithms can provide better location estimation accuracy than their distributed counterparts, the lower bound variances found from CRB analysis for the centralized localization algorithms can also be regarded as the lower bound variances for the corresponding distributed localization algorithms.

In what follows, the CRB analysis for centralized location estimation in single-hop WSNs will be presented in Section 5.5.1. Two centralized localization algorithms are considered, the CL-basic and the CL-refine algorithms, respectively.

In the CL-basic algorithm, only the distances between unknown nodes and anchor nodes are reported to and used by the sink to estimate the locations of unknown nodes in the network. In the CL-refine algorithm, local refinement is used, i.e. the locally available distances between two neighboring nodes are also reported to and used by the sink for location estimation. Similar local refinement is used in the third phase of some distributed localization algorithms. CRB analysis is extended to the location estimation in multi-hop WSNs in Section 5.5.2.

5.5.1 Location Estimation in One-hop Wireless Sensor Networks

In a one-hop WSNs each sensor node is within communication range of any other node. In the CL-refine algorithm, therefore, the locations of anchor nodes and the measured distances between any pair of nodes are used to determine the locations of unknown nodes. In the CL-basic algorithm, however, only the locations of anchor nodes and the measured distances between any unknown node and any anchor node are used to determine the locations of unknown nodes.

Generally, the CRB is a lower bound on the variance of any unbiased estimator of a deterministic parameter, and is given by the inverse of the Fisher information. Denoting $\hat{\mathbf{x}}$ and $\hat{\mathbf{y}}$ as the unbiased estimator of the coordinates vectors $\mathbf{x}$ and $\mathbf{y}$, respectively:

$$\hat{\mathbf{x}} = [\hat{x}_1, \ldots, \hat{x}_{N_u}]^T, \;\; \hat{\mathbf{y}} = [\hat{y}_1, \ldots, \hat{y}_{N_u}]^T, \tag{5.12}$$

the unbiased estimator of the unknown nodes' locations, denoted by $\hat{\mathbf{\Theta}}$, is given by

$$\hat{\mathbf{\Theta}} = \left[\hat{\theta}_1, \ldots, \hat{\theta}_{N_u}, \hat{\theta}_N, \ldots, \hat{\theta}_{2N_u}\right]^T = [\hat{\mathbf{x}}^T, \hat{\mathbf{y}}^T]^T. \tag{5.13}$$

For any unbiased estimator $\hat{\mathbf{\Theta}}$, the CRB states that

$$\mathbb{C}(\hat{\mathbf{\Theta}}) \geq [\mathcal{I}(\mathbf{\Theta})]^{-1}, \tag{5.14}$$

where $\mathbb{C}(\hat{\mathbf{\Theta}})$ is the covariance matrix of $\hat{\mathbf{\Theta}}$ and $\mathcal{I}(\mathbf{\Theta})$ is the Fisher information matrix (FIM) of the parameter vector $\mathbf{\Theta}$.

$$\mathcal{I}(\mathbf{\Theta}) = \begin{bmatrix} \mathbf{I}_{x,x} & \mathbf{I}_{x,y} \\ \mathbf{I}_{x,y}^T & \mathbf{I}_{y,y} \end{bmatrix}, \tag{5.15}$$

in which $\mathbf{I}_{x,x}$, $\mathbf{I}_{y,y}$, and $\mathbf{I}_{x,y}$ are the FIM of vector $\mathbf{x}$, the FIM of vector $\mathbf{y}$, and the FIM between vector $\mathbf{x}$ and $\mathbf{y}$, respectively.

The calculation of the FIM of the parameter vector $\mathbf{\Theta}$ is broken down into calculations of the Fisher information of multiple parameter scalars. Consider the measurement of the one-hop propagation delay between any node k and node l ($k, l \in [1, N]; k \neq l$), and let θ_i ($i \in \{[1, N_u] \bigcup [N+1, N+N_u]\}$) represent one of $(x_1, \ldots, x_{N_u}, y_1, \ldots, y_{N_u})$. As the measured propagation delay $\hat{t}_{k,l}$ is Gaussian, the likelihood function of the unknown parameter θ_i is:

$$\begin{aligned} L\left(\theta_i|\hat{t}_{k,l}\right) &= f\left(\hat{t}_{k,l}|\theta_i\right) \\ &= \frac{1}{\sqrt{2\pi}\sigma_{k,l}} e^{-\frac{\left(\hat{t}_{k,l}-t_{k,l}\right)^2}{2\sigma_{k,l}^2}}. \end{aligned} \tag{5.16}$$

The score, denoted by $V(\theta_i)$, is determined by the partial derivative of the logarithm of the likelihood function with respect to parameter θ_i and is given by:

$$\begin{aligned} V(\theta_i) &= \frac{\partial}{\partial\theta_i} \log L\left(\theta_i|\hat{t}_{k,l}\right) \\ &= \frac{\hat{t}_{k,l}-t_{k,l}}{\sigma_{k,l}^2} \cdot \frac{\partial t_{k,l}}{\partial\theta_i} + \left[\frac{\left(\hat{t}_{k,l}-t_{k,l}\right)^2}{\sigma_{k,l}^3} - \frac{1}{\sigma_{k,l}}\right] \frac{\partial\sigma_{k,l}}{\partial\theta_i}. \end{aligned} \tag{5.17}$$

The squared score is then given by:

$$[V(\theta_i)]^2 = \frac{\left(\hat{t}_{k,l}-t_{k,l}\right)^2}{\sigma_{k,l}^4}\left(\frac{\partial t_{k,l}}{\partial\theta_i}\right)^2 + \left[\frac{\left(\hat{t}_{k,l}-t_{k,l}\right)^4}{\sigma_{k,l}^6} - \frac{2\left(\hat{t}_{k,l}-t_{k,l}\right)^2}{\sigma_{k,l}^4} + \frac{1}{\sigma_{k,l}^2}\right]\left(\frac{\partial\sigma_{k,l}}{\partial\theta_i}\right)^2$$

$$+ 2 \left[\frac{\left(\hat{t}_{k,l} - t_{k,l}\right)^3}{\sigma_{k,l}^5} - \frac{\hat{t}_{k,l} - t_{k,l}}{\sigma_{k,l}^3} \right] \frac{\partial t_{k,l}}{\partial \theta_i} \cdot \frac{\partial \sigma_{k,l}}{\partial \theta_i}. \tag{5.18}$$

Since for unbiased parameter estimation the expectation of the score is zero, the Fisher information $I(\theta_i)$, defined as the variance of the score, is determined by the expectation of the squared score:

$$\begin{aligned} I(\theta_i) &= \mathbb{E}\left\{[V(\theta_i)]^2 | \theta_i\right\} \\ &= \frac{1}{\sigma_{k,l}^2} \left(\frac{\partial t_{k,l}}{\partial \theta_i} \right)^2 + \frac{2}{\sigma_{k,l}^2} \left(\frac{\partial \sigma_{k,l}}{\partial \theta_i} \right)^2. \end{aligned} \tag{5.19}$$

As information is additive, the Fisher information carried by multiple independent random variables $\hat{t}_{k,l}$ $(k, l \in [1, N]; k \neq l)$ about an unknown parameter θ_i is the sum of the Fisher information carried by each random variable separately, i.e.:

$$\begin{aligned} \mathcal{I}(\theta_i) &= \sum_{k=1}^{N} \sum_{l=1}^{N} I(\theta_i) \\ &= \sum_{k=1}^{N} \sum_{l=1}^{N} \left[\frac{1}{\sigma_{k,l}^2} \left(\frac{\partial t_{k,l}}{\partial \theta_i} \right)^2 + \frac{2}{\sigma_{k,l}^2} \left(\frac{\partial \sigma_{k,l}}{\partial \theta_i} \right)^2 \right], \end{aligned} \tag{5.20}$$

where $\sigma_{n,n} = \infty$ for all $n \in [1, N]$, and the standard deviation $\sigma_{k,l}$ for any pair of sensor nodes k and l without connection is set to be infinity.

For the parameter vector $\mathbf{\Theta}$ (given by (5.8)), the Fisher information takes the form of a $2N_u \times 2N_u$ matrix, with typical elements:

$$\begin{aligned} \left(\mathcal{I}(\mathbf{\Theta})\right)_{i,j} &= \sum_{k=1}^{N} \sum_{l=1}^{N} \mathbb{E}\left[V(\theta_i) V(\theta_j) | \theta_i, \theta_j\right] \\ &= \sum_{k=1}^{N} \sum_{l=1}^{N} \left[\frac{1}{\sigma_{k,l}^2} \cdot \frac{\partial t_{k,l}}{\partial \theta_i} \cdot \frac{\partial t_{k,l}}{\partial \theta_j} + \frac{2}{\sigma_{k,l}^2} \cdot \frac{\partial \sigma_{k,l}}{\partial \theta_i} \cdot \frac{\partial \sigma_{k,l}}{\partial \theta_j} \right], \end{aligned} \tag{5.21}$$

where, by considering equations (5.9) and (5.10), the partial derivative of $t_{k,l}$ with

respect to θ_i ($i \in \{[1, N_u] \bigcup [N+1, N+N_u]\}$), is given by:

$$\frac{\partial t_{k,l}}{\partial \theta_i} = \begin{cases} \frac{1}{c} \cdot \frac{x_k - x_l}{\sqrt{(x_k - x_l)^2 + (y_k - y_l)^2}}, & \text{when } i = k; \\ \frac{1}{c} \cdot \frac{x_l - x_k}{\sqrt{(x_k - x_l)^2 + (y_k - y_l)^2}}, & \text{when } i = l; \\ \frac{1}{c} \cdot \frac{y_k - y_l}{\sqrt{(x_k - x_l)^2 + (y_k - y_l)^2}}, & \text{when } i = N + k; \\ \frac{1}{c} \cdot \frac{y_l - y_k}{\sqrt{(x_k - x_l)^2 + (y_k - y_l)^2}}, & \text{when } i = N + l; \\ 0, & \text{otherwise.} \end{cases} \tag{5.22}$$

Due to the signal attenuation over the channel, the variance of measurement noise should increase with propagation distance. The standard deviation of the one-hop measurement noise between node k and node l is assumed to be proportional to $d_{k,l}^{\eta}$, i.e.:

$$\sigma_{k,l} = \sigma_0 \cdot d_{k,l}^{\eta} = \sigma_0 \cdot c^{\eta} \cdot t_{k,l}^{\eta}, \tag{5.23}$$

where σ_0 is the basic standard deviation associated with the measurement noise, and η is the propagation exponent. The partial derivative of $\sigma_{k,l}$ with respect to θ_i ($i \in \{[1, N_u] \bigcup [N+1, N+N_u]\}$) in (5.21) is then given by:

$$\frac{\partial \sigma_{k,l}}{\partial \theta_i} = \sigma_0 \cdot c^{\eta} \cdot \eta \cdot t_{k,l}^{\eta-1} \cdot \frac{\partial t_{k,l}}{\partial \theta_i}, \tag{5.24}$$

where $\frac{\partial t_{k,l}}{\partial \theta_i}$ is given by (5.22).

Combining (5.14), (5.21), (5.22), and (5.24), the CRB for one-hop localization algorithms is given by $[\mathcal{I}(\mathbf{\Theta})]^{-1}$.

5.5.2 CRB for Multi-hop Wireless Sensor Networks

In multi-hop WSNs, some unknown nodes may be indirectly connected to anchor nodes. To estimate the distance between any indirectly connected unknown node

and anchor node, the shortest path routing algorithm is used. The shortest paths and the nodes in the shortest paths are recorded and used by the CL-basic and the CL-refine localization algorithms.

To enable the calculation of the CRB for multi-hop networks, multiple single-hop range measurements between any indirectly connected pair of unknown node and anchor node need to be translated into a virtual one-hop range measurement. The measurement errors also need to be translated into the corresponding one-hop measurement error. This operation depends on the properties of single-hop range measurement errors. Specifically, when the single-hop range measurement error is dependent on the range between two nodes, the shortest path metric is used to calculate the corresponding one-hop measurement error. In what follows, the CRB for multi-hop WSNs will be analyzed in detail.

For any pair of indirectly connected node k and node l ($k, l \in [1, N]; k \neq l$), it is assumed that the shortest path between node k and node l consists of r ($r \geq 1$) hops and $r-1$ relay nodes, which are numbered as m_1 to m_{r-1} ($m_1, \ldots, m_{r-1} \in [1, N]$) from node k towards node l. Let

$$m_0 = k, \;\; m_r = l, \tag{5.25}$$

Node m_0 and node m_r then denote the source node k and the destination node l, respectively. According to the Sum-dist method introduced in Section 5.3.1 for multi-hop localization algorithms, the multi-hop ranging measurement between node k and node l is estimated by the sum of the ranging measurement in each hop, i.e.:

$$\hat{d}_{k,l} = \sum_{s=0}^{r-1} \hat{d}_{m_s, m_{s+1}} = c \sum_{s=0}^{r-1} \hat{t}_{m_s, m_{s+1}}. \tag{5.26}$$

Since the multi-hop propagation delay between node k and node l is defined as:

$$t_{k,l} = \sum_{s=0}^{r-1} t_{m_s,m_{s+1}}, \tag{5.27}$$

the measured multi-hop propagation delay between node k and node l is:

$$\hat{t}_{k,l} = \sum_{s=0}^{r-1} \hat{t}_{m_s,m_{s+1}}, \tag{5.28}$$

and the multi-hop measurement noise $e_{k,l}$ is given by:

$$e_{k,l} = \sum_{s=0}^{r-1} e_{m_s,m_{s+1}}. \tag{5.29}$$

As the one-hop measurement noises $e_{m_s,m_{s+1}}$ $(0 \leq s \leq r-1)$ are assumed to be zero-mean, Gaussian, and independent of one another, the multi-hop measurement noise $e_{k,l}$ is also zero-mean and Gaussian. Using (5.23), the variance of $e_{k,l}$ is given by:

$$\sigma_{k,l}^2 = \sum_{s=0}^{r-1} \sigma_{m_s,m_{s+1}}^2 = \sigma_0^2 \cdot c^{2\eta} \cdot \sum_{s=0}^{r-1} t_{m_s,m_{s+1}}^{2\eta}. \tag{5.30}$$

Considering (5.10), the partial derivative of $t_{k,l}$ with respect to an unknown parameter θ_i $(i \in \{[1, N_u] \bigcup [N+1, N+N_u]\})$ is given by:

$$\frac{\partial t_{k,l}}{\partial \theta_i} = \sum_{s=0}^{r-1} \frac{\partial t_{m_s,m_{s+1}}}{\partial \theta_i}$$

$$= \begin{cases} \frac{1}{c} \cdot \frac{x_k - x_{m_1}}{d_{k,m_1}}, & \text{when } i = k; \\ \frac{1}{c} \cdot \left(\frac{x_{m_s} - x_{m_{s-1}}}{d_{m_s,m_{s-1}}} + \frac{x_{m_s} - x_{m_{s+1}}}{d_{m_s,m_{s+1}}} \right), & \text{when } i = m_s, 1 \leq s \leq r-1; \\ \frac{1}{c} \cdot \frac{x_l - x_{m_{r-1}}}{d_{m_{r-1},l}}, & \text{when } i = l; \\ \frac{1}{c} \cdot \frac{y_k - y_{m_1}}{d_{k,m_1}}, & \text{when } i = N + k; \\ \frac{1}{c} \cdot \left(\frac{y_{m_s} - y_{m_{s-1}}}{d_{m_s,m_{s-1}}} + \frac{y_{m_s} - y_{m_{s+1}}}{d_{m_s,m_{s+1}}} \right), & \text{when } i = N + m_s, 1 \leq s \leq r-1; \\ \frac{1}{c} \cdot \frac{y_l - y_{m_{r-1}}}{d_{m_{r-1},l}}, & \text{when } i = N + l; \\ 0, & \text{otherwise.} \end{cases} \tag{5.31}$$

Considering (5.30) and using (5.10) and (5.22), the partial derivative of $\sigma_{k,l}$ with respect to θ_i is then given by:

$$\begin{aligned} \frac{\partial \sigma_{k,l}}{\partial \theta_i} &= \sigma_0 \cdot c^\eta \cdot \eta \cdot \left(\sum_{s=0}^{r-1} t_{m_s,m_{s+1}}^{2\eta} \right)^{-\frac{1}{2}} \cdot \sum_{s=0}^{r-1} \left(t_{m_s,m_{s+1}}^{2\eta-1} \cdot \frac{\partial t_{m_s,m_{s+1}}}{\partial \theta_i} \right) \\ &= \sigma_0 \cdot \eta \cdot \left(\sum_{s=0}^{r-1} d_{m_s,m_{s+1}}^{2\eta} \right)^{-\frac{1}{2}} \cdot G, \end{aligned} \tag{5.32}$$

where G is an auxiliary variable expressed by:

$$G = \begin{cases} (x_k - x_{m_1})\, d_{k,m_1}^{2\eta-2}, & \text{when } i = k; \\ \left(x_{m_s} - x_{m_{s-1}}\right) d_{m_s,m_{s-1}}^{2\eta-2} + \left(x_{m_s} - x_{m_{s+1}}\right) d_{m_s,m_{s+1}}^{2\eta-2}, & \text{when } i = m_s, 1 \leq s \leq r-1; \\ \left(x_l - x_{m_{r-1}}\right) d_{l,m_{r-1}}^{2\eta-2}, & \text{when } i = l; \\ (y_k - y_{m_1})\, d_{k,m_1}^{2\eta-2}, & \text{when } i = N + k; \\ \left(y_{m_s} - y_{m_{s-1}}\right) d_{m_s,m_{s-1}}^{2\eta-2} + \left(y_{m_s} - y_{m_{s+1}}\right) d_{m_s,m_{s+1}}^{2\eta-2}, & \text{when } i = N + m_s, 1 \leq s \leq r-1; \\ \left(y_l - y_{m_{r-1}}\right) d_{l,m_{r-1}}^{2\eta-2}, & \text{when } i = N + l; \\ 0, & \text{otherwise.} \end{cases} \tag{5.33}$$

Combining (5.14), (5.21), (5.31), (5.32), and (5.33), the CRB for multi-hop

localization algorithms is given by $[\mathcal{I}(\mathbf{\Theta})]^{-1}$.

5.6 Simulation Results

In this section, some typical simulation results will be presented relating to the analytical and simulated location estimation performances of the localization algorithms. The simulations have tested various combinations of node and anchor node densities, network area, anchor placement, and range measurement error patterns. Only a part of the simulation results will, however, be presented here due to the space limit.

It is assumed that the underlying physical layer uses ultra-wideband (UWB) systems for node communication. The basic standard deviation associated with the measurement noise is set to be $\sigma_0 = 3 \times 10^{-9}$ (seconds). Four network scenarios are investigated using different network areas and numbers of sensor nodes. For each network scenario, three relation models between single-hop measurement noise and single-hop propagation distance are tested, with the propagation exponent η set to 0.05, 0.2, and 0.5, respectively. The CRB is computed for both the CL-basic and the CL-refine localization algorithms. By combining two first-phase methods (Sum-dist and DV-hop) and two second-phase methods (Min-max and Trilateration) introduced in Section 5.3, four distributed localization algorithms are simulated. These four algorithms are denoted by SD-Min (distance determined by Sum-dist method, location computed by Min-max method), SD-Lat (distance determined by Sum-dist method, location computed by trilateration method), DV-Min (distance determined by DV-hop method, location computed by Min-max method), and DV-Lat (distance determined by DV-hop method, location computed by trilateration method), respectively. Each simulation value is obtained by averaging over 30 simulations.

5.6.1 Small Network Scenario

The values of system parameters, used to investigate small networks, are summarized in Table 5.1. Using the input system parameters from Table 5.1, a network topology is generated randomly as shown in Figure 5-1. The same network topology is used for the three propagation exponent cases: $\eta = [0.05, 0.2, 0.5]$.

Table 5.1: System parameters for small network scenario

Network	Network Area	Communication Range	No. Nodes N	No. Anchors N_k
Small	75 x 75	40	20	6

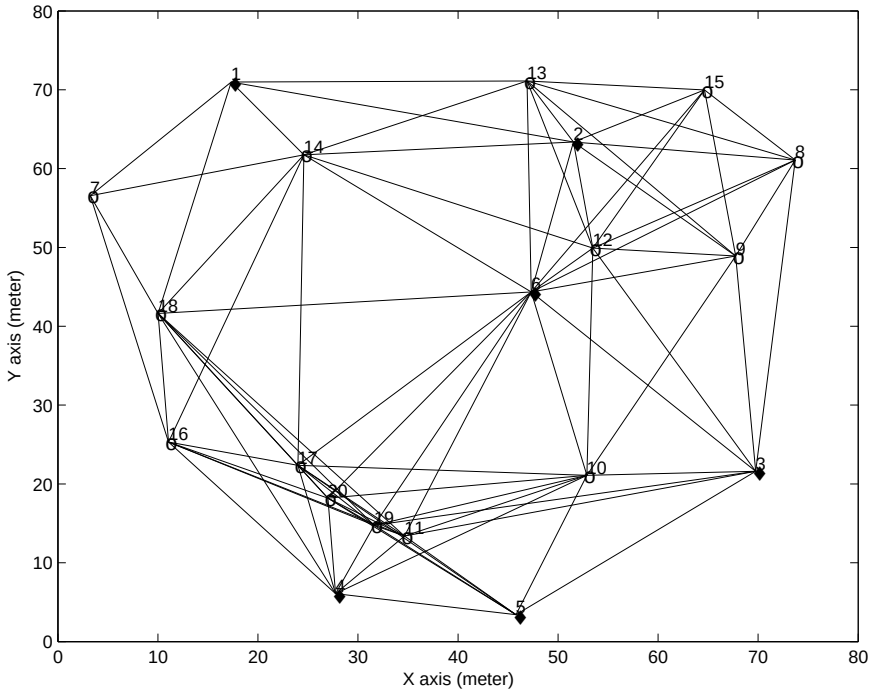

Figure 5-1: Small network scenario of 20 sensor nodes, among which 6 nodes are anchor nodes (denoted by dark diamonds) and 14 nodes are unknown nodes (denoted by circles).

Table 5.2 lists the averaged location estimation deviations obtained by the CRB method for the two centralized algorithms and by simulation for the two

Sum-dist based distributed algorithms for the three propagation exponent cases in the small network, when averaged over all the unknown nodes. "cl-r-x", "cl-r-y", "cl-b-x", and "cl-b-y" denote the results of X and Y coordinates obtained using the CL-refine and the CL-basic algorithms, respectively. "sd-m-x", "sd-m-y", "sd-l-x", and "sd-l-y" denote the results of X and Y coordinates obtained using the SD-Min and the SD-Lat algorithms, respectively. As DV-hop based algorithms are insensitive to the variance of the range measurements, the obtained location estimation deviations using both the DV-Min and the DV-Lat algorithms are zero as expected and, therefore, are not presented here. Table 5.3 lists the location estimation errors obtained using the four distributed algorithms for the three propagation exponent cases in the small network, when averaged over all the unknown nodes. Similarly, "dv-m-x", "dv-m-y", "dv-l-x", and "dv-l-y" denote the results of X and Y coordinates obtained using the DV-Min and the DV-Lat algorithms, respectively. The location estimation deviations, average estimation errors, and estimated locations of the two centralized and four distributed algorithms for the small network are also presented in three groups of figures, Figures 5-2 - 5-4 for $\eta = 0.05$, Figures 5-5 - 5-7 for $\eta = 0.2$, and Figures 5-8 - 5-10 for $\eta = 0.5$, respectively.

Table 5.2: Averaged location estimation deviations of centralized algorithms and Sum-dist based distributed algorithms for small network

η	cl-r-x	cl-r-y	cl-b-x	cl-b-y	sd-m-x	sd-m-y	sd-l-x	sd-l-y
0.05	0.642	0.642	0.717	0.638	0.73	0.753	1.67	0.753
0.2	1.02	1.02	1.2	1.1	1.02	1.2	2.36	1.2
0.5	2.56	2.56	3.33	3.15	2.5	2.75	5.37	2.75

Figure 5-2 shows the location estimation deviations obtained by the CRB of the two centralized algorithms (CL-basic and CL-refine) and by simulation of the two distributed algorithms (SD-Min and SD-Lat) in the small network, on

Table 5.3: Averaged location estimation errors of Sum-dist and DV-hop based distributed algorithms for small network

η	sd-m-x	sd-m-y	sd-l-x	sd-l-y	dv-m-x	dv-m-y	dv-l-x	dv-l-y
0.05	12.2774	4.8689	3.4830	2.3367	15.4988	10.0848	7.3626	7.1369
0.2	12.3790	5.0816	3.4315	2.7861	15.4988	10.0848	7.3626	7.1369
0.5	13.4252	6.8351	6.7644	7.1597	15.4988	10.0848	7.3626	7.1369

the X and Y coordinates of the unknown nodes, when the distance exponent is $\eta = 0.05$. The upper subfigure relates to the estimation of the X coordinate whilst the lower subfigure relates to that of the Y coordinate. From Figure 5-2 it is observed that for the small network and low range measurement variance, the CL-basic algorithm achieves close location estimation performance to that of the CL-refine algorithm, with less than 0.1 m of deviation difference between the two centralized algorithms for both X and Y coordinates of most unknown nodes. As the CL-refine algorithm requires more measurement effort, computation, and communication overhead than the CL-basic algorithm, the CL-basic algorithm is preferred when the CL-refine algorithm does not show significant performance advantages. The location estimation deviations of both centralized algorithms are lower than those of the SD-Min algorithm. The location estimation deviation of the SD-Lat algorithm is higher than that of the SD-Min algorithm when $\eta = 0.05$, however, as shown in Table 5.3, the average estimation error of the SD-Lat algorithm is lower than that of the SD-Min algorithm.

Figure 5-3 shows the average location estimation errors obtained by simulation of the four distributed algorithms (SD-Min, SD-Lat, DV-Min, and DV-Lat) in the small network scenario, on the X and Y coordinates of the unknown nodes, when the distance exponent is $\eta = 0.05$. As the CRB analysis is mainly used for unbiased estimation, the average estimation errors for the two centralized algorithms (CL-basic and CL-refine) are assumed to be zero and, therefore, are not

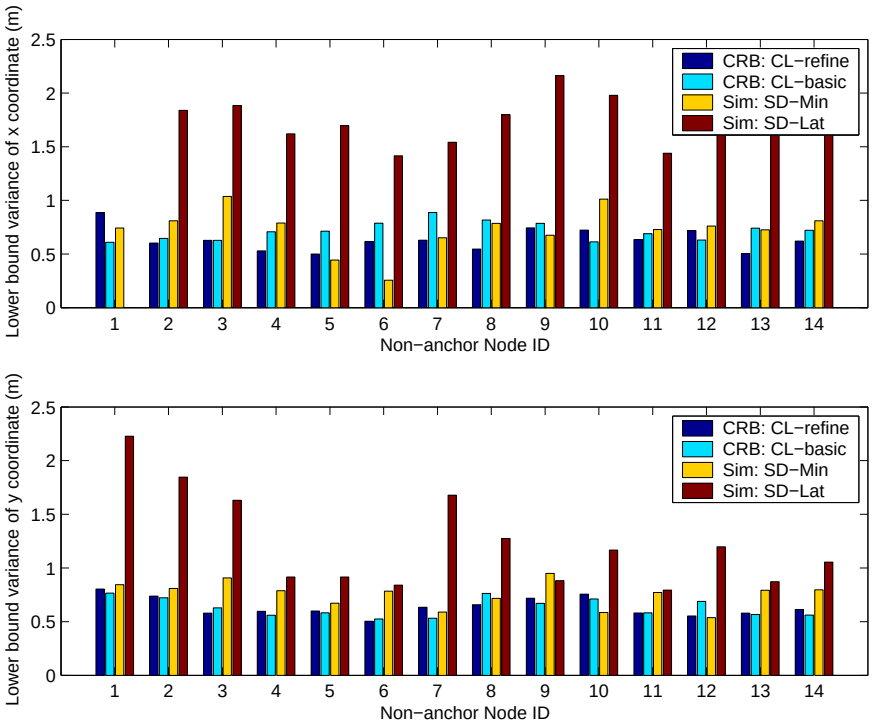

Figure 5-2: Location estimation deviations obtained by CRB and simulation for small network scenario when $\eta = 0.05$.

presented here. The results shown in Figure 5-3 show that for the small network and low range measurement error, Sum-dist based algorithms significantly outperform DV-hop based algorithms. It is also observed that the performance of the SD-Lat algorithm is better than that of the SD-Min algorithm, especially on the X coordinate estimation. The observed advantage of Sum-dist based algorithms are consistent with the results averaged over all the unknown nodes in Table 5.3.

For illustration purpose, the original and estimated node locations for the small network scenario when $\eta = 0.05$ are plotted in Figure 5-4. The original position of each sensor node is indicated by its ID, with a line connecting its estimated location. The estimated locations obtained using SD-Min, SD-Lat, DV-Min, and DV-Lat are plotted in Figure 5-4(a), 5-4(b), 5-4(c), and 5-4(d), respectively.

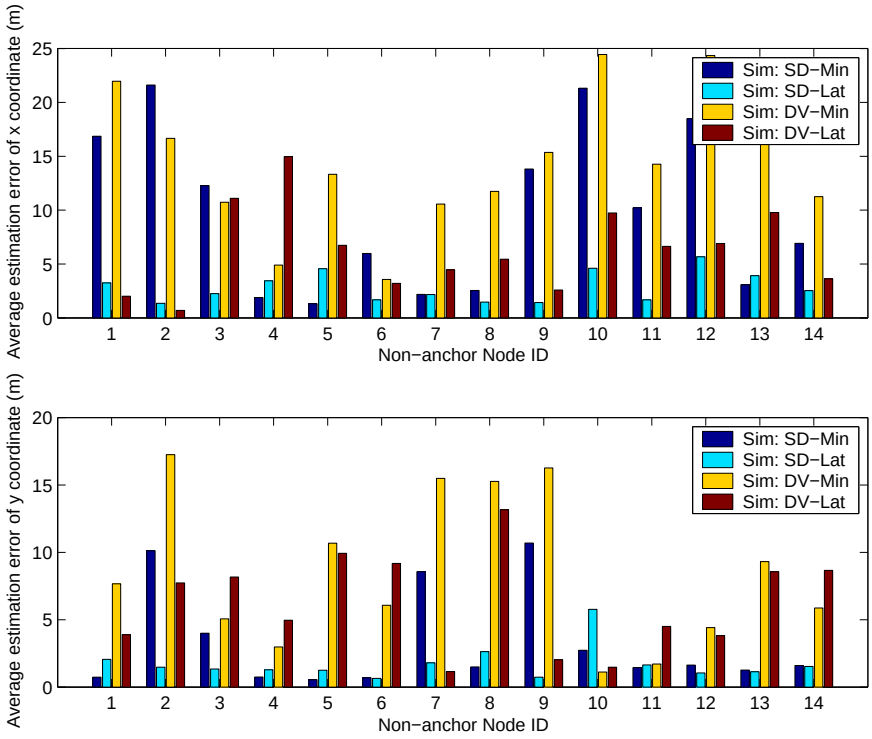

Figure 5-3: Location estimation errors of distributed algorithms for small network scenario when $\eta = 0.05$.

For the small network, when $\eta = 0.2$, the location estimation deviations, the location estimation errors, and the original and estimated node locations are plotted in Figure 5-5, Figure 5-6, and Figure 5-7, respectively. From the results shown in Figure 5-5, Figure 5-6, Table 5.2 and Table 5.3, it is observed that there is significant change in the location estimation deviations between $\eta = 0.05$ and $\eta = 0.2$, but the change in the averaged estimation errors is negligible.

With an increase in dependence of the range measurement noise on propagation distance, significant impact of the ranging measurement error on the localization performance is observed even for the small network scenario. Figure 5-8 shows the location estimation deviations obtained by the CRB of the two centralized algorithms (CL-basic and CL-refine) and by simulation of the two Sum-dist based algorithms (SD-Min and SD-Lat) in the small network, on the

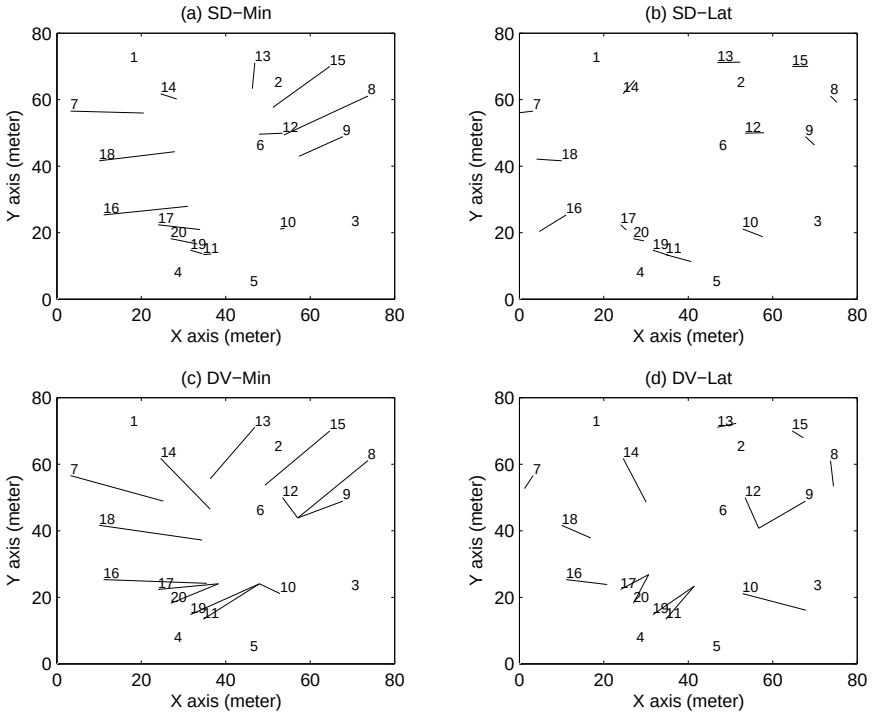

Figure 5-4: Original and estimated node locations for small network scenario when $\eta = 0.05$. Each original position is indicated by the sensor node ID and is connected by a line with its estimated location.

X and Y coordinates of the unknown nodes, when $\eta = 0.5$. From the results in Table 5.2, it is observed that when $\eta = 0.5$, the location estimation deviations using the four investigated algorithms increase by more than 300% compared to those when $\eta = 0.05$.

Table 5.3 shows that the algorithm most affected by the increase in η is SD-Lat. The averaged estimation errors of the SD-Min algorithm increase slightly, while those of both the DV-Min and the DV-Lat algorithms remain the same. However, for the small network, the averaged estimation errors of the SD-Lat algorithm when $\eta = 0.5$ are still slightly lower than those of the DV-Min and the DV-Lat algorithms when $\eta = [0.05, 0.2, 0.5]$.

The original and estimated node locations when $\eta = 0.5$ are plotted in Figure 5-10. It is worth pointing out that even in the small network scenario each node

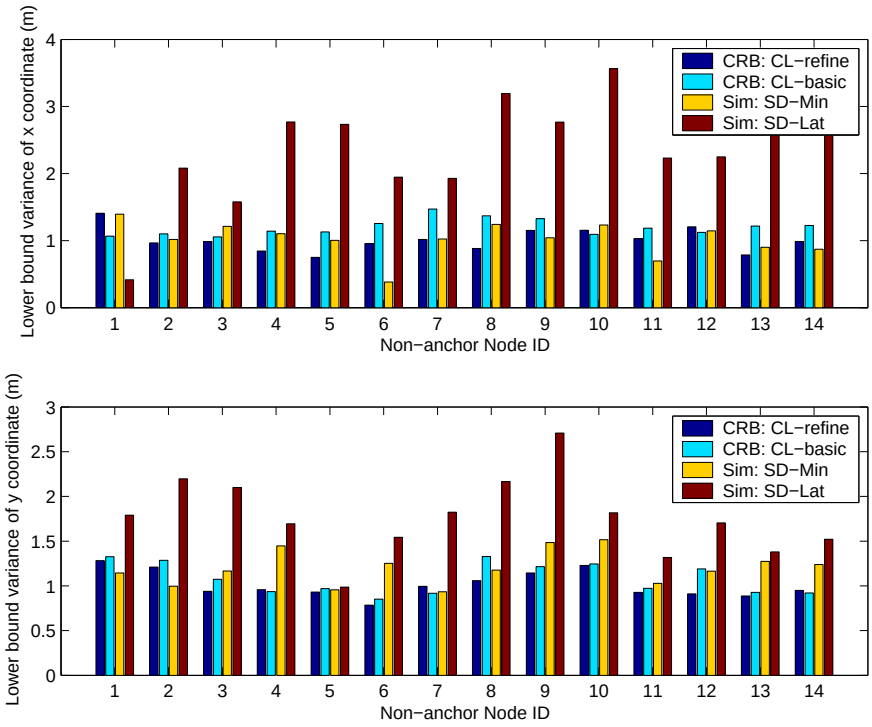

Figure 5-5: Location estimation deviations obtained by CRB and simulation for small network scenario when $\eta = 0.2$.

needs multi-hop communication to determine the distances to some anchor nodes. Range measurement errors may, therefore, be introduced and accumulated, and eventually affect the location estimation performance.

5.6.2 Large Network Scenario

The values of system parameters, used to investigate large networks, are summarized in Table 5.4, with 60 sensor nodes in total among which 10 nodes are anchor nodes. A randomly generated network topology with the above system parameters is shown in Figure 5-11.

Similar to the small network scenario, Table 5.5 lists the averaged location estimation deviations obtained by the CRB method for the two centralized algorithms and by simulation for the two Sum-dist based distributed algorithms for

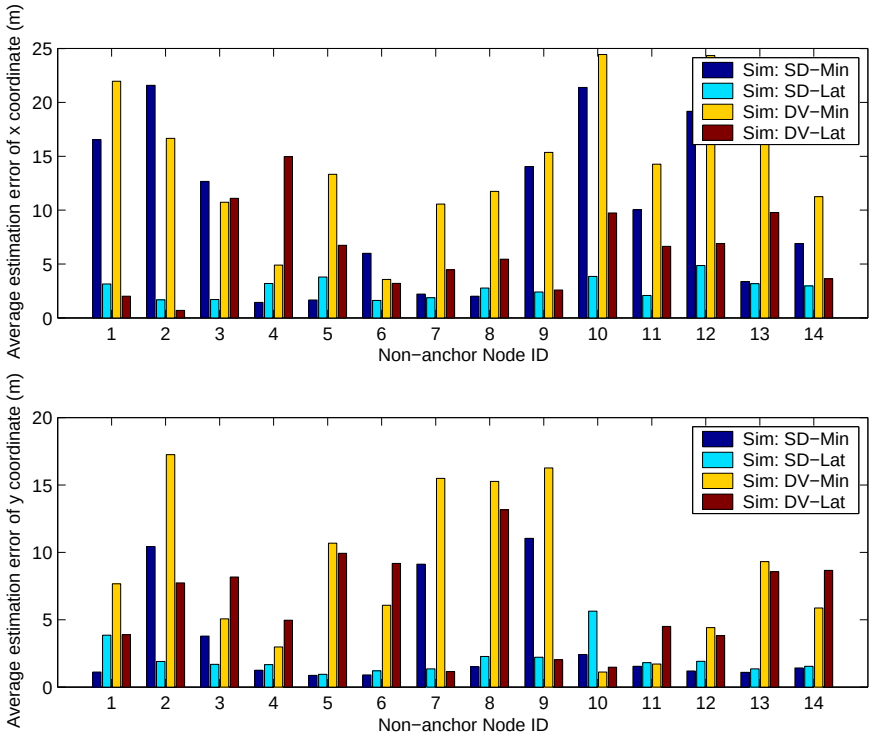

Figure 5-6: Location estimation errors of distributed algorithms for small network scenario when $\eta = 0.2$.

Table 5.4: System parameters for large network scenario

Network	Network Area	Communication Range	No. Nodes N	No. Anchors N_k
large	180x180	64	60	10

the three propagation exponent cases in the large network, when averaged over all the unknown nodes. Table 5.6 lists the location estimation errors obtained using the four distributed algorithms for the three propagation exponent cases in the large network, when averaged over all the unknown nodes. The location estimation deviations, average estimation errors, and estimated locations of the two centralized and four distributed algorithms for the large network are also presented in three groups of figures, Figures 5-12 - 5-14 for $\eta = 0.05$, Figures 5-15 - 5-17 for $\eta = 0.2$, and Figures 5-18 - 5-20 for $\eta = 0.5$, respectively.

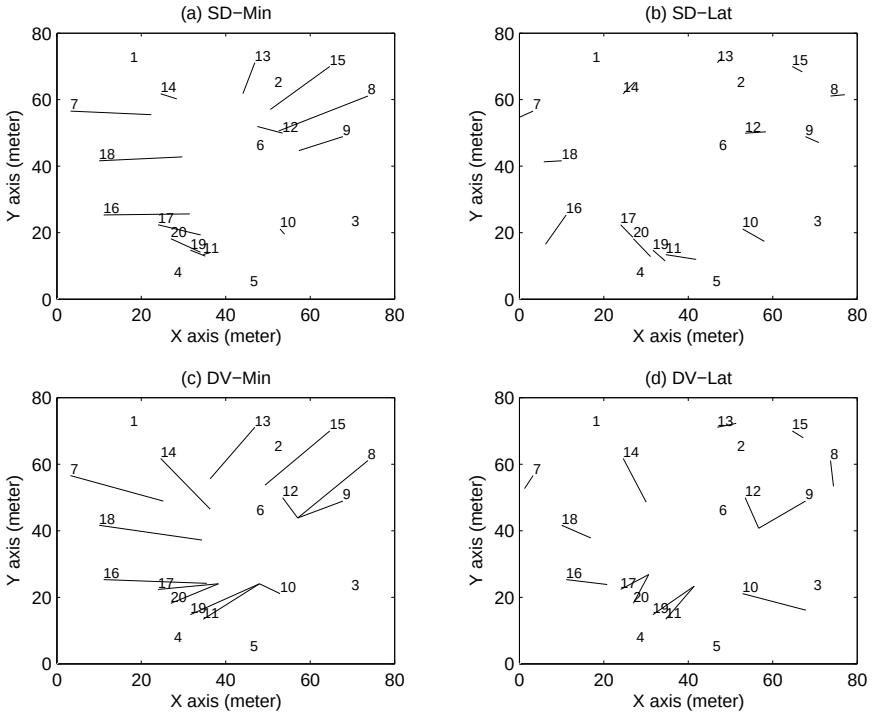

Figure 5-7: Original and estimated node locations for small network scenario when $\eta = 0.2$. Each original position is indicated by the sensor node ID and is connected by a line with its estimated location.

Figure 5-12 shows the location estimation deviations obtained by the CRB of the two centralized algorithms (CL-basic and CL-refine) and by simulation of the two distributed algorithms (SD-Min and SD-Lat) in the large network, on the X and Y coordinates of the unknown nodes, when the distance exponent is $\eta = 0.05$. Figure 5-13 shows the average location estimation errors obtained by simulation of the four distributed algorithms (SD-Min, SD-Lat, DV-Min, and DV-Lat) in the large network, on the X and Y coordinates of the unknown nodes, when the distance exponent is $\eta = 0.05$.

From the results shown in Figure 5-12 and Table 5.5, it is observed that the estimation deviation does not change much due to the increase in network size for low range measurement variance. However, the average estimation errors increase by almost 100% for all the distributed algorithms with the increase of network

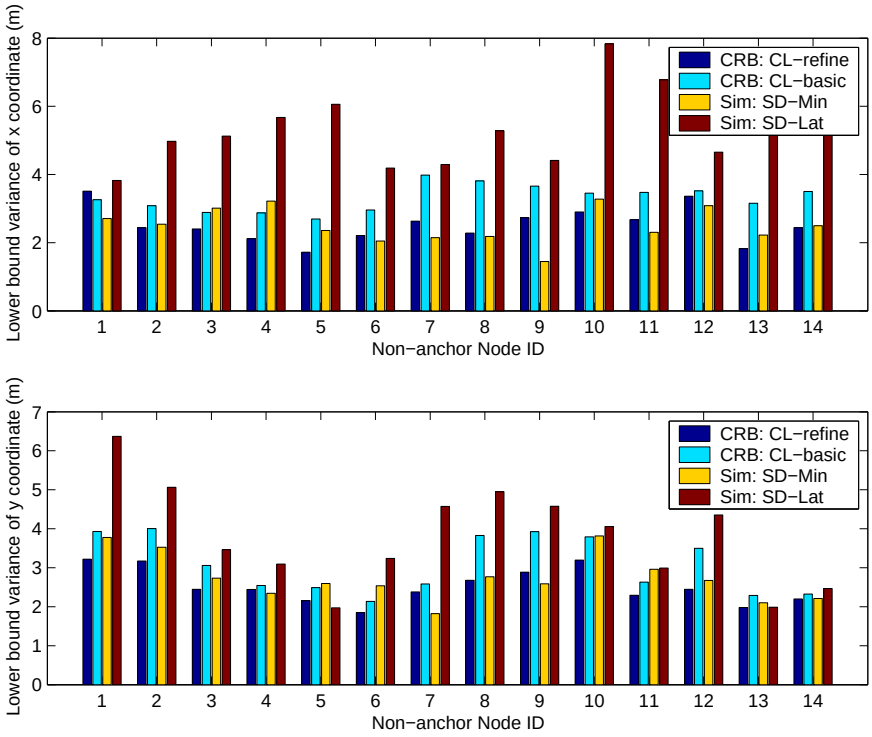

Figure 5-8: Location estimation deviations obtained by CRB and simulation for small network scenario when $\eta = 0.5$.

size, as shown in Figure 5-13 and Table 5.6.

By comparing the location estimation deviation and error results for $\eta = 0.05$ and $\eta = 0.2$ shown in Figure 5-15, Figure 5-16, Table 5.5, and Table 5.6, it is observed that for the large network scenario there is significant change in the estimation deviations but negligible change in the estimation errors. This is the same as was observed for the small network scenario.

The location estimation deviation and error results presented in Figure 5-18 and Figure 5-19 show again that the dependence of range measurement noise on propagation distance has large impact on the location estimation performance, and that Sum-dist based algorithms perform better than their DV-hop based counterparts. From the investigated small and large network scenarios, it is also observed that the CL-refine algorithm performs only slightly better than the CL-

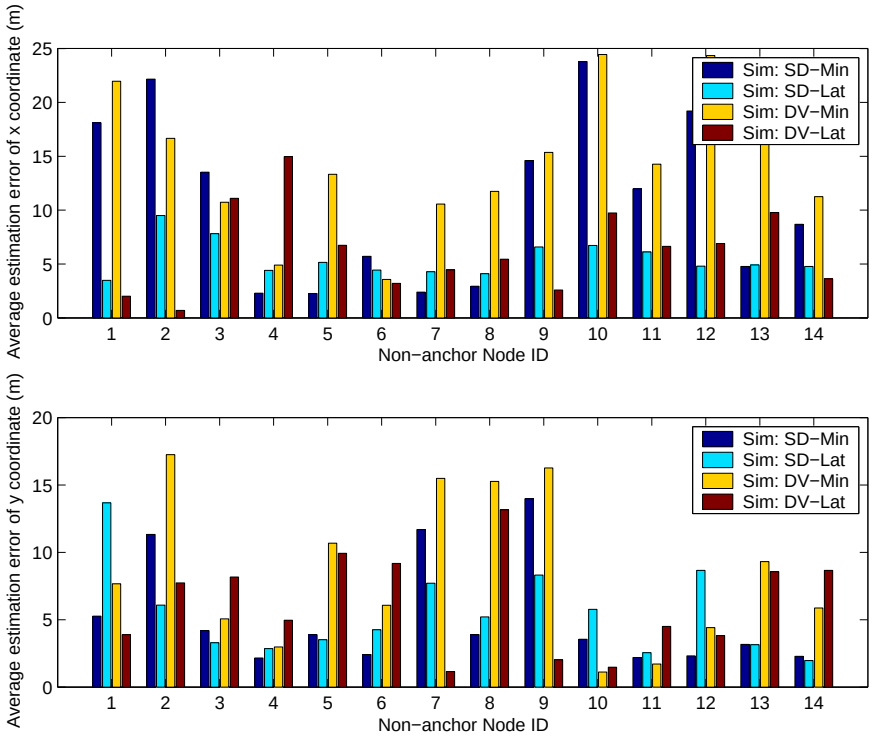

Figure 5-9: Location estimation errors of distributed algorithms for small network scenario when $\eta = 0.5$.

basic algorithm. The local information, i.e. the distances between neighboring nodes, does not, therefore, effectively improve the overall location estimation performance.

5.7 Discussions

5.7.1 More Results with Other Network Sizes

Due to space limitation, the network topologies generated with 40 and 100 sensor nodes will not be presented. The values of system parameters, used to investigate the two networks, are summarized in Table 5.7.

The averaged location estimation deviations obtained by CRB method for the two centralized algorithms and by simulation for the two Sum-dist based

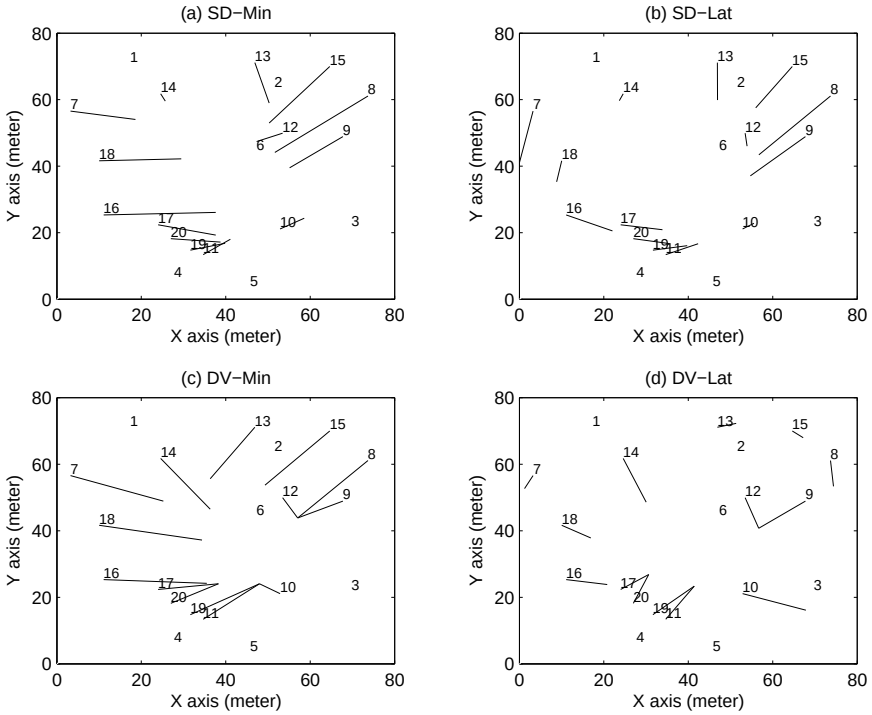

Figure 5-10: Original and estimated node locations for small network scenario when $\eta = 0.5$. Each original position is indicated by the sensor node ID and is connected by a line with its estimated location.

distributed algorithms are presented in Table 5.8 for the network of 40 sensor nodes with 10 anchor nodes. The averaged location estimation errors for this network obtained by simulation of the four distributed algorithms are presented in Table 5.9.

Similarly, Table 5.10 shows the averaged location estimation deviations obtained by the CRB method for the two centralized algorithms and by simulation for the two Sum-dist based distributed algorithms for the network of 100 sensor nodes with 20 anchor nodes. The averaged location estimation errors for this network obtained by simulation of the four distributed algorithms are presented in Table 5.11. From the extra location estimation results for the network scenarios with 40 and 100 sensor nodes, the similar performance trends are observed with those discussed for the small and the large network scenarios in the previous

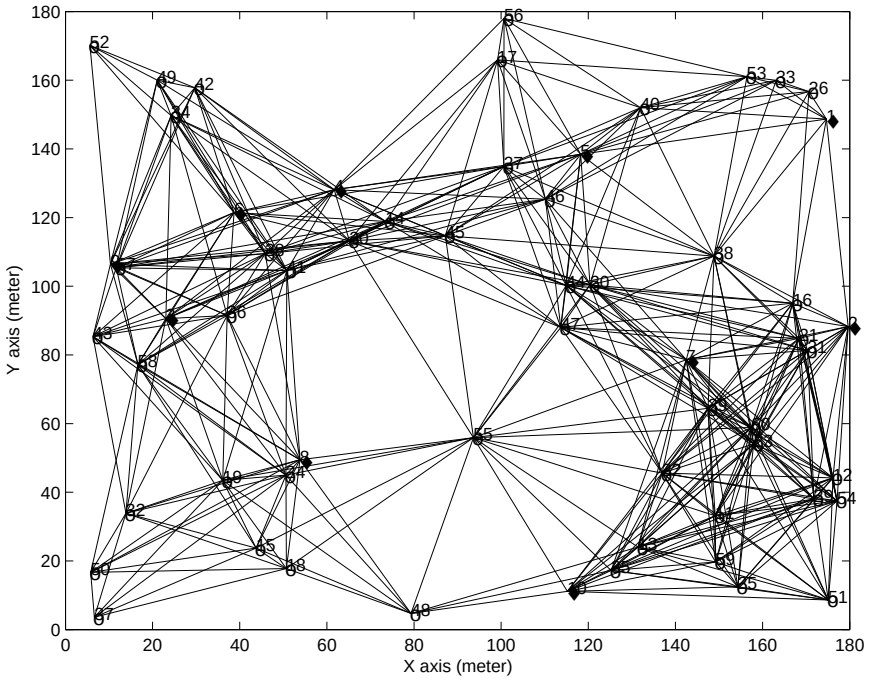

Figure 5-11: Large network scenario of 60 sensor nodes, among which 10 nodes are anchor nodes (denoted by dark diamonds) and 50 nodes are unknown nodes (denoted by circles).

subsections.

5.7.2 Localization for Source Detection Applications

In the previous sections, the CRB analysis method for multi-hop WSNs has been introduced and evaluated. By comparison with the simulation based evaluation approach, it is found that the CRB can provide reasonable location estimation

Table 5.5: Averaged location estimation deviations of centralized algorithms and Sum-dist based distributed algorithms for large network

η	cl-r-x	cl-r-y	cl-b-x	cl-b-y	sd-m-x	sd-m-y	sd-l-x	sd-l-y
0.05	0.568	0.532	0.538	0.58	0.752	0.703	1.2	0.703
0.2	0.974	0.915	1.05	1.09	1.25	1.19	2.11	1.19
0.5	2.84	2.68	3.86	3.76	3.8	2.98	4.82	2.98

Table 5.6: Averaged location estimation errors of Sum-dist and DV-hop based distributed algorithms for large network

η	sd-m-x	sd-m-y	sd-l-x	sd-l-y	dv-m-x	dv-m-y	dv-l-x	dv-l-y
0.05	15.9531	20.6182	6.1938	7.6218	24.3566	28.6600	13.2143	19.1699
0.2	15.9736	20.7782	6.2116	8.1584	24.3566	28.6600	13.2143	19.1699
0.5	18.4150	22.8965	11.2861	13.0514	24.3566	28.6600	13.2143	19.1699

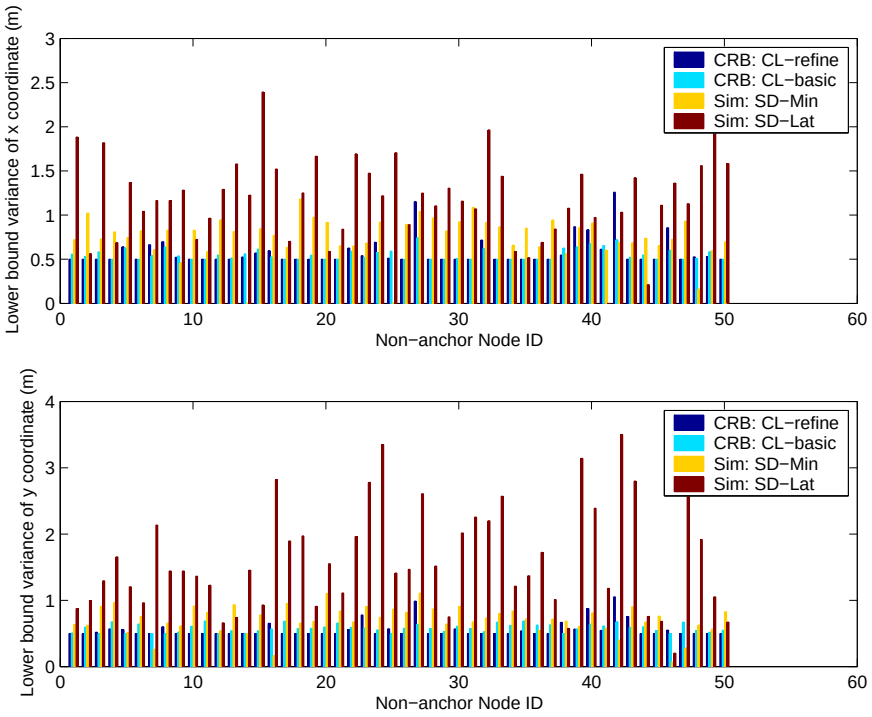

Figure 5-12: Location estimation deviations obtained by CRB and simulation for large network scenario when $\eta = 0.05$.

bounds for the investigated distributed algorithms. However, there are several challenges to applying the CRB analysis method in practical applications, such as remote source detection and tracking applications.

For example, the CRB method requires that all the distances between an unknown node and an anchor node are available before analysis, which is a difficult condition to fulfill in practical applications because of the unknown node loca-

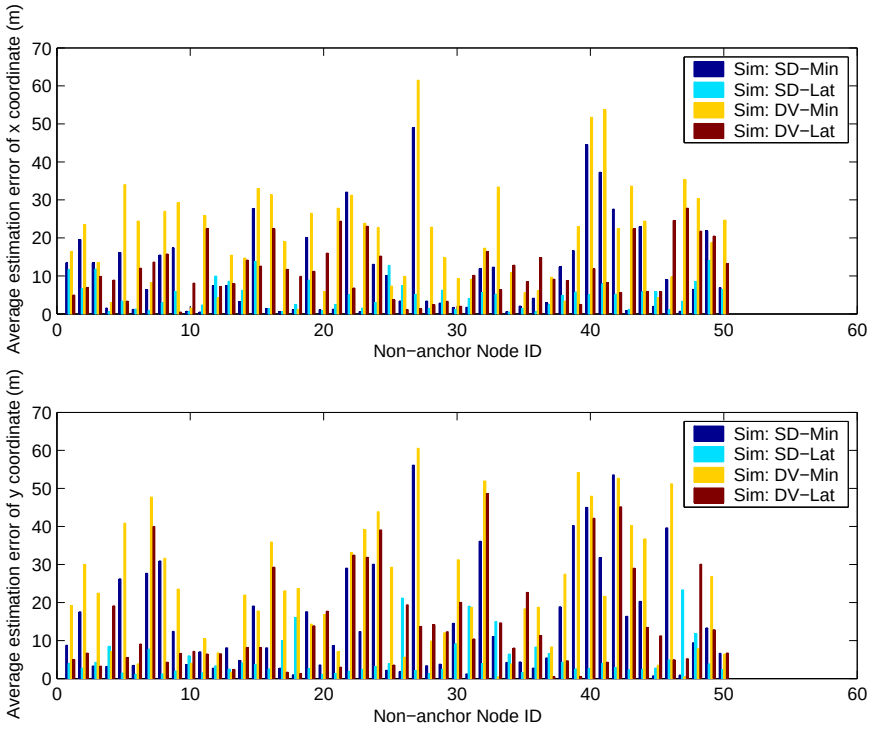

Figure 5-13: Location estimation errors of distributed algorithms for large network scenario when $\eta = 0.05$.

tions. The available information may only consist of the size of network area, number of sensor nodes to be deployed, deviation of range measurement error and so on. If the above-mentioned information is available, a possible way of applying CRB analysis is to generate a number of network topologies randomly with which the previously introduced CRB analytical method can be used. After performing the CRB analysis with the randomly generated network topologies, a basic understanding of the performance of localization algorithms can be obtained

Table 5.7: System parameters for other network scenarios

Network	Network Area	Communication Range	No. Nodes N	No. Anchors N_k
medium	150x150	60	40	10
super	320x320	75	100	20

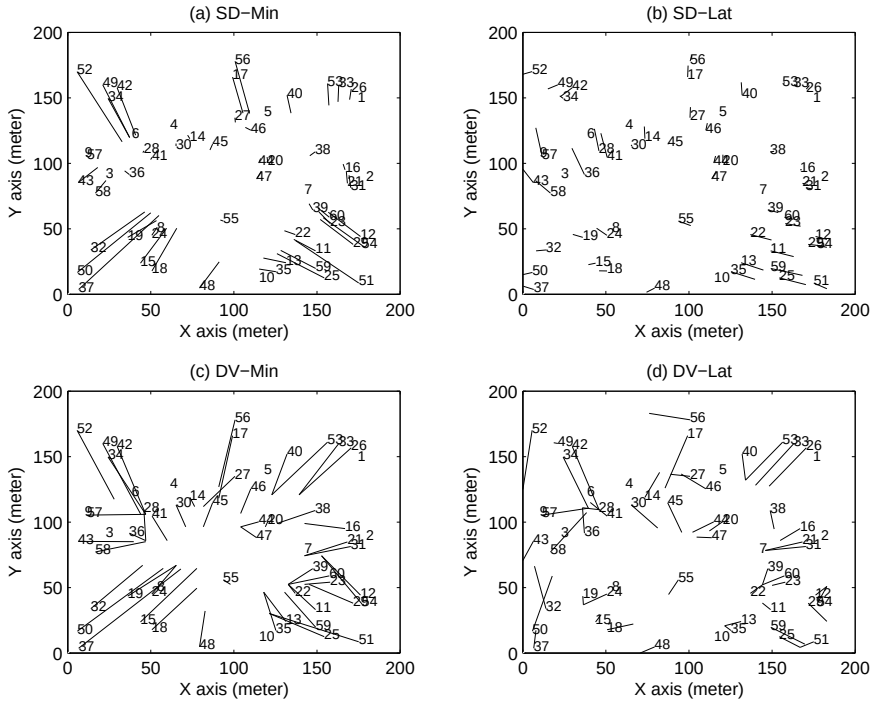

Figure 5-14: Original and estimated node locations for large network scenario when $\eta = 0.05$. Each original position is indicated by the sensor node ID and is connected by a line with its estimated location.

with the specific network environment.

Another challenge is that the proposed CRB analytical method only provides lower bounds on the variances for unbiased localization algorithms. In practice, however, it is very difficult to find distributed algorithms with unbiased location estimation. A bridge between the lower bounds on the estimation variances and the estimation accuracy of algorithms needs to be built.

When considering the specific remote source detection and tracking applications, there are several ways of using the evaluation methods of localization algorithms and the information of node locations. For example, after obtaining a coarse location estimation accuracy of the localization algorithms, the parameters associated with distributed source coding and source detection can be configured for a better performance. In addition, the number and the location of sensor

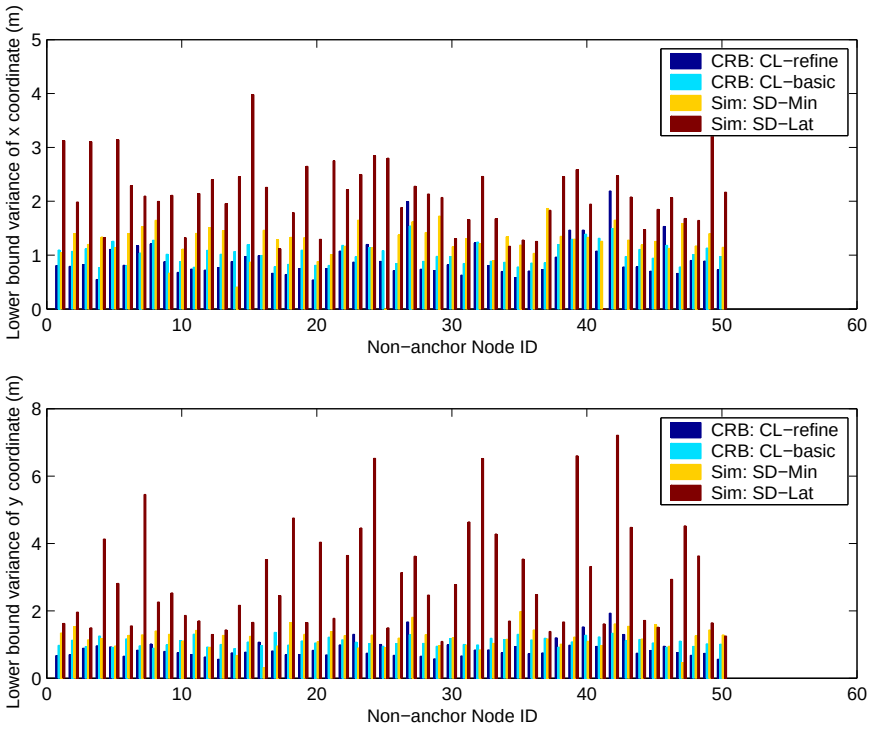

Figure 5-15: Location estimation deviations obtained by CRB and simulation for large network scenario when $\eta = 0.2$.

nodes required to track the detected targets can also be determined by taking into account the estimation accuracy.

Table 5.8: Averaged location estimation deviations of centralized algorithms and Sum-dist based distributed algorithms for network of 40 nodes

η	cl-r-x	cl-r-y	cl-b-x	cl-b-y	sd-m-x	sd-m-y	sd-l-x	sd-l-y
0.05	0.494	0.484	0.571	0.552	0.732	0.801	1.51	0.801
0.2	0.85	0.835	1.05	1.02	1.22	1.28	2.54	1.28
0.5	2.48	2.45	3.5	3.46	3.3	3.2	4.94	3.2

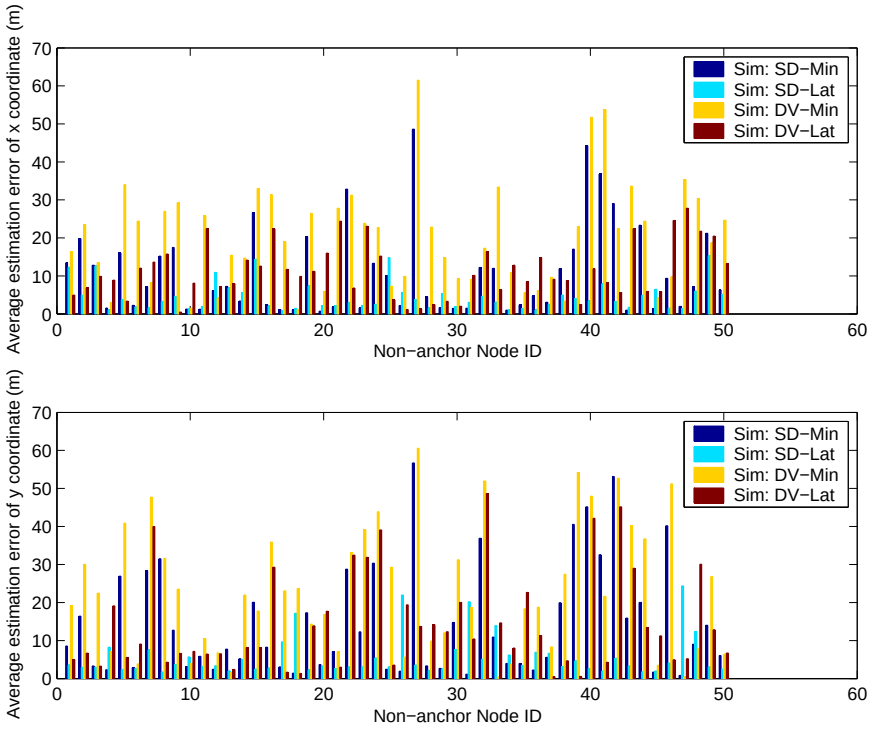

Figure 5-16: Location estimation errors of distributed algorithms for large network scenario when $\eta = 0.2$.

5.8 Summary

This chapter has investigated the location estimation performance of several localization algorithms for multi-hop WSNs. A CRB-based analytical approach is proposed for two centralized localization algorithms, which can provide a lower bound on the variances of location estimation. In addition, a simulation-based approach is introduced for four distributed localization algorithms to evaluate the efficiency of the CRB-based analytical approach. Numerical results show that the CRB-based analytical approach can efficiently provide lower bounds on the variances of location estimation for distributed localization algorithms.

The results suggest that it is possible to design an efficient and scalable evaluation tool for localization algorithms for large scale WSNs. Such an evaluation tool will be useful for the design, selection and configuration of localization al-

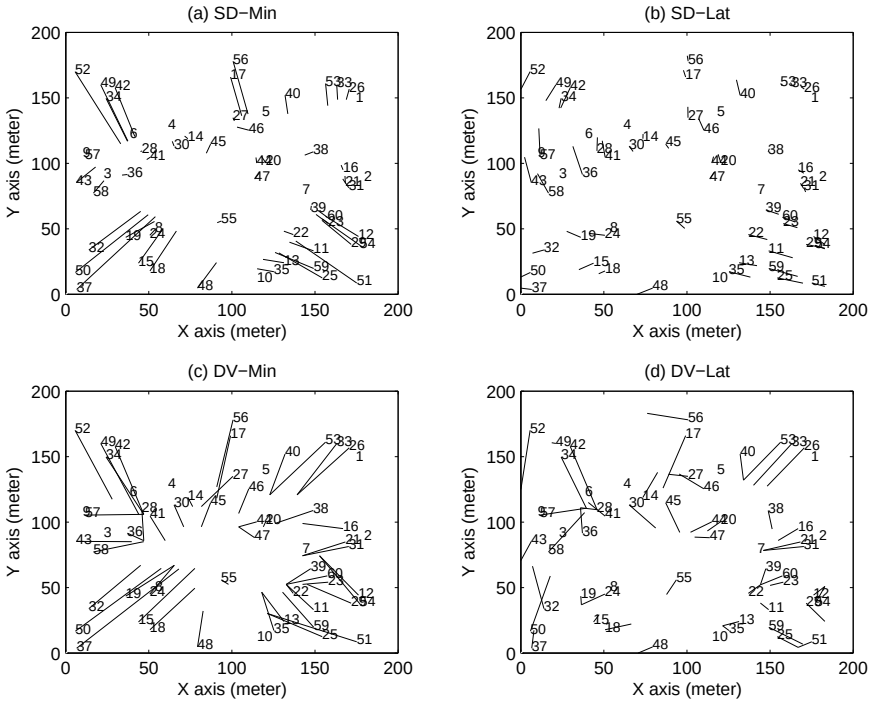

Figure 5-17: Original and estimated node locations for large network scenario when $\eta = 0.2$. Each original position is indicated by the sensor node ID and is connected by a line with its estimated location.

gorithms in large scale WSNs, where simulation-based evaluation approaches are impractical. Also discussed are issues relating to the application of the CRB-based analytical approach and location information to remote source detection and tracking applications.

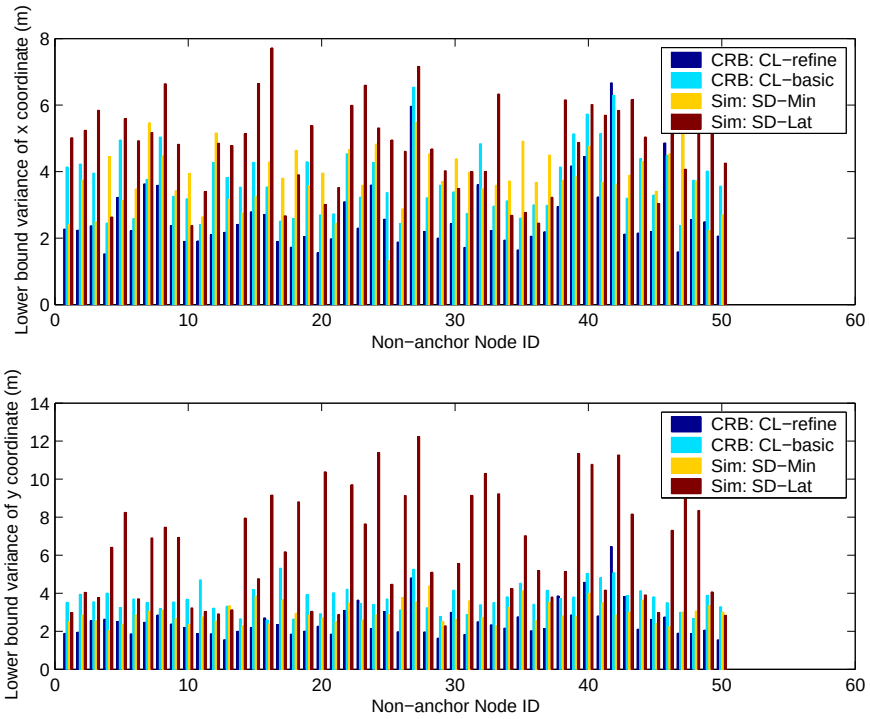

Figure 5-18: Location estimation deviations obtained by CRB and simulation for large network scenario when $\eta = 0.5$.

Table 5.9: Averaged location estimation errors of Sum-dist and DV-hop based distributed algorithms for network of 40 nodes

η	sd-m-x	sd-m-y	sd-l-x	sd-l-y	dv-m-x	dv-m-y	dv-l-x	dv-l-y
0.05	20.0036	11.6822	2.1405	3.2374	26.3730	20.6546	13.2216	13.3414
0.2	20.5209	12.0700	3.1836	3.4403	26.3730	20.6546	13.2216	13.3414
0.5	22.8204	14.1292	10.3676	9.3201	26.3730	20.6546	13.2216	13.3414

Table 5.10: Averaged location estimation deviations of centralized algorithms and Sum-dist based distributed algorithms for network of 100 nodes

η	cl-r-x	cl-r-y	cl-b-x	cl-b-y	sd-m-x	sd-m-y	sd-l-x	sd-l-y
0.05	0.519	0.616	0.423	0.412	0.86	0.784	1.61	0.784
0.2	0.911	1.07	0.861	0.852	1.48	1.37	2.67	1.37
0.5	2.79	3.26	3.43	3.49	4.43	4.16	6.62	4.16

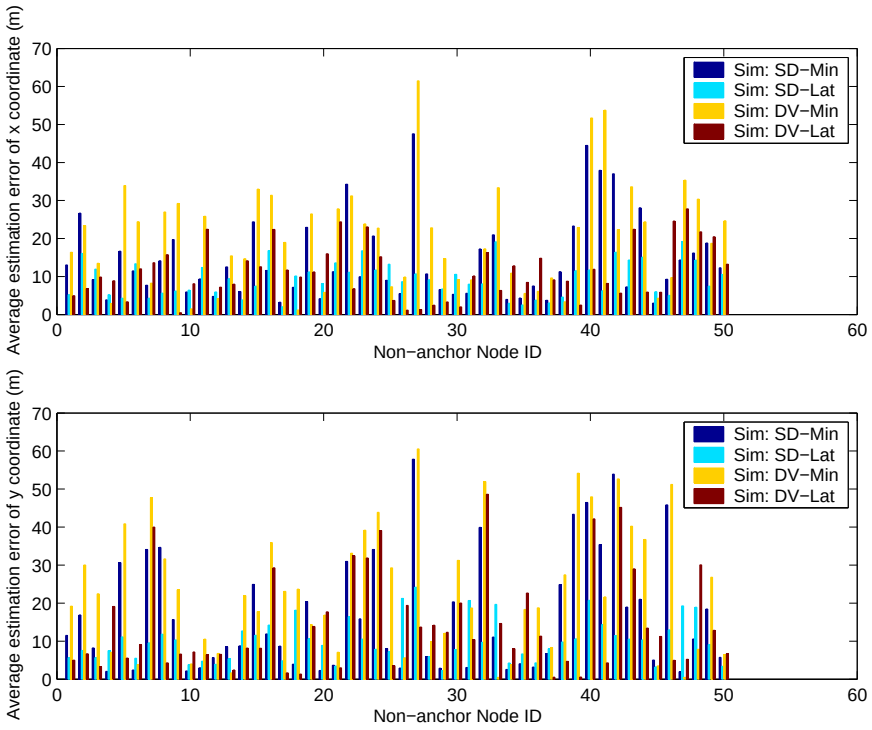

Figure 5-19: Location estimation errors of distributed algorithms for large network scenario when $\eta = 0.5$.

Table 5.11: Averaged location estimation errors of Sum-dist and DV-hop based distributed algorithms for network of 100 nodes

η	sd-m-x	sd-m-y	sd-l-x	sd-l-y	dv-m-x	dv-m-y	dv-l-x	dv-l-y
0.05	20.1804	19.8152	7.0629	9.4841	30.6701	30.1349	22.9455	15.4576
0.2	20.6383	20.2857	7.5496	8.5120	30.6701	30.1349	22.9455	15.4576
0.5	26.3615	24.7551	20.1107	13.1987	30.6701	30.1349	22.9455	15.4576

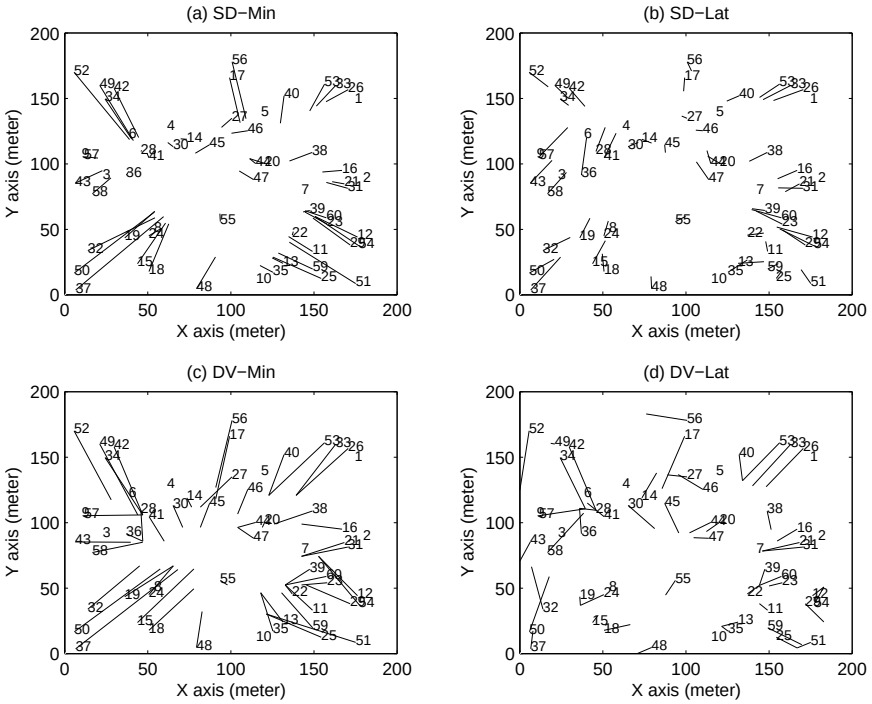

Figure 5-20: Original and estimated node locations for large network scenario when $\eta = 0.5$. Each original position is indicated by the sensor node ID and is connected by a line with its estimated location.

Chapter 6

Conclusions and Future Work

WSNs provide bridges between the virtual world of information technology and the real physical world. It represents a fundamental paradigm shift from traditional inter-human personal communications to autonomous inter-device communications. However, it also brings big challenges on the design and optimization of the network architecture and protocols. This thesis has been concerned with aspects of DSC and sensor node localization for the applications of target detection and tracking in WSNs. The focus on DSC scheme is the design and analysis of a novel random-binning based encoding and decoding algorithm. The random-binning based algorithm is further extended to produce an adaptive and energy-efficient DSC scheme. For the problem of sensor node localization, CRB is applied to evaluate the localization algorithms for large scale WSNs. The CRB-based analytical approach is developed and evaluated by comparing to the simulation results. The above research work on DSC and CRB analysis thereby contributes to the goal of evaluating and optimizing application performance while minimizing energy and bandwidth consumptions in WSNs. Section 6.1 presents a summary of this thesis. Some suggested themes for future work are discussed in section 6.2.

6.1 Conclusion and Summary

Chapter 2 provides the background regarding to the relevant aspects of WSNs for the research on distributed source coding and localization algorithms. The architecture of WSNs and overall protocol stacks are introduced. Several existing collaborative in-network processing techniques are also briefly compared.

In order to reduce the energy consumption and bandwidth requirement, the means of distributed source doing is investigated with which the data to be transmitted from sensor nodes to the sink can be reduced while satisfying the application requirements. In Chapter 3, after the problem formulation of DSC, a random-binning based DSC algorithm is proposed. The encoding and decoding methods for the random-binning based algorithm are presented. An analytical model is developed to evaluate the decoding performance of the algorithm and to find the proper setting of the coding parameters, such as coding rate and number of sensors participating in the coding procedure. A simulation method is designed to evaluate the algorithm's performance, which shows the efficiency and robustness of the random-binning based algorithm.

The random-binning based algorithm is then applied as a core of a distributed compression scheme for WSNs. In the proposed scheme, multiple sensor readings are jointly encoded with the side information implicitly provided by the sink at the same time. The problems of constructing and utilizing the side information required by the DSC scheme and the control of coding rate are solved. By fully utilizing the spatial correlation between multiple sensor observations, this DSC scheme achieves high coding efficiency and reduces bandwidth consumption. The decoding error performance of the distribute source coding scheme is analyzed and simulated. The proposed scheme is shown to be feasible and desirable for resource-constrained wireless sensor nodes.

In WSNs, the conditions of the channel (e.g. channel noise) and the network

(e.g. packet loss rate and available bandwidth) may change quickly. In addition, if a target appears and is detected, the sensor nodes that are required to collaborate to track the target should be adaptively configured during the movement of the detected target. Therefore, when a DSC scheme is applied to compressing sensor readings, it should be designed to be robust and adaptive to the changing network conditions. In Chapter 4, an adaptive end-to-end DSC control mechanism is proposed. Analytical models are developed for the SDR, bandwidth and energy efficiency performances of the DSC scheme to help understand the impacts of DSC parameters, transmission strategies and network conditions. A multi-mode power model for wireless sensor communications is used to evaluate the overall network energy consumption performance. A detailed packet format and a communication protocol are also implemented to facilitate the adaptive control. Simulation results show the efficiency of the proposed adaptive DSC control mechanism.

As sensor nodes normally have no network identifications, the locations of sensor nodes are vital for WSN applications. The location information can also be used to improve the design of WSN protocols. In Chapter 5, a general CRB analysis is introduced and then extended to develop an analytical approach to evaluate localization algorithms for large scale multi-hop WSNs. The performance of the proposed analytical evaluation tool is assessed by comparison with simulation results. With the CRB-based evaluation tool, two centralized localization algorithms are analyzed and compared with four distributed localization algorithms. The sensitivity of the location estimation performance to the range measurement error, node density, and anchor node density is also investigated. The CRB-based evaluation approach is shown to be efficient and scalable in the evaluation and optimization of localization algorithms for large scale WSNs. In addition, the tradeoffs between the location estimation accuracy, algorithm com-

plexity, and communication overheads can be made with the evaluation approach. The application of CRB-based evaluation approach to the target detection and tracking is also discussed.

6.2 Future Work

This thesis has proposed some distributed source coding schemes and an analytical approach for the evaluation of localization algorithms in large scale WSNs. Some aspects of the techniques still remain to be considered in more detail.

- In this thesis, all active sensor nodes, i.e. nodes sending readings to the sink, participating in the DSC encoding procedure are considered to have the same distance to the detected target and the signals to be encoded are independent and identically distributed. In a real network, however, some sensor nodes may be far away from the detected target or at a location with severe channel fading. Some further methods, such as adaptive decoding, to consider the diversity of locations and received signal strength may be desired.

- In the design and adaptive control of the DSC scheme, the detected target is assumed to be motionless during the DSC operations. In a practical network, however, the target may continuously move. The target movement should be taken into account in the DSC scheme design and optimization. For example, prediction of the target movement can be used to help the design and configuration of DSC schemes, such as adaptation of DSC parameters and change of the nodes involved in reporting their sensor readings and participating in the DSC scheme.

- In the design of the DSC scheme, only one target and one sink are assumed to exist in the network, and the signal to be estimated is assumed to be

Gaussian with AWGN. The Gaussian assumption is also typically applied for sensor localization problem. In a real network, however, multiple targets may appear simultaneously and multiple sinks may be deployed. Non-Gaussian scenarios may be experienced. The feasibility and optimization of the distributed source compression and sensor node localization under such network conditions should be studied.

- DSC is an end point based signal compression method, in which only the nodes detecting the target and reporting sensor readings will participate in the DSC encoding procedure. On the other hand, as a data compression approach, data aggregation happens in the nodes along the path from the reporting nodes to the sink. It would, therefore, be interesting to compare the two data compression approaches, study and improve the performance when both approaches are used in the network.

- In the investigation of localization algorithms in Chapter 5, only one type of range measurement technique is assumed for all the sensor nodes over the network. In practice, however, sensor nodes may use one or several different range measurement techniques to measure the distances to their neighbor nodes. In such networks, the impacts of the heterogeneity of the range measurement techniques on the analytical evaluation approach should be investigated.

- Due to the limited energy, communication, and computation resources, the problems in the protocol designs for different network layers in WSNs intertwine. The impact of the protocols used in the other layers, such as routing, channel access, and sleeping, on the DSC scheme can be analyzed. Cross-layer design will help improve the overall network performance in terms of energy consumption, location estimation, DSC decoding performance and

so on.

Author's Publications

1. Z. Tang, I. A. Glover, D. M. Monro, and J. He, "Distributed source coding based signal estimation in wireless sensor networks," in *Proc. 5th Postgraduate Symposium on the Convergence of Telecommunications, Networking and Broadcasting (PGNET 2004)*, Liverpool, UK, Jun. 28-29, 2004, pp. 223-228.

2. Z. Tang, I. A. Glover, D. M. Monro, and J. He, "Adaptive remote signal coding and recovery in wireless sensor networks," in *Proc. 12th IEEE International Conference on Networking (ICON 2004)*, Singapore, Nov. 16-19, 2004, Vol. 2, pp. 655-659.

3. Z. Tang, I. A. Glover, D. M. Monro, and J. He, "An energy aware cluster based routing protocol for wireless sensor network," in *Proc. EPSRC, IEEE, IEE, Postgraduate Research Conference (PREP 2005)*, Lancaster, UK, Mar. 30-Apr. 1, 2005.

4. Z. Tang, I. A. Glover, D. M. Monro, and J. He, "Adaptive control scheme for jointly distributed source coding in wireless sensor networks," in *Proc. 2nd International Conference on Telecommunications and Computer Networks (IADAT-tcn 2005)*, Portsmouth, UK, Sept. 7-9, 2005.

5. Z. Tang, I. A. Glover, A. N. Evans, D. M. Monro, and J. He, "An adaptive distributed source coding scheme for wireless sensor networks," in *Proc. 12th European Wireless Conference (EW 2006)*, Athens, Greece, Apr. 2-5, 2006.

6. Z. Tang, I. A. Glover, A. N. Evans, and J. He, "Performance analysis of location estimation in multi-hop wireless sensor networks," in *Proc. 2nd International Symposium on Broadband Communications (ISBC'06)*, Moscow, Russia, Sept. 10-14, 2006.

7. Z. Tang, I. A. Glover, D. M. Monro, and J. He, "A distributed source coding scheme for source estimation in wireless sensor networks," *IEICE Transactions on Communications*, vol. E90-B, no.1, pp. 152-155, Jan. 2007.

8. Z. Tang, I. A. Glover, A. N. Evans, and J. He, "Energy efficient transmission protocol for distributed source coding in sensor networks," in *Proc. IEEE International Conference on Communications (ICC 2007)*, Glasgow, UK, Jun. 24-28, 2007, pp. 3870-3875.

9. Z. Tang, I. A. Glover, A. N. Evans, and J. He, "An energy-efficient adaptive DSC scheme for wireless sensor networks," *Signal Processing, Special Section: Information Processing and Data Management in Wireless Sensor Networks*, vol. 87, No. 12, pp. 2896-2910, Dec. 2007.

10. J. He, Z. Tang, D. Kaleshi, and A. Munro, "A simple analytical model for the random access channel in WCDMA," *Electronics Letters*, vol. 43, no. 19, pp. 1034-1036, Sept. 2007.

References

[1] B. Warneke, M. Last, B. Leibowitz, and K.S.J. Pister, "Smart dust: communicating with a cubic-millimeter computer," *IEEE Computer*, vol. 34, No. 1, pp. 44-51, Jan. 2001.

[2] I. F. Akyildiz, W. Su, Y. Sankarasubramaniam, and E. Cayirci, "A survey on sensor networks," *IEEE Communications Magazine*, vol. 40, No. 8, pp. 102-114, Aug. 2002.

[3] H. Karl and A. Willig, *Protocols and Architectures for Wireless Sensor Networks*. John Wiley & Sons, 2005.

[4] V. Raghunathan, S. Ganeriwal, and M. Srivastava, "Emerging techniques for long lived wireless sensor networks," *IEEE Communications Magazine*, vol. 44, No. 4, pp. 108-114, Apr. 2006.

[5] E. Fasolo, M. Rossi, J. Widmer, and M. Zorzi, "In-network aggregation techniques for wireless sensor networks: a survey," *IEEE Wireless Communications*, vol. 14, No. 2, pp. 70-87, Apr. 2007.

[6] D. Niculescu, "Communication paradigms for sensor networks," *IEEE Communications Magazine*, vol. 43, No. 3, pp. 116-122, Mar. 2005.

[7] J. Baillieul and P. J. Antsaklis, "Control and communication challenges in networked real-time systems," *Proceedings of the IEEE*, vol. 95, No. 1, pp. 9-28, Jan. 2007.

[8] I. Demirkol, C. Ersoy, and F. Alagoz, "MAC protocols for wireless sensor networks: a survey," *IEEE Communications Magazine*, vol. 44, No. 4, pp. 115-121, Apr. 2006.

[9] J. N. Al-Karaki and A. E. Kamal, "Routing techniques in wireless sensor networks: a survey," *IEEE Wireless Communications*, vol. 11, No. 6, pp. 6-28, Dec. 2004.

[10] C. Wang and L. Xiao, "Sensor localization under limited measurement capabilities," *IEEE Network*, vol. 21, No. 3, pp. 16-23, May-Jun. 2007.

[11] C. Wang, K. Sohraby, B. Li, M. Daneshmand, and Y. Hu, "A survey of transport protocols for wireless sensor networks," *IEEE Network*, vol. 20, No. 3, pp. 34-40, May-Jun. 2006.

[12] D. Djenouri, L. Khelladi, and A. N. Badache, "A survey of security issues in mobile ad hoc and sensor networks," *IEEE Communications Surveys & Tutorials*, vol. 7, No. 4, pp. 2-28, Fourth Quarter 2005.

[13] A. Giridhar and P. R. Kumar, "Toward a theory of in-network computation in wireless sensor networks," *IEEE Communications Magazine*, vol. 44, No. 4, pp. 98-107, Apr. 2006.

[14] G. Sun, J. Chen, W. Guo, and K. J. R. Liu, "Signal processing techniques in network-aided positioning: a survey of state-of-the-art positioning designs," *IEEE Signal Processing Magazine*, vol. 22, No. 4, pp. 12-23, Jul. 2005.

[15] S. Hadim and N. Mohamed, "Middleware: middleware challenges and approaches for wireless sensor networks," *IEEE Distributed Systems Online*, vol. 7, No. 3, Mar. 2006.

[16] J. A. Paradiso and T. Starner, "Energy scavenging for mobile and wireless electronics," *IEEE Pervasive Computing*, vol. 4, No. 1, pp. 18-27, Jan.-Mar. 2005.

[17] J. Liu, M. Chu, and J. E. Reich, "Multitarget tracking in distributed sensor networks," *IEEE Signal Processing Magazine*, vol. 24, No. 3, pp. 36-46, May 2007.

[18] I. I. Hussein and D. M. Stipanovi, "Effective coverage control for mobile sensor networks with guaranteed collision avoidance," *IEEE Transactions on Control Systems Technology*, vol. 15, No. 4, pp. 642-657, Jul. 2007.

[19] D. Niculescu and B. Nath, "Error characteristics of ad hoc positioning systems (APS)," in *Proc. 5th ACM International Symposium on Mobile Ad Hoc Networking and Computing (MobiHoc'04)*, Tokyo, Japan, May 2004, pp. 20-30.

[20] N. Patwari, J. N. Ash, S. Kyperountas, A. O. Hero, III, R. L. Moses, and N. S. Correal, "Locating the nodes: cooperative localization in wireless sensor networks," *IEEE Signal Processing Magazine*, vol. 22, No. 4, pp. 54-69, Jul. 2005.

[21] F. Sivrikaya and B. Yener, "Time synchronization in sensor networks: a survey," *IEEE Network*, vol. 18, No. 4, pp. 45-50, Jul.-Aug. 2004.

[22] Q. Wang, Y. Zhu, and L. Cheng, "Reprogramming wireless sensor networks: challenges and approaches," *IEEE Network*, vol. 20, No. 3, pp. 48-55, May-Jun. 2006.

[23] J.-P. Kaps, G. Gaubatz, and B. Sunar, "Cryptography on a speck of dust," *Computer*, vol. 40, No. 2, pp. 38-44, Feb. 2007.

[24] Y. Wang, G. Attebury, and B. Ramamurthy, "A survey of security issues in wireless sensor networks," *IEEE Communications Surveys & Tutorials*, vol. 8, No. 2, pp. 2-23, Second Quarter 2006.

[25] Y. Yu, V. K. Prasanna, and B. Krishnamachari, *Information Processing and Routing in Wireless Sensor Networks*, World Scientific, 2006.

[26] D. Cook and S. Das, *Smart Environments: Technology, Protocols and Applications*, John Wiley & Sons, 2004.

[27] P. Remagnino, G. L. Foresti, T. Ellis, *Ambient Intelligence: A Novel Paradigm*, New York: Springer, 2005.

[28] J. Cai and D. J. Goodman, "General packet radio service in GSM," *IEEE Communications Magazine*, vol. 35, No. 10, pp. 122-131, Oct. 1997.

[29] G. Brasche and B. Walke, "Concepts, services, and protocols of the new GSM phase 2+ general packet radio service," *IEEE Communications Magazine*, vol 35., No. 8, pp. 94-104, Aug. 1997.

[30] H. Ekstrom, A. Furuskar, J. Karlsson, M. Meyer, S. Parkvall, J. Torsner, and M. Wahlqvist, "Technical solutions for the 3G long-term evolution," *IEEE Communications Magazine*, vol. 44, No. 3, pp. 38-45, Mar. 2006.

[31] "IEEE standard for local and metropolitan area networks part 16: air interface for fixed broadband wireless access systems," 2004.

[32] IEEE 802.22 WRAN WG Website: IEEE 802 LAN/MAN Standards Committee 802.22 WG on WRANs (Wireless Regional Area Networks), http://www.ieee802.org/22/, Sept. 2007.

[33] IEEE 802.11: the working group setting the standards for wireless LANs, http://www.ieee802.org/11/, Sept. 2007.

[34] "Supplement to IEEE standard for information technology telecommunications and information exchange between systems - local and metropolitan area networks - specific requirements. Part 11: wireless LAN medium access control (MAC) and physical layer (PHY) specifications: high-speed physical layer in the 5 GHz band," 1999.

[35] "IEEE standard for information technology - telecommunications and information exchange between systems - local and metropolitan area networks specific requirements part 15.4: wireless medium access control (MAC) and physical layer (PHY) specifications for low-rate wireless personal area networks (LR-WPANS)," 2003.

[36] ZigBee Alliance, http://www.zigbee.org/en/index.asp, Sept. 2007.

[37] Crossbow Technology, http://www.xbow.com, Sept. 2007.

[38] C. Intanagonwiwat, R. Govindan, and D. Estrin, "Directed diffusion: a scalable and robust communication paradigm for sensor networks," in *Proc. 6th Annual ACM/IEEE International Conference on Mobile Computing and Networking (MobiCom'00)*, Boston, MA, Aug. 2000, pp. 56-67.

[39] W. R. Heinzelman, A. Chandrakasan, and H. Balakrishnan, "Energy-efficient communication protocol for wireless microsensor networks,"in *Proc. 33rd Annual Hawaii International Conference on System Sciences*, Hawaii, HI, USA, Jan. 2000, vol. 2.

[40] A. Hossain, "An intelligent sensor network system coupled with statistical process model for predicting machinery health and failure," in *Proc. 2nd ISA/IEEE Sensors for Industry Conference (SIcon 02)*, Houston, TX, USA, Nov. 2002, pp. 52-56.

[41] P. Jiang, H. Ren, L. Zhang, Z. Wang, and A. Xue, "Reliable application of wireless sensor networks in industrial process control," in *Proc. 6th World Congress on Intelligent Control and Automation (WCICA 2006)*, Dalian, China, Jun. 2006, vol. 1, pp. 99-103.

[42] F. Chiti, A. De Cristofaro, R. Fantacci, D. Tarchi, G. Collodo, G. Giorgetti, and A. Manes, "Energy efficient routing algorithms for application to agro-food wireless sensor networks," in *Proc. IEEE International Conference on Communications (ICC 2005)*, Seoul, Korea, May 2005, vol. 5, pp. 3063-3067.

[43] D. M. Doolin and N. Sitar, "Wireless sensors for wildfire monitoring," in *Proc. SPIE Symposium on Smart Structures and Materials*, San Diego, CA, USA, Mar. 2005, vol. 5765, pp. 477-484.

[44] L. Yu, N. Wang, and X. Meng, "Real-time forest fire detection with wireless sensor networks," in *Proc. International Conference on Wireless Communications, Networking and Mobile Computing (WCNM 2005)*, Wuhan, China, Sep. 2005, vol. 2, pp. 1214-1217.

[45] A. Mainwaring, J. Polastre, R. Szewczyk, D. Culler, and J. Anderson, "Wireless sensor networks for habitat monitoring," in *Proc. 1st ACM International Workshop on Wireless Sensor Networks and Applications (WSNA'02)*, Atlanta, GA, USA , Sep. 2002, pp. 88-97.

[46] E. S. Biagioni and K. W.Bridges, "The application of remote sensor technology to assist the recovery of rare and endangered species," *International Journal of High Performance Computing Applications*, vol. 16, No. 3, pp. 315-324, Aug., 2002.

[47] James San Jacinto Mountains Reserve, http://www.jamesreserve.edu/index.lasso, Sept. 2007.

[48] P. Juang, H. Oki, Y. Wang, M. Martonosi, L. Peh, and D. Rubenstein, "Energy-efficient computing for wildlife tracking: design tradeoffs and early experiences with ZebraNet," in *Proc. ACM International Conference on Architectural Support for Programming Languages and Operating Systems (ASPLOS'02)*, San Jose, CA, USA , Oct. 2002, pp. 96-107.

[49] Intel Research Seattle, University of Washington: Caregiver's Assistant and CareNet Display: Making Eldercare Easier, http://www.intel.com/research/exploratory/wireless_sensors.htm#seattle, Sept. 2007.

[50] N. Xu, S. Rangwala, K. K. Chintalapudi, D. Ganesan, A. Broad, R. Govindan, and D. Estrin, "A wireless sensor network for structural monitoring,"

in *Proc. ACM Conference on Embedded Networked Sensor Systems (SenSys'04)*, Baltimore, MD, USA, Nov. 2004, pp. 13-24.

[51] K. Chintalapudi, T. Fu, J. Paek, N. Kothari, S. Rangwala, J. Caffrey, R. Govindan, E. Johnson, and S. Masri, "Monitoring civil structures with a wireless sensor network," *IEEE Internet Computing*, vol. 10, No. 2, pp. 26-34, Mar./Apr., 2006.

[52] J. S. Sandhu, A. M. Agogino, and K. Agogino, "Wireless sensor networks for commercial lighting control: decision making with multi-agent systems," in *Proc. 19th National Conference on Artificial Intilligence (AAAI-04) Workshop on Sensor Networks*, San Jose, CA, USA, Jul. 2004.

[53] TinyOS community forum: an open-source OS for the networked sensor regime,
http://www.tinyos.net, Sept. 2007.

[54] TinyDB: a declarative database for sensor networks,
http://telegraph.cs.berkeley.edu/tinydb, Sept. 2007.

[55] W. R. Heinzelman, J. Kulik, and H. Balakrishnan, "Adaptive protocols for information dissemination in wireless sensor networks," in *Proc. 5th Annual ACM/IEEE International Conference on Mobile Computing and Networking (MobiCom'99)*, Seattle, WA, USA, pp. 174-185, Aug. 1999.

[56] B. Deb, S. Bhatnagar, and B. Nath, "ReInForM: reliable information forwarding using multiple paths in sensor networks," in *Proc. 28th Annual IEEE Conference on Local Computer Networks (LCN'03)*, Bonn, Germany, Oct. 2003, pp. 406-415.

[57] C.-Y. Wan, A. T. Campbell, and L. Krishnamurthy, "PSFQ: a reliable transport protocol for wireless sensor networks," in *Proc. 1st ACM International Workshop on Wireless Sensor Networks and Applications (WSNA'02)*, Atlanta, GA, USA, Sept. 2002, pp. 1-11.

[58] F. Stann and J. Heidemann, " RMST: reliable data transport in sensor networks," in *Proc. 1st IEEE International Workshop on Sensor Network Protocols and Applications (SNPA 2003)*, Anchorage, AK, May 2003, pp. 102-112.

[59] C.-Y. Wan, S. B. Eisenman, and A. T. Campbell, "CODA: congestion detection and avoidance in sensor networks," in *Proc. 1st ACM Conference on Embedded Networked Sensor Systems (SenSys'03)*, Los Angeles, CA, USA, Nov. 2003, pp. 266-279.

[60] Y. Sankarasubramaniam, O. B. Akan, and I. F. Akyildiz, "ESRT: event-to-sink reliable transport in wireless sensor networks," in *Proc. 4th ACM International Symposium on Mobile Ad Hoc Networking and Computing (MobiHoc'03)*, Annapolis, MD, USA, Jun. 2003, pp. 177-188.

[61] D. Slepian and J. K. Wolf, "Noiseless coding of correlated information sources," *IEEE Transactions on Information Theory*, vol. 19, No. 4, pp. 471-480, Jul. 1973.

[62] T. M. Cover and J. A. Thomas, *Elements of Information Theory*. New York: John Wiley & Sons, 1991.

[63] Z. Xiong, A. D. Liveris and S. Cheng, "Distributed source coding for sensor networks," *IEEE Signal Processing Magazine*, vol. 21, No. 5, pp. 80-94, Sept. 2004.

[64] A. D. Wyner and J. Ziv, "The rate-distortion function for source coding with side information at the decoder," *IEEE Transactions on Information Theory*, vol. 22, No. 1, pp. 1-10, Jan. 1976.

[65] S. S. Pradhan, J. Kusuma, and K. Ramchandran, "Distributed compression in a dense microsensor network," *IEEE Signal Processing Magazine*, vol. 19, No. 2, pp. 51-60, Mar. 2002.

[66] T. S. Han and K. Kobayashi, "A unified achievable rate region for a general class of multiterminal source coding systems," *IEEE Transactions on Information Theory*, vol. 26, No. 3, pp. 277-288, May 1980.

[67] H. Yamamoto, "Wyner-Ziv theory for a general function of the correlated sources," *IEEE Transactions on Information Theory*, vol. 28, No. 5, pp. 803-807, Sept. 1982.

[68] A. D. Kaspi and T. Berger, "Rate-distortion for correlated sources with partially separated encoders," *IEEE Transactions on Information Theory*, vol. 28, No. 6, pp. 828-840, Nov. 1982.

[69] T. Berger, Z. Zhang, and H. Viswanathan, "The CEO problem," *IEEE Transactions on Information Theory*, vol. 42, No. 3, pp. 887-902, May 1996.

[70] H. Viswanathan and T. Berger, "The quadratic Gaussian CEO problem," *IEEE Transactions on Information Theory*, vol. 43, No. 5, pp. 1549-1559, Sept. 1997.

[71] Y. Oohama, "Gaussian multiterminal source coding," *IEEE Transactions on Information Theory*, vol. 43, No. 6, pp. 1912-1923, Nov. 1997.

[72] Y. Oohama, "The rate-distortion function for the quadratic Gaussian CEO problem," *IEEE Transactions on Information Theory*, vol. 44, No. 3, pp. 1057-1070, May 1998.

[73] Y. Oohama, "Rate-distortion theory for Gaussian multiterminal source coding systems with several side informations at the decoder," *IEEE Transactions on Information Theory*, vol. 51, No. 7, pp. 2577-2593, Jul. 2005.

[74] P. Ishwar, R. Puri, S. S. Pradhan, and K. Ramchandran, "On rate-constrained estimation in unreliable sensor networks," in *Proc. 2nd International Symposium on Information Processing in Sensor Networks (IPSN'03)*, Palo Alto, CA, USA, Apr. 22-23, 2003, pp. 179-192.

[75] S. S. Pradhan and K. Ramchandran, "Distributed source coding using syndromes (DISCUS): design and construction," in *Proc. IEEE Data Compression Conference (DCC'99)*, Snowbird, UT, USA, Mar. 1999, pp. 158-167.

[76] J. Chou, S. S. Pradhan, and K. Ramchandran, "Turbo and trellis-based constructions for source coding with side information," in *Proc. IEEE Data Compression Conference (DCC 2003)*, Snowbird, UT, USA, Mar. 2003, pp. 25-27.

[77] X. Wang and M. T. Orchard, "Design of trellis codes for source coding with side information at the decoder," in *Proc. IEEE Data Compression Conference (DCC 2001)*, Snowbird, UT, USA, Mar. 2001, pp. 361-370.

[78] J. Garcia-Frias and Y. Zhao, "Compression of correlated binary sources using turbo codes," *IEEE Communications Letters*, vol. 5, No. 10, pp. 417-419, Oct. 2001.

[79] J. Garcia-Frias and Y. Zhao, "Compression of binary memoryless sources using punctured turbo codes," *IEEE Communications Letters*, vol. 6, No. 9, pp. 394-396, Sept. 2002.

[80] Y. Zhao and J. Garcia-Frias, "Joint estimation and compression of correlated nonbinary sources using punctured turbo codes," *IEEE Transactions on Communications*, vol. 53, No. 3, pp. 385-390, Mar. 2005.

[81] A. Aaron and B. Girod, "Compression with side information using turbo codes," in *Proc. IEEE Data Compression Conference (DCC 2002)*, Snowbird, UT, USA, Apr. 2002, pp. 252-261.

[82] V. Stankovic, A. D. Liveris, Z. Xiong, and C. N. Georghiades, "Design of Slepian-Wolf codes by channel code partitioning," in *Proc. IEEE Data Compression Conference (DCC 2004)*, Snowbird, UT, USA, Mar. 2004, pp. 302-311.

[83] A. D. Liveris, Z. Xiong, and C. N. Georghiades, "Compression of binary sources with side information at the decoder using LDPC codes," *IEEE Communications Letters*, vol. 6, No. 10, pp. 440-442, Oct. 2002.

[84] M. Sartipi and F. Fekri, "Source and channel coding in wireless sensor networks using LDPC codes," in *Proc. 1st Annual IEEE Communications Society Conference on Sensor and Ad Hoc Communications and Networks (SECON 2004)*, Santa Clara, CA, USA, Oct. 2004, pp. 309-316.

[85] M. Sartipi and F. Fekri, "Distributed source coding in wireless sensor networks using LDPC coding: the entire Slepian-Wolf rate region," in *Proc. IEEE Wireless Communications and Networking Conference (WCNC 2005)*, New Orleans, LA, USA, Mar. 2005, pp. 1939-1944.

[86] J. Chou, D. Petrovic, and K. Ramchandran, "A distributed and adaptive signal processing approach to exploiting correlation in sensor networks," *Ad Hoc Networks*, vol. 2, No. 4, pp. 387-403, Oct. 2004.

[87] A. S. Y. Poon, "An energy-efficient reconfigurable baseband processor for wireless communications," *IEEE Transaction on Very Large Scale Integration (VLSI) Systems*, vol. 15, No. 3, pp. 319-327, Mar. 2007.

[88] S. Hong, S. Kim, M. C. Papaefthymiou, and W. E. Stark, "Power-complexity analysis of pipelined VLSI FFT architectures for low energy wireless commu-

nication applications," in *Proc. 42nd Midwest Symposium on Circuits and Systems*, Las Cruces, NM, USA, Aug. 1999, pp. 313-1944.

[89] S. Hong, R. Gupta, W. E. Stark, and A. O. Hero III, "Performance and complexity analysis of VLSI multi-carrier receivers for low-energy wireless communications," in *Proc. 51st IEEE Vehicular Technology Conference (VTC 2000-Spring)*, Tokyo, Japan, May 2000, pp. 2350-2354.

[90] L. Larson, P. Asbeck, and W. Xiong, "Energy constrained RF transceivers for mobile wireless communications," in *Proc. IEEE Wireless Communications and Networking Conference (WCNC 1999)*, New Orleans, LA, USA, Sept. 1999, pp. 197-200.

[91] S. Cui, A. J. Goldsmith, and A. Bahai, "Energy-constrained modulation optimization," *IEEE Transaction on Wireless Communications*, vol. 4, No. 5, pp. 2349-2360, Sept. 2005.

[92] S. Cui, A. J. Goldsmith, and A. Bahai, "Energy-efficiency of MIMO and cooperative MIMO techniques in sensor networks," *IEEE Journal on Selected Areas in Communications*, vol. 22, No. 6, pp. 1089-1098, Aug. 2004.

[93] R. Prasad, C. Dovrolis, M. Murray, and K. Claffy, "Bandwidth estimation: metrics, measurement techniques, and tools," *IEEE Network*, vol. 17, No. 6, pp. 27-35, Nov. 2003.

[94] V. Rajendran, K. Obraczka and J. J. Garcia-Luna-Aceves, "Energy-efficient collision-free medium access control for wireless sensor networks," in *Proc. 1st International Conference on Embedded Networked Sensor Systems (SenSys'03)*, Los Angeles, CA, USA, Nov. 2003, pp. 181-192.

[95] J. Li and G. Y. Lazarou, "A bit-map-assisted energy-efficient MAC scheme for wireless sensor networks," in *Proc. 3rd International Symposium on Information Processing in Sensor Networks (IPSN'04)*, Berkeley, CA, USA, Apr. 2004, pp. 55-60.

[96] W. Ye, J. Heidemann, and D. Estrin, "An energy-efficient MAC protocol for wireless sensor networks," in *Proc. 21st Annual Joint Conference of the IEEE Computer and Communications Societies (INFOCOM 2002)*, New York, NY, USA, Jun. 2002, pp. 1567-1576.

[97] T. v. Dam and K. Langendoen, "An adaptive energy-efficient MAC protocol for wireless sensor networks," in *Proc. 1st International Conference on Embedded Networked Sensor Systems (SenSys'03)*, Los Angeles, CA, USA, Nov. 2003, pp. 171-180.

[98] J. Polastre, J. Hill, and D. Culler, "Versatile low power media access for wireless sensor networks," in *Proc. 2nd International Conference on Embedded Networked Sensor Systems (SenSys'04)*, Baltimore, MD, USA, Nov. 2004, pp. 95-107.

[99] I. Rhee, A. Warrier, M. Aia, and J. Min, "Z-MAC: a hybrid MAC for wireless sensor networks," in *Proc. 3rd International Conference on Embedded Networked Sensor Systems (SenSys'05)*, San Diego, CA, USA, Nov. 2005, pp. 90-101.

[100] H. Wang, X. Zhang, and A. Khokhar, "An Energy-Efficient Low-Latency MAC Protocol for Wireless Sensor Networks," in *Proc. 49th Annual IEEE Global Telecommunications Conference (GLOBECOM'06)*, San Francisco, CA, USA, Nov. 2006, pp. 1-5.

[101] W. Wang, H. Wang, D. Peng, and H. Sharif, "An Energy Efficient Pre-Schedule Scheme for Hybrid CSMA/TDMA MAC in Wireless Sensor Networks ," in *Proc. 10th IEEE Singapore International Conference on Communication Systems (ICCS 2006)*, Singapore, Oct. 2006, pp. 1-5.

[102] C. Guo, L. C. Zhong, and J. M. Rabaey, "Low power distributed MAC for ad hoc sensor radio networks," in *Proc. Annual IEEE Global Telecommunications Conference (GLOBECOM'01)*, San Antonio, TX, USA, Nov. 2001, pp. 2944-2948.

[103] Z. Chen and A. Khokhar, "Self organization and energy efficient TDMA MAC protocol by wake up for wireless sensor networks," in *Proc. 1st Annual IEEE Communications Society Conference on Sensor and Ad Hoc Communications and Networks (SECON 2004)*, Santa Clara, CA, USA, Oct. 2004, pp. 335-341.

[104] M. J. Miller and N. H. Vaidya, "A MAC protocol to reduce sensor network energy consumption using a wakeup radio," *IEEE Transaction on Mobile Computing*, vol. 4, No. 3, pp. 228-242, May 2005.

[105] K. R. Chowdhury, N. Nandiraju, D. Cavalcanti, and D. P. Agrawal, "CMAC - A multi-channel energy efficient MAC for wireless sensor networks," in *Proc. IEEE Wireless Communications and Networking Conference (WCNC 2006)*, Las Vegas, NV, USA, Apr. 2006, pp. 1172-1177.

[106] C. Shen, C. Srisathapornphat, and C. Jaikaeo, "Sensor information networking architecture and applications," *IEEE Personal Communications*, vol. 8, No. 4, pp. 52-59, Aug. 2001.

[107] Y. Xu, J. Heidemann, and D. Estrin, "Geography-informed energy conservation for Ad Hoc routing," in *Proc. 7th ACM Annual International Conference on Mobile Computing and Networking (MobiCom'01)*, Rome, Italy, pp. 70-84, Jul. 2001.

[108] D. Niculescu and B. Nath, "Ad hoc positioning system (APS)," in *Proc. 44th Annual IEEE Global Telecommunications Conference (GLOBECOM'01)*, San Antonio, TX, USA, Nov. 2001, pp. 2926-2931.

[109] C. Savarese, J. M. Rabaey, and K. Langendoen, "Robust positioning algorithms for distributed ad-hoc wireless sensor networks," in *Proc. the General Track: 2002 USENIX Annual Technical Conference*, Monterey, CA, USA, pp. 317-327, Jun. 2002.

[110] A. Savvides, H. Park, and M. B. Srivastava, "The bits and flops of the n-hop multilateration primitive for node localization problems," in *Proc. 1st ACM International Workshop on Wireless Sensor Networks and Applications (WSNA'02)*, Atlanta, GA, USA, pp. 112-121, Sept. 2002.

[111] The Network Simulator - ns-2,
http://www.isi.edu/nsnam/ns/, Sept. 2007.

[112] OPNET Modeler,
http://www.opnet.com, Sept. 2007

[113] E. G. Larsson, "Cramer-Rao bound analysis of distributed positioning in sensor networks," *IEEE Signal Processing Letters*, vol. 11, No. 3, pp. 334-337, Mar. 2004.

[114] A. Catovic and Z. Sahinoglu, "The Cramer-Rao bounds of hybrid TOA/RSS and TDOA/RSS location estimation schemes," *IEEE Communications Letters*, vol. 8, No. 10, pp. 626-628, Oct. 2004.

[115] A. Savvides, W. L. Garber, R. L. Moses, and M. B. Srivastava, "An analysis of error inducing parameters in multihop sensor node localization," *IEEE Transactions on Mobile Computing*, vol. 4, No. 6, pp. 567-577, Nov.-Dec. 2005.

[116] D. Niculescu, "Positioning in ad hoc sensor networks," *IEEE Network*, vol. 18, No. 4, pp. 24-29, Jul.-Aug. 2004.

[117] K. Langendoen and N. Reijers, "Distributed localization in wireless sensor networks: a quantitative comparison," *Computer Networks*, vol. 43, No. 4, pp. 499-518, Nov. 2003.